Coordination Chemistry Reviews 254 (2010) 2031–2077

Contents lists available at ScienceDirect

Coordination Chemistry Reviews

journal homepage: www.elsevier.com/locate/ccr

Review

Molecular complexes formed by halides of group 4,5,13–15 elements and the thermodynamic characteristics of their vaporization and dissociation found by the static tensimetric method

E.I. Davydova, T.N. Sevastianova, A.V. Suvorov, A.Y. Timoshkin*

Department of Chemistry, St. Petersburg State University, University pr. 26, Old Peterhof, 198504 St. Petersburg, Russia

Contents

Abbreviations: A, acceptor molecule (Lewis acid); AZ, alumazene [2,6-(*i*-Pr)$_2$C$_6$H$_3$NAlMe]$_3$; CVD, chemical vapor deposition; cyt, cytosine; D, donor molecule (Lewis base); DA, donor–acceptor; depe, diethylphosphinoethane detu: (1,3diethylthiourea); deu, (1,3diethylurea); DICNQ, dipyrido[f,h]quinoxaline-6,7-dicarbonitrile; DMA, dimethylacetamide O=C(Me)NMe$_2$; dmap, 4-NMe$_2$-Py; DMF, *N*,*N*,dimethylformamide O=CHNMe$_2$; dmit, 1,3-dimethyl-2(3H)-imidazolethione.; dmpe, dimethylphosphinoethane; DMSO, Me$_2$SO; DO, dioxane C$_4$H$_8$O$_2$; dpm, dipivaloylmethanate (2,2,6,6-tetramethylheptane-3,5,-dionate); dpmpy, 2-Ph$_2$CH-Py; dppe, diphenylphosphinoethane; dppen, Ph$_2$P(CH)$_2$PPh$_2$; dppeS$_2$, SP(Ph$_2$)CH$_2$CH$_2$P(Ph$_2$)S; dppm, diphenylphosphinomethane; Hbta, bezotriazole; LSM, least squares method; *m*, mass of the sample; M, molecular mass; mcyt, 1-methylcytosine; Me$_3$[9]aneN$_3$, 1,4,7-trimethyl-1,4,7-triazacyclononane; morph, morpholine: NH(C$_4$H$_8$)O (coordination via N); mpy, 2-Me-Py; NTMSI, N-trimethylsilylimidazol; *P*, pressure; *P**, hypothetical pressure of the compound, which is computed on assumptions that (1) full amount of the compound exists in the system in the gaseous state, (2) any reactions of the compound are neglected; PhA, *N*-phenylacetamide; phen, 1,10-phenantroline; pic, 4-methylpyridine; pip, piperidine C$_5$H$_{11}$N; P_{total}, total pressure (usually this quantity is measured experimentally); py, pyridine C$_5$H$_5$N; pyz, pyrazine C$_4$H$_4$N$_2$; quin, quinuclidine; *R*, universal gas constant (8.314 J mol^{-1} K^{-1}, 0.082 l atm K^{-1},62,400 Torr ml K^{-1}); S(pz)$_2$, bis(pyrazolyl)sulfane; *T*, temperature, K; terpy, 2,2′,2″-terpyridil (2,6-di-2-pyridylpyridine); TEU, tetraethylurea; THF, tetrahydrofuran; tmeda, tetramethylethylenediamide; tmpH, 2,2,6,6-tetramethylpiperidine; tmtu, N,N,N′,N′-tetramethylthiourea; tmu, N,N,N′,N′-tetramethylurea; tu, thiourea; *V*, volume of the system.

* Corresponding author. Tel.: +7 812 428 4071; fax: +7 812 428 6939.
E-mail address: alextim@AT11692.spb.edu (A.Y. Timoshkin).

0010-8545/$ – see front matter
doi:10.1016/j.ccr.2010.04.001

ARTICLE INFO

Article history:
Received 20 July 2009
Accepted 2 April 2010
Available online 10 April 2010

Keywords:
Donor–acceptor complexes
Adducts
Structure
Thermodynamics
Vaporization
Dissociation
Tensimetry
Static method

ABSTRACT

Donor–acceptor molecular complexes (adducts AD_x) play important role in modern technology. They are prospective single-source precursors for the synthesis of solid phases by the chemical vapor deposition (CVD) method. Stability of the complex in the gas phase is an important issue for many practical applications. High-temperature thermodynamic data for adducts are not readily available, which underlines the fundamental need for the systematic study of processes which adducts undergo upon heating. Such processes are: the congruent or incongruent vaporization (sublimation), the reversible dissociation in the gas phase into the components and the irreversible thermal destruction (pyrolysis).

The static tensimetric method with membrane null-manometer is unique method for studying donor–acceptor interactions both in gaseous and condensed phases. It is a useful method for: (1) the evaluation of the complex composition AD_x; (2) characterization of the nature of the main process which the complex undergoes upon heating; (3) determination of the thermodynamic characteristics of such processes. The static method allows to achieve the true equilibrium state, it is applicable both to the heterogeneous and homogeneous systems and allows one to measure the vapor pressure—temperature dependence for the pressure range 1–1000 Torr and temperatures up to 1100 °C. For the homogeneous systems (processes in the gas phase), the vapor composition and the vapor density can be determined, which allows to calculate partial pressures of three molecular forms in vapors and determine the equilibrium constant at a given temperature. From the temperature dependence of the equilibrium constant, the enthalpies and entropies of the respective process can be evaluated.

In the present review the application of the static tensimetry method for the determination of the nature of the process, vapor composition and thermodynamic characteristics is illustrated on the following examples:

- Sublimation (vaporization) of the adduct without decomposition.
- Reversible gas phase dissociation of the adduct into components.
- Sublimation (vaporization) of the adduct accompanied by its reversible dissociation into components.
- Complete congruent dissociation of the adduct into gaseous components upon heating.
- Incongruent dissociation of the adduct (subsequent dissociation of the solid AD_x adducts into solid AD_{x-1} and gaseous D).
- Appearance of the upper temperature limit due to the irreversible thermal destruction (pyrolysis) of one of the components.

Our results on systematic studies of the thermal decomposition of adducts of group 4,5,13,14,15 element halides (chlorides, bromides and iodides) with group 15, 16 element-containing donors are presented. Experimentally obtained thermodynamic characteristics of vaporization and dissociation for more than 50 adducts are summarized for the first time.

Current approaches towards estimation of the sublimation enthalpies of donor–acceptor complexes are critically evaluated. It is shown, that the widely used approximation (sublimation enthalpy of the complex equals the sublimation enthalpy of 1 mol of the ligand) generally performs very poor and may result in large (about 70 kJ mol^{-1}) errors. Its application is not recommended. Moreover, reported values for the gas-phase metal–ligand bond dissociation energies, based on such approximation, are incorrect and should not be trusted. Approaches based on the structural information appear to be more perspective.

The structural features of the DA complexes of group 4,5,13,14,15 element halides both in gaseous and solid states are also summarized for the first time.

1. Introduction

High-temperature gas phase chemistry plays an important role in modern technology. In particular, the chemical vapor deposition (CVD) method [1–4] is widely used for the production of binary and composite materials, such as semiconductors and refractory nitrides and oxides. Donor–acceptor (DA) molecular complexes AD_x (also called adducts) [5] formed by Lewis acids A and Lewis bases D are prospective single-source precursors for the synthesis of the solid phases [6–14]. Donor–acceptor interactions often stabilize unusual structures. For example, inorganic heterocycles of the N_3P_2, N_4As, N_4P series have been stabilized by Shulz [15–17].

Saturated vapor pressure of the single-source precursor and its stability in the gas phase are the two most important issues for its practical application. Thus, there is a fundamental need for the systematic study of processes which adducts undergo upon heating. Such processes are: congruent or incongruent vaporization (sublimation), reversible dissociation in the gas phase (into donor and acceptor components) and irreversible thermal destruction (pyrolysis). Homogeneous gas-phase dissociation of the DA complexes is

of fundamental interest for the direct determination of the energy of DA bond rupture in the gas phase.

The group 4,5,13,14 element halides EX_n are typical Lewis acids which readily form stable donor–acceptor complexes with nitrogen- and oxygen-containing donors. In past 20 years there has been an impressive progress in structure determination of molecular complexes. Despite many experimental studies, structural aspects of donor–acceptor interactions are not well addressed in the literature. In the first part of the present review the structural features of molecular complexes of group 4,5,13–15 element halides are summarized.

Thermal stability, vaporization behavior and thermodynamic characteristics of the vaporization processes of molecular complexes are only scarcely explored. In reviews of sublimation and vaporization enthalpies by Chickos and Acree in 2002–2003 [18,19] data for only several DA complexes are provided. Sublimation/vaporization enthalpies for several adducts have been determined by the isoteniscope variant of a static method and the Knudsen effusion method. Dissociation enthalpies of gaseous molecular complexes were the subject of early tensimetry studies by Brown [20] and Tamres [21–23]. As noted by Burkinshaw and Mortimer [24] in their 1983 review, results obtained in earlier studies with the isoteniscope method could be the subject of large systematic errors due to the presence of the volatile impurities. Many gas phase dissociation enthalpies of the complexes have been obtained by thermochemical cycles from measurements in solutions. In such an approach, estimated values for the vaporization enthalpies of adducts are widely used. Such estimations are often made "on a somewhat arbitrary basis" [24, p. 125]. Special reviews devoted to the thermodynamic properties of gaseous donor–acceptor complexes are also few in number. The thermochemistry of the gaseous transition metal complexes with ligands of 15 and 16 group elements have been reviewed in 1983 by Burkinshaw and Mortimer [24]. In 1993, Airoldi and Chagas [25] summarized thermochemistry of coordination compounds of group 12 metal halides (Zn, Cd, Hg). Thermochemistry of selected $TiCl_4$ complexes has been reviewed by Sevast'yanova and Suvorov [26], and that of metal halide complexes with donor ligand pyridine – in 1999 [27]. The relationship between structural and thermodynamic properties of molecular complexes has been investigated by Romm et al. [28].

In the second part of the present review we briefly describe static tensimetric method and consider its capabilities. Several case studies will be explored in detail to illustrate the determination of complex composition, and the determination of thermodynamic characteristics of processes which donor–acceptor complexes undergo upon heating. We also summarize results obtained within last decades in our laboratory with static tensimetric method for the donor–acceptor complexes formed by group 4,5,13–15 element halides with donor molecules of group 15 and 16 elements. On the basis of our studies we will show that the widely used estimation of the enthalpy of the sublimation of the complex as the enthalpy of sublimation of 1 mol of the ligand [29] is completely erroneous for the complexes of group 13 metal halides, and should not be used as a general rule.

2. Molecular donor–acceptor complexes of group 4,5,13–15 element halides

2.1. General characteristic

Primary objects, studied by the static tensimetric method in the present review, are molecular complexes of group 4,5,13–15 metal halides. The reaction between a Lewis acid (electron pair acceptor) and a Lewis base (electron pair donor) results in the formation of the electron donor–acceptor [5] (DA) complex, also called a charge transfer complex or a Lewis adduct. The first molecular complex BF_3NH_3 was produced in early nineteenth century by Gay-Lussac [30] by the following reaction:

$$HBF_4(g) + 2NH_3(g) = BF_3{\cdot}NH_3(s) + NH_4F(s)$$

The most common method of the adduct synthesis is an interaction between stoichiometric amounts of donor and acceptor molecules, which can be carried out either directly (without a solvent) or in the non-polar solvent medium.

$$A + D = A{\cdot}D$$

Complexes of A·2D and A·3D compositions can be obtained in excess of the donor. For example, the reaction of 1:1 SiF_4·IPr complex with excess of the N-heterocyclic carbene ligand IPr gives 1:2 complex SiF_4·2IPr [31].

Substitution of one donor molecule by another is usually carried out in solution and is a useful route to new complexes. It was used to produce $[TiCl_4(TPPO)_2]$ from $[TiCl_4(NH_3)_2]$ [32] and $[SnF_4(Ph_3PO)_2]$ from $[SnF_4(MeCN)_2]$ [33].

Alternative routes, such as oxidative addition, are rarely used. Complexes of SnI_4 and $SnBr_4$ were obtained [34] with qualitative yield, by the reaction of metallic tin with two equivalents of $^nPr_3PI_2$ and Me_2SBr_2, respectively:

$$Sn + 2^nPr_3PI_2 = SnI_4{\cdot}2P^nPr_3;$$

$$Sn + 2Me_2SBr_2 = SnI_4{\cdot}2SMe_2$$

Interestingly, in the later case a mixture of *cis* and *trans* isomers was produced.

Synthesis of $SnCl_4$·DICNQ was achieved by slow oxidation of solution containing $SnCl_2$ and DICNQ in methanol – ethylacetate (1:3) [35]. Disproportionation of InI in the Py/m-xylene (2:1) solution at room temperature yielded *mer*-InI_3·3Py [36].

A distinct feature of adduct compounds is their molecular structure, which is retained both in gaseous and condensed states. For example, group 13 metal halide monoammiacates $EX_3{\cdot}NH_3$ were the subject of numerous experimental studies in all states of aggregation. Gas phase electron diffraction studies have been performed by Hargittai et al. [37–40] and Haaland et al. [41] and indicated ethane-like molecules with direct E–N bond. Extensive spectral studies indicate that the molecular structure of gaseous $EX_3{\cdot}NH_3$ adducts [42,43] is retained both in liquid, glassy, and solid states [44,45]. Comparisons of IR and Raman spectra for the $AlCl_3NH_3$ adduct in gaseous, liquid, and solid states are presented in Fig. 1. Differences in spectra are interpreted in terms of H. . .Cl hydrogen bonding and the partial ionization in the liquid state [42]. Significant H. . .X hydrogen bonding in the melt leads to the fact that $EX_3{\cdot}NH_3$ adducts usually form supercooled melts and relatively stable glassy states. For example, the glass, obtained by quenching of the cell with melted $AlCl_3{\cdot}NH_3$ in water, is stable for several weeks [42]. Ionization degree of molten $EX_3{\cdot}NH_3$ adducts is usually small. At 200 °C the ionization constant for the process:

$$2AlCl_3{\cdot}NH_3 = [AlCl_2(NH_3)_2]^+ + [AlCl_4]^-$$

was estimated as 3×10^{-3} [42].

More recently, the crystal structure determinations of $AlX_3{\cdot}NH_3$ [46] and $GaBr_3{\cdot}NH_3$ [47] directly confirmed molecular structures of the solid adducts with evident H. . .X hydrogen bonding (Fig. 2). In contrast, the complexes with excess ammonia molecules usually have ionic structures; thus complexes of the $AlX_3{\cdot}5NH_3$ composition in the solid state are formulated as $[Al(NH_3)_5X]^{2+}2X^-$ [48].

Comparative theoretical study [47] revealed that the molecular structure of $EX_3{\cdot}NH_3$ adducts is primary due to much stronger hydrogen bonding and larger stability of the head-to-tail dimers

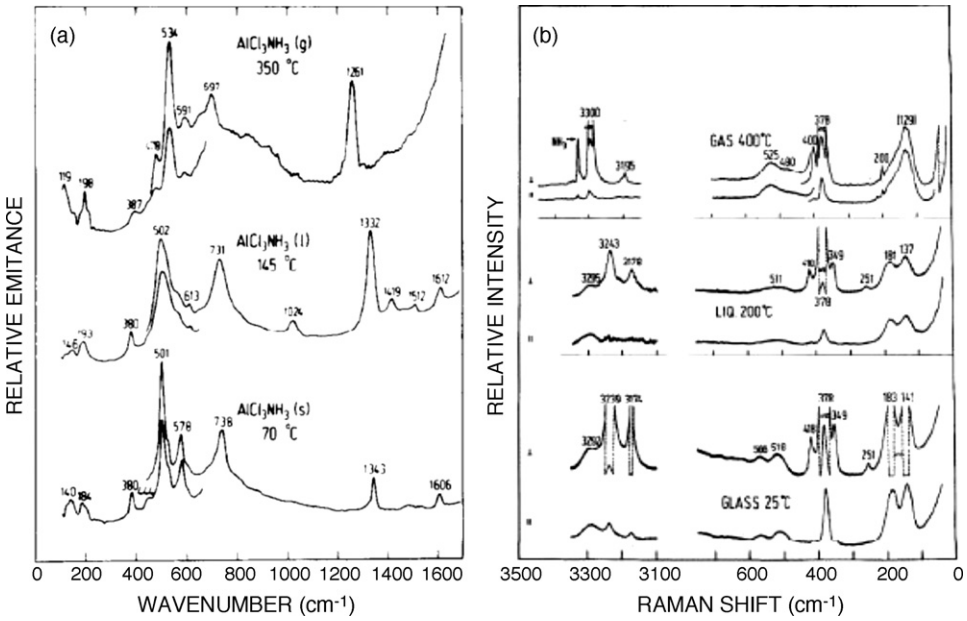

Fig. 1. Infrared emission (a) and Raman (b) spectra of $AlCl_3NH_3$ adduct in gaseous, liquid and solid states. Taken from Refs. [43,44], respectively. Gas phase Raman spectra are from Ref. [45].

and tetramers $(EX_3NH_3)_{2,4}$ as compared to the contact ion pairs $\{[EX_2(NH_3)_2]^+ \ldots [EX_4]^-\}_{1,2}$. The hydrogen bonding plays an important role in structures of all ammonia complexes. Extensive hydrogen bonded network with two different hydrogen-bonded interactions was observed in the structure of *trans*-$SnF_4 \cdot 2ND_3$ adduct obtained by high-resolution neutron powder diffraction [49]. Head-to-tail packing of the $GaCl_3 \cdot NH^iPr_2$ adduct is also facilitated by H...Cl interactions (Fig. 3) [50]. Interestingly, the structures of complexes of group 13 and 14 metal *fluorides* with ammonia are quite different from that of their heavier halogenides. A typical feature of *fluoride* complexes is the increase of coordination number of the central atom and formation of 2D or 3D polymeric networks (coordination polymers). For example, the crystal structure of $GaF_3 \cdot NH_3$ is formed by two-dimensional layers of octahedral $[GaF_5NH_3]$, the gallium atom has coordination number 6 [51]. Both $ZrF_4 \cdot NH_3$ and $HfF_4 \cdot NH_3$ form conjugated layers of bicapped trigonal prisms $[M(NH_3)F_7]$, which are connected via edges and corners [52].

Adducts formed by other donors exhibit similar features. Raman spectra of $MCl_3 \cdot POCl_3$ (M = Al,Ga) [53,54], and $MCl_4 \cdot POCl_3$ (M = Zr,Hf) [55] in the gas, liquid and glassy state indicate molecular complexes of 1:1 stoichiometry formed via oxygen atom of $POCl_3$. Molecular structure of $AlCl_3 \cdot OPCl_3$ in the solid state was confirmed by the single crystal X-ray diffraction [56]. IR spectra of solid complexes of AlX_3 with pyridines and pyridine-N-oxides [57] are indicative of their molecular structure. X-ray powder diffraction data for AlX_3 adducts with pyridines are reported by Wilson and Worrall [58]. The low conductivity of liquid adducts [59,60] is also consistent with their molecular structures. Comparative X-ray and spectral studies of the $EX_3 \cdot$terpy adducts also indicate their molecular structures [61].

The growth of single crystals of adducts is sometimes limited due to their low solubility. In case of $SnCl_4 \cdot 2Py$, which is insoluble in common organic solvents, single crystals were grown from pyridine solution held at ca 220 °C in sealed ampoule for 3 days and allowed to cool slowly [62]. Growth of single crystals of adducts by slow sublimation in vacuum is also a useful method [47].

In recent years, there are many theoretical studied devoted to donor–acceptor interactions. A brief summary of the recent theoretical works on 13–15 donor–acceptor complexes can be found in [63]. Although detailed comprehensive report on theoretical studies of donor–acceptor complexes lies out of scope of

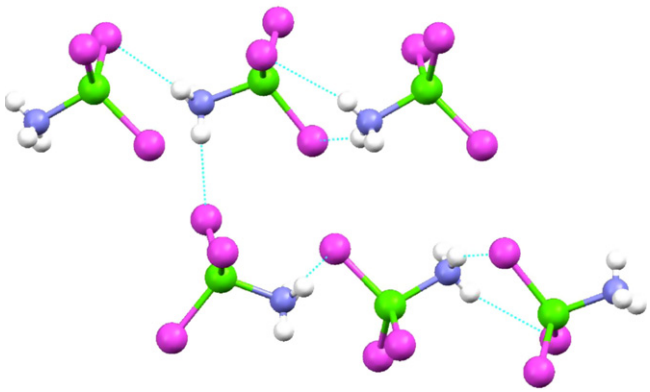

Fig. 2. Solid state structure of $GaBr_3 \cdot NH_3$ adduct [47]. Projection of the structure down the *b*-axis.

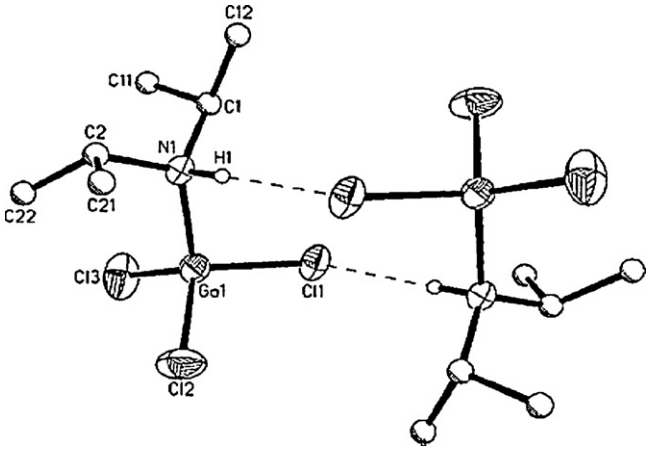

Fig. 3. Structure of the $GaCl_3 \cdot NH^iPr_2$ adduct, stabilized by short Cl···H contacts. Taken from Ref. [50].

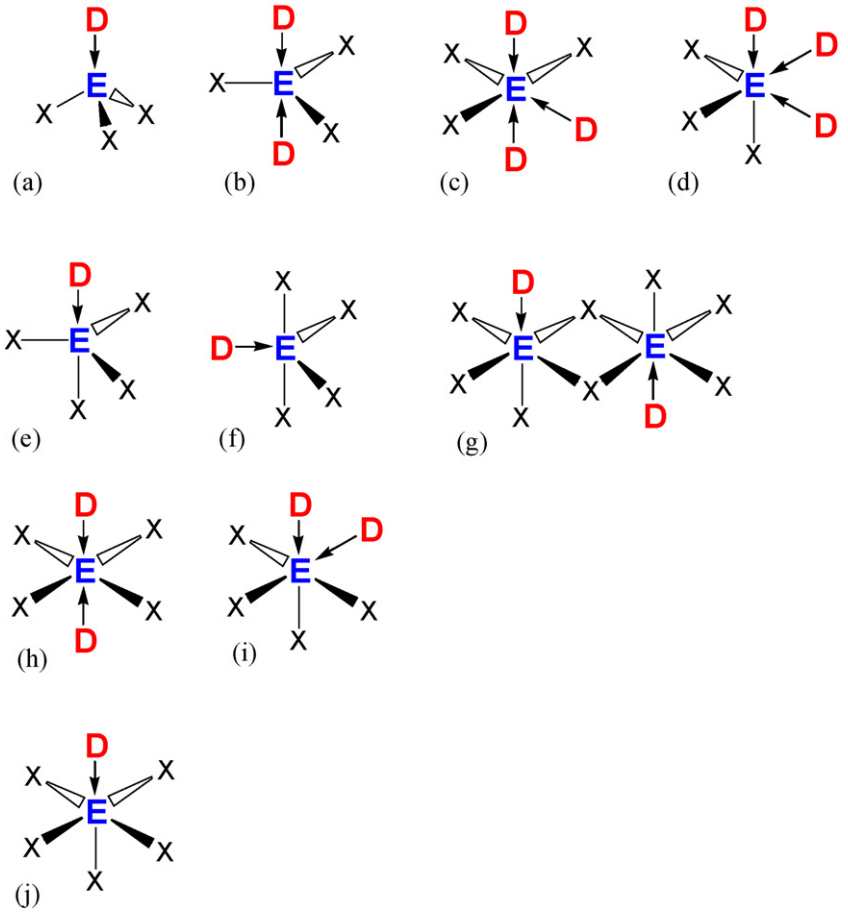

Fig. 4. Major structural types of the donor–acceptor complexes of group 13 (a–d), 4 and 14 (e–i), 5 and 15 (j) element halides: (a) tetrahedral $EX_3{\cdot}D$; (b) trigonal pyramidal $EX_3{\cdot}2D$; (c) meridional isomer *mer*-$EX_3{\cdot}3D$; (d) facial isomer *fac*-$EX_3{\cdot}3D$; (e) axial isomer *ax*-$EX_4{\cdot}D$; (f) equatorial isomer *eq*-$EX_4{\cdot}D$; (g) X-bridged dimer $[EX_4{\cdot}D]_2$; (h) trans isomer *trans*-$EX_4{\cdot}2D$; (i) cis isomer *cis*-$EX_4{\cdot}2D$; (j) $EX_5{\cdot}D$.

the present review, some related works will be briefly mentioned below.

Comparative theoretical studies of complexes of group 13 metal halides [64–68] and group 14 metal halides [69–75] provided important conclusions concerning the trends in the donor–acceptor bond energies and reorganization energies. In particular, the greater Lewis acidity of BCl_3 compared to BF_3 attracted considerable attention and was discussed in detail [76–78]. The role of terminal atoms in the complex formation was addressed in [64]. Analysis of the geometrical and energetic changes upon complex formation, based on *ab initio* studies performed by Horvath and Hargittai [79,80], revealed that formation of 13–15 tetrahedral adduct from planar EX_3 and pyramidal ammonia molecules proceeds without an energetic barrier. In contrast, formation of complexes with group 14 metal halides requires some barrier, due to larger distortion energy of tetrahedral acceptor molecules EX_4. The barrier height depends on the stoichiometry and the type of complex and increases in order *eq*-$ECl_4{\cdot}Py$ < *cis*-$ECl_4{\cdot}2Py$ < $ECl_4{\cdot}2,2'$-bipy (E = Si, Ge) [71]. An approach towards the rigorously defined quantum-chemical analysis of donor–acceptor bond formation was presented by Frenking [81] and used for a theoretical study of 13–15 adducts [82].

2.2. Structural features of adduct compounds

Since the crystal structure is an important factor determining the complex volatility (value of the sublimation enthalpy and vapor pressure at a given temperature), a short summary of structural characteristics of adducts will be presented. In last 15 years there have been made an amazing progress in structure determination for adducts formed by group 13,14,15 element halides. These data for the first time will be summarized in the present review. We have focused our attention only on complexes which exhibit molecular structures in the solid state.

Major structural types of the molecular complexes of group 4, 5, and 13–15 element halides with coordination numbers 4, 5 and 6 are schematically presented in Fig. 4. Although coordination numbers higher than 6 are known for the molecular complexes of group 4 metal halide adducts [83,84] and adducts of indium trihalides [85], the structural features of such compounds will not be considered in the present report.

2.2.1. Tetrahedral $EX_3{\cdot}D$ adducts

The structural parameters of experimentally known gaseous complexes are summarized in Table 1, and those of the solid adducts are presented in Table 2. Comparison of structural data indicates, that the donor–acceptor bond distances for gaseous compounds are noticeably larger than that for the solid adducts. More clearly it can be seen from Table 3, where the donor–acceptor bond distances for gaseous and solid adducts are summarized. With the single exception for the $AlCl_3{\cdot}NMe_3$ adduct, the donor–acceptor bond lengths in condensed phase are by 0.01–0.11 Å shorter than those in gaseous state. Mean bond shortening for the solid adducts amounts about 4.3%. In respect with the observed general trend, the structural parameters for some adducts, in particularly the bond distances in $AlCl_3{\cdot}NMe_3$ and $BCl_3{\cdot}PMe_3$ require re-examination. Note, that extremely large differences were observed for weak (or so called "partially bonded") adducts of BF_3 with HCN and CH_3CN,

Table 1
Structural properties of gaseous adducts.

Complex	r(E–D), Å	r(E–X), Å	Method[a]	Ref.
$BF_3{\cdot}NH_3$	1.59(3)		MW	[86]
$BF_3{\cdot}NMe_3$	1.664(11)	1.354(6)	ED	[39]
$BF_3{\cdot}NMe_3$	1.674(4)	1.374(2)	ED + MW	[87]
$BF_3{\cdot}NMe_3$	1.636(4)		MW	[88]
$BF_3{\cdot}NMe_3$	1.636(4)	1.387(5)	MW	[89]
$BF_3{\cdot}Py$	1.669(7)	1.366(2)	ED	[90]
$BF_3{\cdot}Py$	1.610(3)		MW	[91]
$BF_3{\cdot}Pyz$	1.605(3)		MW	[91]
$BF_3{\cdot}$pyrimidine	1.606(3)		MW	[91]
$BF_3{\cdot}HCN$	2.473(29)		MW	[92]
$BF_3{\cdot}NCMe$	2.011(7)		MW	[93]
$BF_3{\cdot}OMe_2$	1.730(50)	1.361(8)	ED	[94]
$BCl_3{\cdot}NMe_3$	1.659(6)	1.839(4)	ED	[39]
$BCl_3{\cdot}NMe_3$	1.652(9)	1.836(2)	ED	[95]
$BCl_3{\cdot}Py$	1.706(12)	1.830(3)	ED	[90]
$BCl_3{\cdot}PMe_3$	1.941(16)	1.851(7)	ED	[96]
$BBr_3{\cdot}Py$	1.694(17)	1.986(3)	ED	[90]
$BBr_3{\cdot}NMe_3$	1.663(13)	2.001(3)	ED	[95]
$BBr_3{\cdot}PMe_3$	1.946(29)	2.010(9)	ED	[97]
$AlCl_3{\cdot}NH_3$	1.996(19)	2.100(5)	ED	[40]
$AlCl_3{\cdot}NMe_3$	1.945(35)	2.121(4)	ED	[41]
$AlBr_3{\cdot}NH_3$	1.997(19)	2.264(5)	ED	[37]
$GaCl_3{\cdot}NH_3$	2.057(11)	2.142(5)	ED	[38]
$GaBr_3{\cdot}NH_3$	2.081(23)	2.288(5)	ED	[37]
$AlBr_3{\cdot}SbBr_3$	2.52(2)	2.30(2)	ED	[98]
axial-$SiF_4{\cdot}NH_3$	2.090	1.608eq; 1.612ax	MW	[99]

[a]ED – electron diffraction; MW – microwave spectroscopy.

this problem was in details addressed by Leopold et al. [100]. Difference for the more strongly bound $BF_3{\cdot}NH_3$ adduct is less dramatic [101]. Shorting of the DA bond distance of the solid adduct is primarily due to the increase of the molecular dipole moment in a polar (or polarizable) medium (so called "dipolar enhancement" mechanism) [100]. High-accuracy computations on BF_3 complexes with nitriles by Phillips and Cramer [102–104] aim to resolve the long standing experiment–theory structure discrepancies [105] for the weak adducts.

Interestingly, in early electron diffraction study the structure of gaseous $AlBr_3{\cdot}SbBr_3$ complex was interpreted as ethane-like molecule with direct Al–Sb bond [98]. Based on these data, formation of 1:1 gaseous adducts was assumed in tensimetry studies of $AlBr_3$–$SbBr_3$ [106] and $GaCl_3$–$SbCl_3$ [107] systems. In this respect it is noticeable that X-ray structure determination for the $GaCl_3$–$SbCl_3$ compound showed ionic structure $[SbCl_2]^+[GaCl_4]^-$ in the solid state [108].

Complexes of EX_3 with such donor molecules as ammonia, primary and secondary amines, water, and alcohols, feature hydrogen bonds in the solid state. In particular, BF_3 complexes with water and methanol form 3D and 1D H-bonded networks, respectively [109].

2.2.2. Trigonal bipyramidal $EX_3{\cdot}2D$ adducts

Although for $EX_3{\cdot}2D$ three different isomers are theoretically possible (with donor molecules occupying two, one and zero equatorial positions), all structurally characterized complexes with monodentate ligands always have donor molecules in the axial positions (Fig. 4b). Only in case of bidentate chelating donors, such as tetramethylethylenediamine, the donor molecule occupies one equatorial position, as for example in $InI_3{\cdot}$tmeda [282]. Major structural parameters of adducts are summarized in Table 4, and the structure of $AlCl_3{\cdot}2NMe_3$ [264] is presented as an illustrative example in Fig. 5.

As can be seen from Table 5, the donor–acceptor bond length noticeably increases (by 0.03–0.33 Å) upon addition of the second donor ligand D to $EX_3{\cdot}D$ adduct. Interestingly, there is no further elongation of the In–O bond upon further increasing of the coordination number from five (2.258(2) Å for $InCl_3{\cdot}2THF$) to six (2.258(56) Å for *mer*-$InCl_3{\cdot}3THF$).

It should be noted, that since the In atom prefer higher coordination number 6, indium halides easily form tris-adducts or oligomer structures with halide bridges. For example, tetrameric $4InCl_3{\cdot}6NHEt_2$ is formed by four octahedra fused by Cl edges [296].

2.2.3. Octahedral $EX_3{\cdot}3D$ adducts

In case of aluminum and gallium compounds, interaction with the excess of monodentate donor molecules often leads

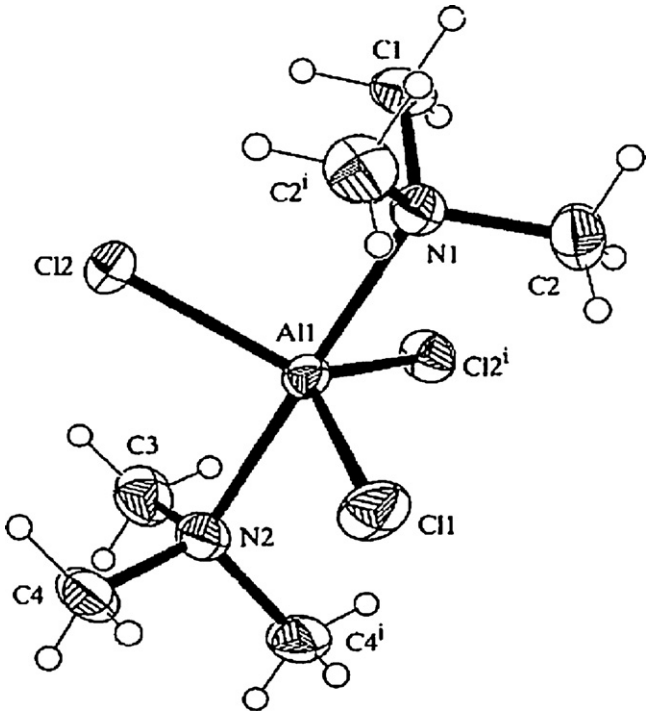

Fig. 5. Solid state structure of $AlCl_3{\cdot}2NMe_3$ adduct. Taken from Ref. [264].

Table 2
Structural properties of tetrahedral EX_3 adducts.

Complex	r(E–D), Å	r(E–X), Å	Ref.
$BF_3{\cdot}NH_3$	1.60	1.38	[110,111]
$BF_3{\cdot}NH_3$	1.5788(15)	1.3837(3); 1.3900(4); 1.3903(4)	[112]
$BF_3{\cdot}ND_3$[a] (neutron diffraction)	1.554(5)	1.393(9); 1.394(9); 1.400(8)	[101]
$BF_3{\cdot}NH_2Me$	1.57	(1.39)	[111,113]
$BF_3{\cdot}NMe_3$	1.585(30)	1.39	[111,114]
$BF_3{\cdot}Py$	1.530(20)	1.410(2)	[115]
$BF_3{\cdot}Py$	1.604(5)	1.330; 1.347; 1.357(4)	[116]
$BF_3{\cdot}$dmap	1.589(5)	1.292(16); 1.310(13); 1.365(13)	[117]
$BF_3{\cdot}NCH$	1.638(2)	1.352(2); 1.362(2); 1.369(2)	[118]
$BF_3{\cdot}NCMe$	1.635	(1.33)	[111,119]
$BF_3{\cdot}NCMe$	1.630(4)	1.334(5); 1.353(3)	[120]
$BF_3{\cdot}NCPh$	1.630(3)	1.364(2); 1.365(3)	[121]
$BF_3{\cdot}NCCH_2F$	1.635(6)	1.340(6); 1.354(6); 1.362(6)	[103]
$BF_3{\cdot}NCCH_2Cl$	1.640(3); 1.649(2)	1.345(3); 1.358(3); 1.355(3); 1.364(3)	[103]
$BF_3{\cdot}NCCH_2I$	1.643(12)	1.374(12); 1.341(13); 1.356(13)	[103]
4-N-$BF_3{\cdot}$1-Me,5-CH_2Ph-1,2,4,3-triazaphosphole	1.597(5)	1.373(7); 1.379(7)	[122]
2-N-$BF_3{\cdot}$4,5-diisopropyl-1,2,4,3-triazaphosphole	1.585(2)	1.367(2); 1.375(2); 1.390(2)	[123]
$BF_3{\cdot}$c,c,c,c-[4.5.5.5]-1-Azafenestrane	1.597(7)	1.375(7); 1.395(7); 1.400(7)	[124]
$2BF_3{\cdot}$1,3-dimethyl-1,3-diazolidine	1.650 (2); 1.651(2)	1.372–1.387(2)	[125]
$BF_3{\cdot}$quin	1.601(7)	1.364(4); 1.392 (8)	[126]
$BF_3{\cdot}$imidazole	1.544(7)	1.379(9); 1.378(8); 1.354(9)	[127]
$BF_3{\cdot}$1-[bis(diisopropylamino)boryl]imidazole	1.579(2); 1.575(2)	1.356(2); 1.403(3); 1.353(2) 1.388(2); 1.365(2); 1.371(2)	[128]
$BF_3{\cdot}$8-(2,6-dimethyllpiperidino)-2-methyl-1,9-diaza-8-borabicyclo[4.3.0]nonan	1.66(1)	1.37(1); 1.37(1); 1.38(1)	[129]
$S(pz{\cdot}BF_3)_2$	1.629(3); 1.601(2)	1.354(3)–1.377(3)	[130]
$BF_3{\cdot}N(SiMe_3)PEt_3$	1.578(3)	1.399(3); 1.397(2); 1.380(3)	[131]
$BF_3{\cdot}NHPPh_3$	1.504(8)	1.417(6); 1.394(5); 1.379(6)	[132]
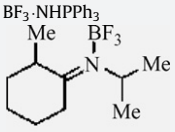 **25**	1.630(2)	1.376(2); 1.372(2); 1.379(2)	[133]
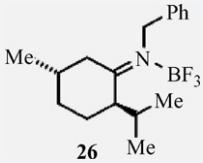 **26**	1.621(3)	1.374(3; 1.368(3); 1.370(3)	[133]
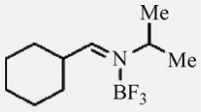 **24**	1.619(2)	1.376(2); 1.366(2); 1.368(2)	[133]
$BF_3{\cdot}NH_2CH_2C_6H_5$	1.60(1)	1.31(2); 1.37(1); 1.46(1)	[391]
$BF_3{\cdot}OH_2$	1.532(6)	1.382; 1.383; 1.399(6)	[109]
$BF_3{\cdot}O(CH_3)H$	1.524(4)	1.355; 1.357; 1.399(4)	[109]
$BF_3{\cdot}$(S,S)-1-Oxo-2,5-trans-diphenylphospholane	1.481(11)	1.359(14); 1.370(16); 1.48(2)	[135]
$BF_3{\cdot}$(E)-3-diethylamino-3-phenyl-2-propenal	1.496(3)	1.370(3)–1.382(3)	[136]
$BF_3{\cdot}$2-methylacrolein	1.587(8)	1.324(11); 1.366(11); 1.369(10)	[137]
$BF_3{\cdot}$diphenyl-2-hydroxy-3,5-di-*tert*-butylphenyl phosphinate	1.528(3)	1.352(4); 1.366(4); 1.389(4)	[138]
$BF_3{\cdot}$dibenzylidene acetone	1.533(4)	1.364(4); 1.372(4); 1.381(4)	[139]
$BF_3{\cdot}$benzylidene acetone	1.5579(18)	1.3538(18); 1.3594(19); 1.3692(19)	[139]
$BF_3{\cdot}$methyl cinnamate	1.5559(17)	1.3504(19); 1.3505(18); 1.3525(19)	[139]
$BF_3{\cdot}O{=}CHPh$	1.591(6)		[140]
$BF_3{\cdot}O{=}PPh_3$	1.516(6)	1.357(5); 1.353(6); 1.334(6)	[141]
$BF_3{\cdot}O{=}AsPh_3$	1.486(5)	1.354(5); 1.362(5); 1.352(5)	[141]
$BF_3{\cdot}$1,3-Dimesitylimidazol-2-ylidene	1.635(5)	1.323	[142]
$BF_3{\cdot}$4,5-dichloro-1,3-dimesitylimidazol-2-ylidene	1.669(6)	1.365	[142]
$BF_3{\cdot}$dimethylsulfoxonium methylide $BF_3{\cdot}CH_2S(O)Me_2$	1.650(2)	1.394(2); 1.400(2); 1.400(2)	[143]
Bis-[2-(2-(trifluoroborane)-3-methylimidazolin-2-yliden-1-yl)ethyl]ether	1.644(2)	1.382(2)–1.3944(16)	[144]
$BF_3{\cdot}C(NMe^tBu)$anthryl	1.688(3)	1.372(3); 1.373(3); 1.384(3)	[145]
$BF_3{\cdot}$carbene $(C(NMe)_2(CMe)_2)$ 2,3,4,5-Tetramethylimidazol-2-ylidene	1.638(6); 1.654(6)	1.386(5); 1.387(6); 1.394(6); 1.381(6); 1.387(5); 1.393(5)	[146]
$BF_3{\cdot}PEt_3$	2.0280(14)	1.378(2); 1.383(2); 1.384(2)	[147]
$BCl_3{\cdot}NH_3$	1.579(4)	1.830(4); 1.847(4); 1.834(3)	[148]
$BCl_3{\cdot}NMe_3$	1.610(6)		[88]
$BCl_3{\cdot}NMe_3$	1.611	1.836; 1.847	[149]
$BCl_3{\cdot}NMe_3$	1.575(11)	1.831(10) (1.827; 1.839)	[150]
$BCl_3{\cdot}NMe_2F$	1.631(7)	1.77(2); 1.827(5); 1.87(2)	[151]
$BCl_3{\cdot}NMe_2Cl$	1.670(30)	1.830(20)	[152]
$BCl_3{\cdot}Py$	1.592(3)	1.835; 1.836; 1.839 (3)	[153]

Table 2 (*Continued*)

Complex	*r*(E–D), Å	*r*(E–X), Å	Ref.
BCl_3·NCMe	1.562(8)	1.826(7); 1.825(4)	[120]
BCl_3·2-Cl-l,3-dimethyl-1,3,2-diazaborolidin	1.600(7); 1.575 (10)	1.828(7); 1.845(7); 1.852(6); 1.783(7); 1.835(7); 1.842(8)	[154]
BCl_3·imidazole	1.543 (3)	1.847(2); 1.848(2); 1.865(2)	[155]
BCl_3·OEt_2	1.5430(19)	1.8292(18); 1.8250(17); 1.8361(18)	[156]
BCl_3·O=P$(OPh)_3$	1.511(5)	1.821(4); 1.834(5); 1.818(5)	[157]
BCl_3·9-fluorenone	1.514(4)	1.811(7); 1.833(5); 1.836(4)	[217]
BCl_3·PMe_3	1.957(5)	1.855(5)	[159]
BCl_3·P$(SiMe_3)_3$	2.022(9)	1.841(9); 1.845(9); 1.857(9)	[160]
BCl_3·PVi_3	1.970(2)	1.841(3); 1.845(2); 1.847(2)	[147]
BCl_3·PPh_3	2.006(3)	1.835(3); 1.837(3); 1.852(3)	[161]
BCl_3·$PPhMe_2$	1.963(2)	1.836(2); 1.838(2); 1.839(2)	[161]
Cl_3B·P$(Ph)_2CH_2(Ph)_2$P·BCl_3	1.980(3); 1.995(3)	1.835–1.850(3)	[161]
BCl_3·As$(SiMe_3)_3$	2.118(6)	1.822; 1.837; 1.838(7)	[162]
BCl_3·$AsMe_3$	2.065(6)	1.828(7); 1.830(4)	[164]
BCl_3·SC_4H_8	1.960(3)	1.820(3); 1.828; 1.832(3)	[165]
BBr_3·NMe_3	1.603(20)		[88]
BBr_3·NMe_3	1.594(8)	2.002(7); 2.021(4)	[166]
BBr_3·NMe_3	1.602	2.002; 2.035	[149]
BBr_3·Py	1.590(20)	1.990(20)	[169]
BBr_3·PMe_3	1.924(12)	2.022(7)	[159]
BBr_3·PPh_3	1.988(10)	1.978(9); 2.005(8); 2.013(9)	[168]
BBr_3·PBr_3·	2.010(20)	1.960(20); 1.990(10)	[170]
BBr_3·P$(SiMe_3)_3$	1.998(21)	1.995(20); 2.020(18); 2.035(20)	[160]
BBr_3·PVi_3	1.952(2)	2.004(2); 2.005(2); 2.009(2)	[147]
BBr_3·$PHPh_2$	1.965(4)	1.997(4); 2.010(4); 2.013(4)	[171]
BBr_3·$PMePh_2$	1.976(9)	2.004(11); 2.010(11); 2.046(12)	[171]
BBr_3·P^nPr_3	1.95(1)	2.009(3)	[172]
BBr_3·PI_3	2.01(1)	1.987(6); 2.00(1)	[172]
BBr_3·$AsMe_3$	2.04(1)	1.99(1); 2.02(1)	[164]
BBr_3·SC_4H_8	1.966(13)	1.954(12); 1.998(6)	[165]
BBr_3·C{N(^{i}Pr)C(CH_3)}$_2$	1.623(7)	2.013(5); 2.021(5); 2.029(6)	[173]
BI_3·NMe_3	1.584(25)		[88]
BI_3·NMe_3	1.584	2.260; 2.273	[149]
BI_3·PMe_3	1.918(15)	2.249(12)	[159]
BI_3·PVi_3	1.944(4)	2.226(5); 2.228(4); 2.232(4)	[147]
BI_3·As$(SiMe_3)_3$	2.104(15)	2.216; 2.231; 2.262(14)	[162]
BI_3·$AsMe_3$	2.030(10)	2.22(1); 2.23(1)	[164]
BI_3·SC_4H_8	1.920(10)	2.220(20); 2.240(20)	[165]
$AlCl_3$·NH_3	1.921(3)	2.108(1); 2.110(1); 2.115(1)	[46]
$AlCl_3$·NMe_3	1.960(10)	2.110–2.140(10)	[167]
$AlCl_3$·NMe_3	1.949	2.110; 2.121	[174]
$AlCl_3$·NH$(SiMe_3)_2$	1.939(3)	2.115(2); 2.118(1); 2.122(2)	[175]
$AlCl_3$·NHCPhNH^{t}Bu, N-*tert*-butylbenzamidine	1.869(3)	2.123(1); 2.124(1)	[176]
$AlCl_3$·NPhP$(NEt_2)_2$Cl	1.873(2)	2.115(1); 2.119(1); 2.121(1)	[177]
$AlCl_3$·$NHPh_2$	1.983(4)	2.090(3); 2.130(2)	[178]
$AlCl_3$·NH_2^{t}Bu	1.936(4)	2.111(2); 2.120(2); 2.104(2)	[179]
$AlCl_3$·quin	1.959(6)	2.096(4); 2.104(4); 2.105(4)	[180]
$AlCl_3$·Py	1.930(2)	2.1236(9); 2.1261(9); 2.1165(9)	[181]
$AlCl_3$·mpy	1.942(4)	2.109(1); 2.112(4)	[180]
$AlCl_3$·dpmpy	1.954(4)	2.082(2); 2.093(2); 2.100(2)	[180]
$AlCl_3$·dmap	1.900(5); 1.902(8)	2.102–2.128(3)	[182]
$AlCl_3$·tmpH	2.014(2)	2.129(1); 2.136(1)	[183]
$AlCl_3$·N$(SnMe_3)_3$	1.872(12)	2.138(6); 2.124(6); 2.159(6)	[184]
$AlCl_3$·N$(SiMe_3)$BN$(SiMe_3)_2$	1.885(2)	2.133(1); 2.130(1); 2.111(1)	[185]
$AlCl_3$·N$(SiMe_3)$P^iPr_3	1.902(2)	2.1313(12); 2.1372(13); 2.1481(13)	[186]
$AlCl_3$·N$(SiMe_3)PCl_3$	1.942(6)	2.135(3); 2.137(3); 2.138(3)	[187]
$AlCl_3$·N$(SiMe_3)$BN$(SiMe_3)$^{t}Bu	1.886(2)		[185]
$AlCl_3$·NH=CMe_2	1.898(3)	2.1179(8); 2.1197(12)	[188]
$AlCl_3$·N(^{t}Bu)Si^tBu_2, additional Cl–Si interaction	1.809(3)	2.106(2) 2.112(2); 2.318(2) Si–Cl: 2.2315(14)	[188]
$AlCl_3$·NMe_2Si$(NMe_2)_2$Cl	1.990(5); 1.972(5)	2.115 (3) 2.111 (3) 2.112 (3); 2.130 (3) 2.118 (3)	[189]
$AlCl_3$·$C_3N_3Cl_3$	2.042(3); 2.067(4)	2.096(2)–2.120(2)	[190]
$AlCl_3$·$[PCl_2{}^{15}N]_3$	1.977(5); 1.978(5)	2.107–2.110(2)	[191]
$AlCl_3$·5-methyl-1,3,5-dithiazinane	1.993(5)	2.101(3); 2.110(3); 2.112(3)	[192]
$AlCl_3$·P$(SiMe_3)_3$	2.392(4)	2.125(4); 2.118(3); 2.112(4)	[193]
$AlCl_3$·THF	1.798(6)	2.095(3); 2.098(4)	[180]
$AlCl_3$·O$C(NMe_2)_2$	1.769(2)	2.123(2); 2.128(2)	[194]
$AlCl_3$·O=CClPh (preliminary report)	1.84	2.10–2.13	[195]
$AlCl_3$·O=CClPh	1.819(5)	2.079(2); 2.094(3)	[196]
$AlCl_3$·O=CClEt	1.847(6)	2.094(3); 2.092(3); 2.094(4)	[197]
$AlCl_3$·O=C(OEt)Ph	1.761(3)	2.110(2); 2.102(2)	[198]
$AlCl_3$·O=PCl_3	1.780(4)	2.093(2); 2.103(2)	[56]
$AlCl_3$·O=PPh_3	1.733(4)	2.099(2)	[199]
$AlCl_3$·O=P($N^i$$Pr_2$)CHMeCHCHNN$Me_2$	1.748(1)	2.117(1); 2.120(1); 2.112(1)	[200]
$AlCl_3$·2-isocyanatobenzoylchloride	1.786(2)		[201]
$AlCl_3$·9-fluorenone	1.787(3)	2.097(2); 2.109(2); 2.117(2)	[158]
$AlCl_3$·xanthenone	1.764(6)	2.118(4); 2.098(4); 2.116(4)	[158]
$AlCl_3$·dibenzosuberenone	1.762(9)	2.102(5); 2.111(3)	[158]

Table 2 (*Continued*)

Complex	r(E–D), Å	r(E–X), Å	Ref.
$AlCl_3$·*o*-$CH_3C_6H_4COCl$	1.824(4)	2.087(2); 2.093(2); 2.104(1)	[202]
$AlCl_3$·*m*-$CH_3C_6H_4COCl$	1.835 (2)	2.091(1); 2.098(2)	[202]
$AlCl_3$·*p*-$CH_3C_6H_4COCl$	1.828 (2)	2.098(1); 2.100(1); 2.113(1)	[202]
$AlCl_3$·S=PPh_3	2.297(2)	2.107(2); 2.115(2); 2.120(2)	[203]
$AlCl_3$·S=$PCl(N^iPr_2)_2$	2.291(7)	2.100(7); 2.110(7); 2.123(7)	[204]
$AlCl_3$·1,3,4,5-tetramethylimidazole-2(3*H*)-thione	2.2661(13)	2.1242(12); 2.1300(13); 2.1318(12)	[205]
$AlCl_3$·Se=PPh_3	2.452(2)	2.113(3); 2.117(3); 2.119(3)	[203]
$AlCl_3$·1,3,4,5-tetramethylimidazole-2-ylidene	2.009(5)	2.121(5); 2.131(3); 2.134(4)	[205]
$AlCl_3$·[η^1-N-{E,Z-N,N′-bis(2,6-diisopropylphenyl)1,4-diazadiene}]	1.965(2)	2.0996(1); 2.1010(12); 2.1144(11)	[206]
$AlCl_3$·[η^1-N-{E,E-N,N′-bis(2,6-diisopropylphenyl)1,4-diazadiene}]	1.973(4)	2.0893(19); 2.117(2)	[206]
$2AlCl_3$·[η^2-N,N′-{E,E-N,N′-bis(2,6-diisopropylphenyl)-1,4-diazadiene}]	2.003(5)	2.096(2); 2.100(2); 2.104(3)	[206]
$2AlCl_3$·$(Ph_2PN)_2$	1.883(2)		[207]
$2AlCl_3$·$[Ph(Cl)PN]_2$	1.900(2)		[207]
$2AlCl_3$·$(Ph_2PO)_2CH_2$	1.756(5)	2.072(4); 2.116(3); 2.133(4)	[208]
$3AlCl_3$·1,3,5-$C_6H_3(COOMe)_3$	1.789(3); 1.786(3); 1.773(3)	2.073(2)–2.102(2)	[209]
$2AlCl_3$·$C_2H_4(CO_2Et)_2$	1.794(4); 1.803(4)	2.104(2); 2.092(2); 2.090(2); 2.102(3); 2.102(3); 2.088(3)	[210]
$AlCl_3$·$MeNO_2$	1.867(2)	2.103(2); 2.096(1)	[211]
$AlCl_3$·$PhNO_2$	1.856(5)	2.091(3); 2.081(3); 2.093(3)	[211]
$AlCl_3$·OEt_2	1.830(2)	2.0872(12); 2.1212(10); 2.1422(13)	[212]
$AlBr_3$·NH_3	1.925(17); 1.918(17)	2.25–2.275(6)	[46]
$AlBr_3$·$B_3N_3Me_6$	2.011(8)	2.282(3); 2.268(3); 2.273(4)	[213]
$AlBr_3$·NEt_3	1.973(8)	2.290	[214]
$AlBr_3$·tmpH	2.009(5)	2.280(2); 2.283(2); 2.300(2)	[183]
$AlBr_3$·5-methyl-1,3,5-dithiazinane	1.982(5)	2.270(2); 2.272(2)	[192]
$2AlBr_3$·$[N_2Se_2]$	1.92(2)		[215]
cis-[(^{t}BuNH)(PN^tBu)(^{t}BuN·$AlBr_3$){P(H)N^tBu}]	1.901(4)	2.2827(14); 2.3133(14); 2.2990(13)	[216]
$AlBr_3$·$P(SiMe_3)_3$	2.391(6)	2.287(5); 2.290(5); 2.288(5)	[193]
$AlBr_3$·O=PPh_3	1.736(7)	2.245(2); 2.287(2)	[199]
$AlBr_3$·9-fluorenone	1.756(9)	2.239(4); 2.253(4); 2.256(4)	[217]
$AlBr_3$·THF	1.823(8)	2.262(4); 2.264(2)	[218]
$AlBr_3$·OPh_2	1.8905(8)	2.2688(9)	[219]
$AlBr_3$·diglyme	1.933(9); 1.943(6)	2.377(3); 2.481(1)	[220]
$AlBr_3$·1,3-diox	2.052(4)	2.284(3); 2.307(1)	[220]
$AlBr_3$·H_2S	2.40	2.34	[221]
AlI_3·NH_3	1.957(19)	2.481(6); 2.499(6); 2.504(6)	[46]
AlI_3·tmpH	2.038(9)	2.532(3); 2.535(3); 2.540(3)	[183]
AlI_3·isoquin	1.947(9)	2.500(4); 2.508(4); 2.510(4)	[222]
AlI_3·AisoH, H[MeC(N{2,6-^{i}Pr$_2$C$_6$H$_3$})$_2$]	1.935(6)	2.473(2); 2.530(2); 2.531(2)	[223]
GaF_3·NH_3[b]	1.842(14)	1.928(12); 1.9241(6); 1.9336(9)	[51]
$GaCl_3$·$N(SnMe_3)_3$	1.950(7)	2.180(3); 2.183(3); 2.190(3)	[184]
$GaCl_3$·$[PCl_2{}^{15}N]_3$	2.048(3); 2.049(3)	2.1425(10)–2.1505(10)	[191]
$GaCl_3$·N_4PMes*, Mes* = 2,4,6-^{t}Bu$_3$C$_6$H$_2$	1.990(4)	2.136(1); 2.146(1)	[15]
$GaCl_3$·N_3P_2Mes*	1.9830(5)	2.1359(6); 2.1501(6); 2.1550(7)	[17]
$GaCl_3$·$Me_3B_3N_3Me_3$	2.064(4)	2.146; 1.150; 2.162(2)	[224]
[$GaCl_3${2,6-(2,4,6-^{i}Pr$_3$C$_6$H$_2$)$_2$C$_5$H$_3$N}]	2.0563(15)	2.1530(5); 2.1598(6); 2.1725(5)	[225]
$GaCl_3$·2-Chlor-l,3-dimethyl-1,3,2-diazaborolidin	2.018(3)	2.149(1); 2.156(1)	[226]
$GaCl_3$·NCMe	1.9676(18)	2.1379(7); 2.1432(5)	[227]
$GaCl_3$·$NH(SiMe_3)_2$	2.011(4)	2.099(2); 2.169(2); 2.1869(18)	[7]
$GaCl_3$·NH^iPr_2	2.000(3)	2.146; 2.154; 2.178(1)	[50]
$GaCl_3$·(3,5-Me_2-Py)	1.968(1)	2.1517(5); 2.1608(5); 2.1610(4)	[228]
$GaCl_3$·FisoH, H[HC(N{2,6-^{i}Pr$_2$C$_6$H$_3$})$_2$]	1.941(3)	2.1397(11); 2.1676(13); 2.1683(14)	[223]
$GaCl_3$·TMPH	2.050(7)	2.151; 2.161; 2.175(3)	[229]
$GaCl_3$·dmap	1.948(2); 1.946(3)	2.1539(9); 2.1580(10); 2.1609; 2.1614; 2.1628(7)	[230]
$GaCl_3$·Ph_2pzH, 3,5-diphenylpyrazole	1.971(2)	2.1448(13); 2.1568(17); 2.1589(15)	[231]
$GaCl_3$·bis(trimethylsilyl)sulfurdiimide	1.965(2)	2.1597(9); 2.1643(8); 2.166(1)	[16]
$2GaCl_3$·3,3,5,5-tetramethyl-4,3,5,1,2,6-oxadisilathiadiazine	2.073(2)	2.127; 2.130; 2.152(1)	[16]
$2GaCl_3$·$(Ph_2PN)_2$	1.937(4)		[207]
$GaCl_3$·Hbta	1.968(2)	2.137; 2.147; 2.167 (1)	[232]
$GaCl_3$·PPh_3	2.3717(16)	2.1677; 2.1679; 2.1696(15)	[233]
$GaCl_3$·PEt_3	2.3531(5)	2.1746(5); 2.1756(5); 2.1836(5)	[234]
$GaCl_3$·PCl^iPr_2	2.380(10); 2.400(10)	2.140(20); 2.150(10)	[235]
$GaCl_3$·$P(SiMe_3)_3$	2.379(5); 2.380(5)	2.169(4); 2.176(4)	[236]
$GaCl_3$·PMe_3	2.353(2)	2.171(2); 2.176(2)	[237]
$GaCl_3$·Ph_2PPPh_2·$GaCl_3$	2.4285(6)		[238]
$GaCl_3$·dppe·$GaCl_3$	2.3854(8)	2.1608; 2.1620; 2.1648 (8)	[239]
$GaCl_3$·4-bis(trimethylsilyl)amino-1,2,4,3,5-triazadiphosphole	1.978(3)		[240]
$2GaCl_3$·4-bis(trimethylsilyl)amino-1,2,4,3,5-triazadiphosphole	2.035(4); 2.036(4)		[240]
$GaCl_3$·N_4AsMes*, Mes* = 2,4,6-^{t}Bu$_3$C$_6$H$_3$	1.964(2)	2.1463; 2.1499; 2.1503 (9)	[241]
$GaCl_3$·$AsMe_3$	2.4332(12)	2.1709(15); 2.1768(12); 2.1768(12)	[242]
$GaCl_3$·THF	1.919(3)	2.1388(8); 2.1405(11)	[243]
$GaCl_3$·O=PPh_3	1.818(10)	2.111(6); 2.112(6)	[199]
$GaCl_3$·O=PMe_3	1.828(6)	2.159; 2.161; 2.162(2)	[233]
$GaCl_3$·9-fluorenone	1.915(2)	2.125(1); 2.134(1); 2.143(1)	[217]
$GaCl_3$·fluorobenzoyl chloride	1.9646(13)	2.1312(4); 2.1312(4); 2.1342(5)	[244]

Table 2 (*Continued*)

Complex	r(E–D), Å	r(E–X), Å	Ref.
$[(GaCl_3)_2\{\mu\text{-}o\text{-}C_6H_4(CH_2SMe)_2\}]$	2.3573(15)	2.1478(14); 2.1530(16); 2.1650(15)	[245]
$[(GaCl_3)_2\{\mu\text{-}PhS(CH_2)_2SPh\}]\cdot$	2.3892(11)	2.1492(12); 2.1509(12); 2.1473(11)	[245]
$[GaCl_3(SeMe_2)]$	2.4637(7)	2.1700(10); 2.1606(8)	[245]
$[(GaCl_3)_2\{\mu\text{-}^nBuSe(CH_2)_2Se^nBu\}]$	2.4683(11)	2.1624(17); 2.1658(16); 2.1491(17)	[245]
$GaCl_3\cdot$IPr (1,3-bis(2,6-diisopropylphenyl)imidazol-2-ylidene)	2.016(2)	2.173(5); 2.179(5); 2.177(6)	[246]
$GaCl_3\cdot$IMes (1,3-dimesitylimidazol-2-ylidene)	1.954(4)	2.1674(8); 2.1674(10); 2.1910(8)	[246]
$GaCl_3\cdot$IPrMe (1,3-diisopropyl-4,5-dimethylimidazol-2-ylidene)	2.011(4)	2.203(10); 2.197(11); 2.198(11)	[246]
$GaCl_3\cdot$PHC (Bertrand carbene)	1.994(4)	2.1561(15); 2.1787(15); 2.1836(13)	[247]
$GaCl_3\cdot CP(2,4,6^tBu_3C_3H_2)NC(Me)P(2,4,6^tBu_3C_3H_2)$			
$GaBr_3\cdot NH_3$	1.980(4) 1.974(4)	2.2908(7); 2.3027(7); 2.3032(7); 2.2989(7); 2.3006(7); 2.3068(7)	[47]
$GaBr_3\cdot N(SnMe_3)_3$	1.95385(16)	2.342(3)	[184]
$GaBr_3\cdot PPh_3$	2.3848(13); 2.3879(13)	2.3048–2.3212(7)	[233]
$GaBr_3\cdot P(SiMe_3)_3$	2.362(4)	2.315(2)	[236]
$GaBr_3\cdot Et_2P(CH_2)_2PEt_2\cdot GaBr_3$	2.3614(13)	2.3033(8); 2.3226(8); 2.3246(8)	[242]
$2GaBr_3\cdot$dppe dppe = $Ph_2PCH_2CH_2PPh_2$	2.4002(8)	2.2936(6); 2.3031(5); 2.3125(5)	[248]
$GaBr_3\cdot AsMe_3$	2.438(2)	2.3154(19); 2.3226(15); 2.3226(15)	[242]
$GaBr_3\cdot$9-fluorenone	1.936(4)	2.280(1); 2.283(1); 2.288(1)	[217]
$[GaI_3\{$*trans*-(EtO)C(O)C(H)C(H)Ph$]$	1.966(8)	2.5071(15); 2.5113(15); 2.5130(15)	[249]
$GaI_3\cdot As(SiMe_3)_3$	2.423(7)	2.524; 2.528; 2.552 (6)	[250]
$GaI_3\cdot MeS(CH_2)_2SMe\cdot GaI_3$	2.4048(12)	2.5054(7); 2.5316(7); 2.4997(7)	[245]
$GaI_3\cdot SeMe_2$	2.479(2)	2.5209; 2.5222; 2.5277(2)	[6]
$[GaI_3)_2\{o\text{-}C_6H_4(CH_2PPh_2)_2\}]$	2.3872(9); 2.3891(9)	2.5143–2.5516(5)	[233]
$[(GaI_3)_2\{\mu\text{-}Et_2P(CH_2)_2PEt_2\}]$	2.3769(15)	2.5200(10)–2.5418(9)	[242]
$GaI_3\cdot AsMe_3$	2.4593(13)	2.5300(11); 2.5344(9); 2.5344(9)	[242]
$GaI_3\cdot PPh_3$	2.413(4)	2.518(2)	[251]
$GaI_3\cdot PPh_3$	2.416(5)	2.5212(9)	[252]
$GaI_3\cdot P(SiMe_3)_3$	2.347(4)	2.564(2)	[236]
$GaI_3\cdot$dppe$\cdot GaI_3$	2.404(9); 2.410(9)	2.481(5)–2.533(5)	[252]
$GaI_3\cdot AsPh_3$	2.490(1)	2.509(1)	[251]
$[(GaI_3)_2\{\mu\text{-}Ph_2As(CH_2)_2AsPh_2\}]$	2.4875(10) 2.4885(10)	2.4944(9)–2.5329(9)	[242]
$GaI_3\cdot As(p\text{-}MeOC_6H_4)_3$	2.509(3)	2.505(1)	[253]
$InCl_3\cdot N(SnMe_3)_3$	2.148(6)	2.3652(15)	[184]
$InCl_3\cdot$tris(2,4,6-trimethoxyphenyl)phosphine	2.5281(5)	2.3870(6); 2.4029(6); 2.4056(6)	[254]
$[InCl_3\{CN(Mes)C_2H_2N(Mes)\}]$	2.200(7)	2.355(2); 2.349(2); 2.353(2)	[255]
$InBr_3\cdot N(SnMe_3)_3$	2.158(8)	2.5081(9)	[184]
$InBr_3\cdot$IPr, 1,3-bis(2,6-diisopropylphenyl)imidazol-2-ylidene	2.212(8)	2.4935(14); 2.5000(12); 2.4999(13)	[256]
$InBr_3\cdot$IMes, 1,3-bis(2,4,6-trimethylphenyl)imidazol-2-ylidene	2.195(5)	2.4994(8); 2.4935(8); 2.4947(9)	[256]
$InBr_3\cdot CN(^iPr)C_2Me_2N^iPr$	2.199(5)	2.4915(6); 2.5030(6); 2.5063(7)	[257]
$InBr_3\cdot NH_2SiMe_3$	2.210(9)	2.475(2); 2.474(2); 2.485(2)	[258]
$InI_3\cdot PPh_3$	2.603(7)	2.677(1)	[260]
$InI_3\cdot PHPh_2$	2.592(9); 2.605(9)	2.665(5)–2.676(5)	[259]
$InI_3\cdot PH^tBu_2$	2.586(6)	2.679(3); 2.668(2)	[259]
$InI_3\cdot P^iPr_3$	2.569(7)	2.689(3); 2.701(3); 2.705(3)	[261]
$InI_3\cdot P(SiMe_3)_3$	2.537(3)	2.6975(14); 2.6914(16); 2.7252(15)	[10]
$InI_3\cdot O_2C_{13}H_8$ (9-xanthenone)	2.1872(6)	2.654(2); 2.6572(8); 2.672(1)	[262]
$InI_3\cdot AsPh_3$	2.7238(13)	2.6811(6)	[251]
$InI_3\cdot$dppe	2.5871(12)	2.7003(5); 2.7061(5); 2.7420(6)	[248]
$2InI_3\cdot$dppe	2.6035(12); 2.5966(12)	2.6523(6); 2.6833(5); 2.7023(6); 2.6843(6); 2.6773(5); 2.6685(5)	[263]
$2InI_3\cdot$dppeS_2	2.5322(13)	2.6859(5); 2.6901(6); 2.6733(5)	[263]

[a] Neutron diffraction.
[b] Octahedral geometry, coordination polymer.

Table 3
Comparison of structural properties of some EX_3 adducts in gas and crystal state.

Complex	r(E–D)gas, Å	r(E–D)solid, Å	Δr(E–D) (gas)–(solid)	Δr(E–D)/r(E–D)gas, %
$BF_3\cdot HCN$	2.473(29)	1.638(2)	0.835(31)	33.8
$BF_3\cdot CH_3CN$	2.011(7)	1.630(4)	0.381(11)	18.9
$BF_3\cdot NH_3$	1.590(30)	1.579(2)	0.011(32)	0.7
$BF_3\cdot NMe_3$	1.664(11)	1.585(30)	0.079(41)	4.7
$BF_3\cdot NMe_3$	1.636(4)	1.585(30)	0.051(34)	3.1
$BF_3\cdot$Py	1.669(7)	1.604(5)	0.065(12)	3.9
$BCl_3\cdot NMe_3$	1.659(6)	1.575(11)	0.084(17)	5.1
$BCl_3\cdot$Py	1.706(12)	1.592(3)	0.114(15)	6.7
$BCl_3\cdot PMe_3$	1.941(16)	1.957(5)	−0.016(21)	−0.8
$BBr_3\cdot NMe_3$	1.663(13)	1.594(8)	0.069(21)	4.1
$BBr_3\cdot$Py	1.694(17)	1.590(20)	0.104(37)	6.1
$BBr_3\cdot PMe_3$	1.946(29)	1.924(12)	0.022(41)	1.1
$AlCl_3\cdot NH_3$	1.996(19)	1.921(3)	0.075(22)	3.8
$AlCl_3\cdot NMe_3$	1.945(35)	1.960(10)	−0.015(45)	−0.8
$AlBr_3\cdot NH_3$	1.997(19)	1.925(17)	0.072(36)	3.6
$GaBr_3\cdot NH_3$	2.081(23)	1.980(4)	0.101(27)	4.9

Table 4
Structural properties of EX_3·2D adducts with CN. 5.

Complex	r(E–D), Å	r(E–X), Å	Ref.
$AlCl_3$·2NMe_3	2.1580(16); 2.1662(16)	2.1676(10); 2.1725(5)	[264]
$AlCl_3$·2$NHMe_2$	2.051(3); 2.071(3)	2.173–2.178(1)	[265]
$AlCl_3$·2$NHMe_2$	2.066(3); 2.058(3); 2.060(3); 2.078(3)	2.182(2); 2.188(2); 2.190(2); 2.172(2); 2.180(2); 2.182(2)	[266]
$AlCl_3$·2morph	2.064 (3); 2.093 (3)	2.173(1); 2.197(1); 2.181(1)	[267]
$AlCl_3$·2pip	2.070(5)	2.163(2); 2.174(2); 2.190(2)	[180]
$AlCl_3$·2THF	1.990(1)	2.163(1); 2.154(1)	[268]
$AlBr_3$·2(9-fluorenone)	1.907(6); 1.913(7)	2.304(3); 2.312(3); 2.323(3)	[217]
AlI_3·2PEt_3	2.520(4); 2.528(4)	2.598(3); 2.613(3); 2.619(3)	[269]
$GaCl_3$·2(Hbta)	2.169(2)	2.178; 2.204(2)	[232]
$GaBr_3$·2THF	2.141(2)	2.3174(4); 2.3303(6)	[270]
$InCl_3$·2NMe_3	2.320(20); 2.345(19)	2.376(4); 2.343(8)	[271]
$InCl_3$·2$NH(CH_2Ph)_2$	2.310(10)	2.390(4); 2.395(3)	[50]
$InCl_3$·2[5-methyl-1,3,5-dithiazinane]	2.413(3)	2.376(1); 2.383(1)	[192]
$InCl_3$·2tmu	2.183(4)	2.359; 2.382(2)	[272]
$InCl_3$·2tmtu	2.521(2); 2.531(2)	2.410–2.484(3)	[272]
$InCl_3$·2(S=PMe_3)	2.630(3); 2.663(3)	2.393; 2.396; 2.400(2)	[273]
$InCl_3$·2(S=$AsMe_3$)	2.594(40; 2.620(3)	2.406(3); 2.412(3); 2.417(4)	[273]
$InCl_3$·2dmit	2.516(1)	2.402(1); 2.505(1)	[274]
$InCl_3$·2HMPA HMPA: O=$P(NMe_2)_3$	2.175(10); 2.185(11)	2.371(8); 2.358(3); 2.349(7)	[275]
$InCl_3$·2THF	2.257(9)	2.312(5); 2.330(4)	[276]
$InCl_3$·2THF	2.265(5)	2.314(3); 2.339(2)	[277]
$InCl_3$·2THF	2.259(2)	2.345(1); 2.346(2)	[278]
$InCl_3$·2O=CPhMe acetophenone	2.250(2)	2.337(1); 2.363(1)	[279]
$InCl_3$·2PMe_3	2.575(3); 2.576(3)	2.503(3); 2.453(4)	[280]
$InCl_3$·2PPh_3	2.701(5); 2.723(5)	2.377; 2.382; 2.391(5)	[281]
$InCl_3$·2CN(^{i}Pr)$C_2Me_2N^i$Pr	2.220(10); 2.236(9)	2.431(2); 2.586(2); 2.578(2)	[257]
$InBr_3$·2quin	2.364(3)	2.5271(8); 2.5254(5)	[256]
$InBr_3$·N,N′-bis(2,6-diisopropylphenyl)diazabutadiene	2.332(14); 2.314(12)	2.532(2); 2.505(2); 2.539(2)	[256]
$InBr_3$·2(S=PMe_3)	2.653(3); 2.691(3)	2.524; 2.529; 2.531(3)	[273]
$InBr_3$·2(S=$AsMe_3$)	2.615(3); 2.643(3)	2.539; 2.552; 2.554(3)	[273]
$InBr_3$·2dmit	2.528(2); 2.529(2)	2.547–2.680(1)	[274]
$InBr_3$·2CN(^{i}Pr)$C_2Me_2N^i$Pr	2.230(10) 2.231(10)	2.586(6); 2.744(13); 2.737(12)	[257]
$InBr_3$·2THF	2.296(3); 2.288(3); 2.307(3); 2.285(3)	2.4901(7); 2.4839(7); 2.4770(8); 2.4914(7); 2.4811(8); 2.4818(8)	[283]
$InBr_3$·2PMe_2Ph	2.614(3); 2.622(3)	2.565(2); 2.577(2); 2.606(2)	[284]
InI_3·tmeda	2.40(2); 2.36(2)	2.744(2); 2.759(2); 2.801(2)	[282]
InI_3·2$PMePh_2$	2.712(3); 2.719(3)	2.7362(14); 2.762(2); 2.776(2)	[284]
InI_3·2PPh_3	2.86(1); 2.99(1)	2.707(1)	[260]
$[InI_3$·dppe$]_n$[a]	2.758(6); 2.769(7)	2.729(2); 2.730(3); 2.766(3)	[260]
2InI_3·3dppe	2.798(3); 2.819(2)	2.742(2); 2.739(2); 2.713(2)	[280]
InI_3·$[OP(p\text{-}Anis)_3]_2$ O=$P(p$-MeO-$C_6H_4)_3$	2.221(3)	2.7184(3)	[254]
InI_3·2(9-fluorenone)	2.33(1); 2.37(1)	2.644(2); 2.666(2); 2.684(2)	[262]
InI_3·2$AsPh_3$	2.926(2); 2.990(2)	2.7024(5)	[251]
InI_3·2$SeMe_2$	2.7916(2); 2.7951(2)	2.7313(1); 2.7416(1); 2.7490(2)	[6]

[a] Infinite chain.

to formation of ionic species. In contrast, less ionic indium complexes favor molecular structures. For example, while in case of Al and Ga ionic $[M(OC(NH_2)_2)_6]^{3+}3Cl^-$ are formed, In forms molecular adduct *fac*-$InCl_3(OC(NH_2)_2)_3$ [11]. As can be seen from Table 6, InX_3·3D complexes are quite common. Meridional and facial isomers are theoretically feasible, and for monodentate donors both cases are realized in practice (Table 6). Structures of *mer*-$InCl_3$·3THF [291] and *fac*-$InCl_3$·$3H_2O$ [608] adducts are given in Fig. 6. Donor–acceptor bond distances are summarized in Table 6. Design of the tridentate ligand allows to obtain desired *mer*-isomer in case of terpyridil ligand and *fac*-isomer in case of substituted triazacyclononane ligand.

2.2.4. Trigonal bipyramidal EX_4·D adducts

Theoretically for EX_4·D both equatorial and axial isomers are possible. Computational studies by Davydova et al. [71] indicate that structural preference depends on the ligand type. Thus, while for EX_4·NH_3 complexes only axial isomers are predicted to be true minima on PES, for EX_4·Py complexes

Table 5
Comparison of donor–acceptor bond distances in EX_3·D and EX_3·2D adducts.

Complex	r_1(E–D) in EX_3·D, Å	Mean r_2(E–D) in EX_3·2D, Å	Δr(E–D), Å	Δr(E–D)/r_1(E–D), %
$AlCl_3$·NH_3	1.960(10)	2.162(4)	0.202(14)	10.3
$AlCl_3$·THF	1.798(6)	1.990(1)	0.102(7)	5.7
$AlBr_3$·9-fluorenone	1.756(9)	1.910(10)	0.154(19)	8.8
$GaCl_3$·Hbta	1.968(2)	2.169(2)	0.201(4)	10.2
$InBr_3$·CN(^{i}Pr)$C_2Me_2N^i$Pr	2.199(5)	2.231(10)	0.032(15)	1.5
InI_3·$PPhH_3$	2.603(7)	2.930(70)	0.327(77)	12.6
InI_3·dppe	2.5871(12)	2.764(7)[a]	0.177(8)	6.8
InI_3·$AsPhH_3$	2.7238(3)	2.958(32)	0.234(32)	8.6

[a] Infinite chain $[InI_3$·dppe$]_n$.

Table 6
Structural properties of EX_3 adducts with CN. 6.

Complex	r(E–D), Å	r(E–X), Å	Ref.
mer-$GaCl_3$·terpy	2.034(7); 2.110(6); 2.115(6)	mer 2.235(3); ax 2.329(3); ax 2.403(2)	[285]
mer-$InCl_3$·3Py (and solvated Py)	2.302(7); 2.377(21)	mer 2.471(8); ax 2.476(2)	[287]
mer-$InCl_3$·terpy	2.2438(16); 2.2697(17); 2.2769(17)	mer 2.4080(5); ax 2.4735(6); 2.5155(5)	[288]
mer-$InCl_3$·2,6-bis(1-phenyliminoethyl)pyridine	2.247(2); 2.307(2); 2.338(2)	mer 2.401(1); ax 2.466(1); 2.473(1)	[85]
mer-$InCl_3$·3(4-ethylpyridine)	2.284(9); 2.293(9); 2.370(9)	2.426(7); 2.450(6); 2.475(6)	[289]
mer-$InCl_3$·2-[(2-(pyridylamino)phenylazo]pyridine	2.2684(19); 2.2577(19); 2.2220(19)	2.5775(7); 2.3876(7); 2.4968(7)	[290]
fac-$InCl_3·3H_2O$	2.191(2); 2.205(2); 2.207(2); 2.223(2); 2.217(2); 2.224(2)	2.4232(8); 2.4203(8); 2.4358(8); 2.4403(7); 2.4662(7); 2.4568(7)	[608]
mer-$InCl_3$·3THF	2.235(10); 2.304(9); 2.223(11)	mer 2.423(4); ax 2.422(4); ax 2.420(4)	[291]
mer-$InCl_3$·3THF	2.243(3) 2.318(3); 2.226(3)	mer 2.414(1); 2.405(1); 2.404(1)	[292]
fac-$InCl_3$·3DMF	2.214(3); 2.220(2); 2.241(2)	2.439(1); 2.431(1); 2.435(1)	[279]
fac-$InCl_3$·3DMA	2.217(3); 2.180(3)	2.461 (1); 2.440(1)	[279]
fac-$InCl_3$·3 O=C(H)Ph	2.277(12)	2.400(5)	[279]
fac-$InCl_3$·3 DMSO	2.191(2); 2.190(2); 2.204(3)	2.465(1); 2.449(1); 2.466(1)	[293]
mer-$InCl_3$·3 O=PMe_3	2.164(11); 2.171(7)	2.459(4); 2.478(5); 2.495(5)	[293]
fac-$InCl_3$·3 O=PMe_2Ph	2.196(7)	2.484(4)	[293]
fac-$InCl_3$·3 O=$C(NH_2)_2$	2.180(2)	2.4696(8)	[11]
fac-$InBr_3$·3 DMSO	2.199(17); 2.198(15); 2.200(14)	2.625(4); 2.579(4); 2.620(4)	[293]
fac-$InBr_3$·3DMF	2.2287(17); 2.2287(18) 2.2405(17)	2.5893(3); 2.5911(4); 2.5872(3)	[283]
fac-$InBr_3$·Me_3[9]$aneN_3$	2.355(8); 2.360(7); 2.338(7)	2.6054(11); 2.6053(11); 2.5974(11)	[283]
fac-$InBr_3$·bis(2-pyridylmethyl)amine	2.311(6); 2.328(9)	2.5682(13); 2.6060(9)	[286]
mer-$InBr_3$·3Py	2.28(3); 2.31(2); 2.32(2)	mer 2.593(3); ax 2.611(4); 2.618(4)	[294]
mer-InI_3·3Py	2.309(4); 2.323(5)	2.8676(3); 2.8390 (6)	[36]
mer-InI_3·3pic	2.28(3); 2.30(3); 2.34(2)	2.848(4); 2.893(4); 2.803(4)	[295]
mer-$TlCl_3$·3Py	2.380(12); 2.482(15)	mer 2.520(6) ax 2.498(4)	[287]

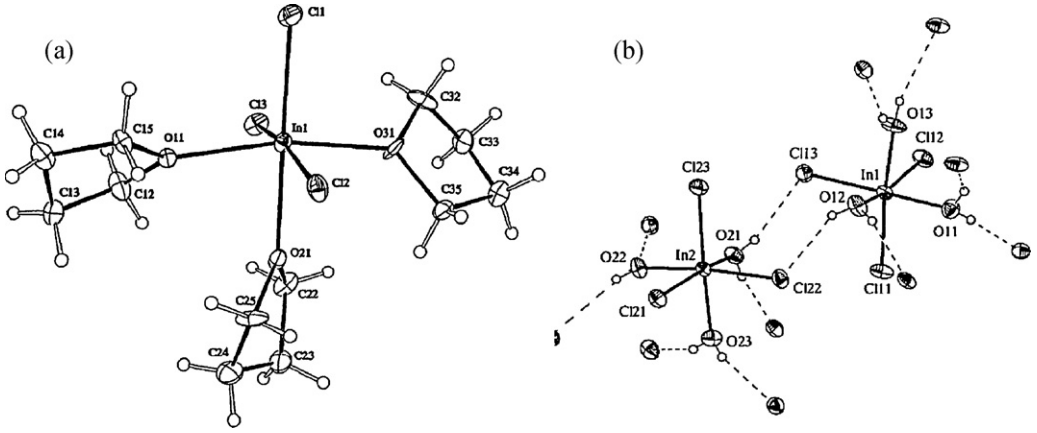

Fig. 6. Solid state structures of (a) *mer*-$InCl_3$·3THF and (b) *fac*-$InCl_3·3H_2O$. Taken from Refs. [291,608], respectively.

the equatorial isomers are more stable. With the increase of the size of the acceptor atom, the energy difference between isomers becomes smaller. Experimental structure determinations show that both isomers are experimentally realized (Table 7). Representative structures of *eq*-$TiBr_4$·(2,6-$Me_2C_5H_3N$) [302] and *ax*-SiF_4·C[N(2,6-$^iPr_2C_6H_3$)CH]$_2$ [31] adducts are given in Fig. 7 and major structural parameters are summarized in Table 7.

2.2.5. Dimeric octahedral $[EX_4·D]_2$ adducts

Since in EX_4·D the central atom has coordination number 5 and is not coordinationally saturated, these adducts can easily dimerize

Table 7
Structural properties of EX_4·D adducts.

Complex	r(E–D), Å	r(E–X_{eq}), Å	r(E–X_{ax}), Å	Ref.
ax-SiF_4·C[N(2,6-$^iPr_2C_6H_3$)CH]$_2$	2.004(2)	1.5736(15); 1.5730(17); 1.5836(17)	1.6462(13)	[31]
eq-$SiCl_4$·C[N(Et)CMe]$_2$ 1,3-diethyl-4,5-dimethylimidazol-2-ylidene)	1.911(7)	2.045(5); 2.070(5)	2.225(4); 2.219(4)	[298]
eq-$SiCl_4$·(C{N(2,6-$^iPr_2C_6H_3$)CH}$_2$)	1.928(2)	2.0696(6)	2.1892(5	[299]
eq-$SiCl_4$·O=$C(NMe_2)_2$	1.696(3)	2.073(3); 2.082(3)	2.176(3); 2.209(3)	[300]
eq-$SiBr_4$·C[N(2,6-$^iPr_2C_6H_3$)CH]$_2$	1.935(2)	2.2360(4)	2.4106(7); 2.3765(7)	[31]
ax-$GeCl_4$·NMe_3	2.19(3)	2.13; 2.15; 2.15(1)	2.24(1)	[301]
ax-$SnBr_4$·$AsPh_3$	2.780(1)	2.484(1); 2.486(2); 2.484(2)	2.522(2)	[8]
eq-$TiCl_4$·(2-MeC_5H_4N)	2.185(3)	2.253(1); 2.211(1)	2.289(1); 2.297(1)	[297]
eq-$TiCl_4$·(2,6-$Me_2C_5H_3N$)	2.190(2)	2.2006(9); 2.2019(8)	2.2613(8) 2.2590(8)	[297]
eq-$TiBr_4$·(2,6-$Me_2C_5H_3N$)	2.181(4); 2.176(9)	2.3585(14); 2.3564(14)	2.4326(8); 2.4372(8)	[302]
eq-$TiBr_4$·(2-MeC_5H_4N)	2.145(7)	2.3245(17); 2.3502(17)	2.4129(17); 2.4202(17)	[303]
$ZrF_4·NH_3$[a]	2.337(4); 2.359(4)	1.973(3); 1.959(3)	2.110–2.192(4)	[52]
$HfF_4·NH_3$[a]	2.290(20); 2.320(20)	1.980(20); 1.960 (20)	2.070–2.220(20)	[52]

[a] Coordination polymer, capped trigonal prism.

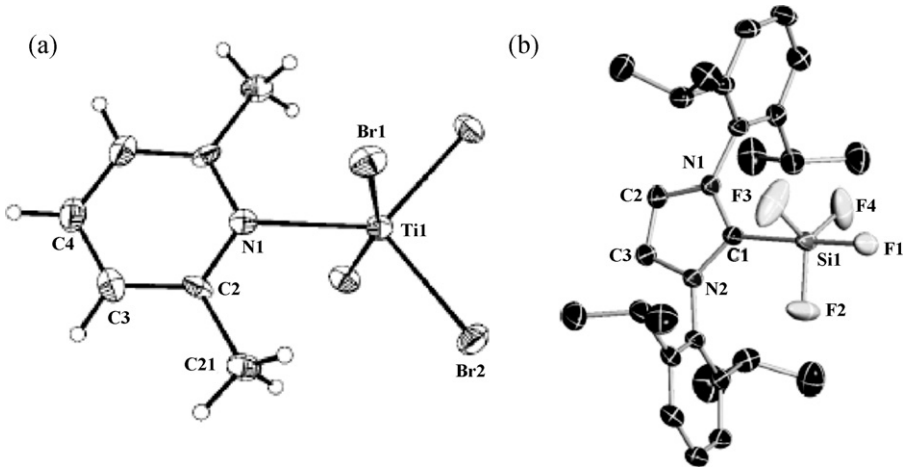

Fig. 7. Solid state structures of (a) *eq*-$TiBr_4$·(2,6-$Me_2C_5H_3N$) and (b) *ax*-SiF_4·C[N(2,6-$^i Pr_2C_6H_3$)CH]$_2$. Taken from Refs. [302,31], respectively.

to increase coordination number to 6 and form $[EX_4{\cdot}D]_2$ dimers with octahedral coordination sphere. Major structural parameters of such dimmers are summarized in Table 8, and the structure of $[TiCl_4{\cdot}CH_3CN]_2$ dimer [311] is presented in Fig. 8.

2.2.6. Octahedral EX_4·2D adducts

In these adducts the central atom achieves coordination number 6 by interaction with two donor molecules, which can be placed in *cis* or *trans* position to each other. Both *cis* and *trans* isomers are experimentally realized, as can be seen on the example of *trans*-$TiCl_4$·2(3,5-$Me_2C_3H_2N_2$) [413] and *cis*-$SnCl_4$·2CH_3CN [365] (Fig. 9). Structural parameters of compounds are summarized in Table 9. Use of the rigid bidentate ligands, such as 1,10-phen and 2,2′-bipy allows to obtain *cis* isomers.

2.2.7. Octahedral EX_5·D adducts

Group 15 element halides form molecular complexes of 1:1 composition. Representative structure of the $TaCl_5$·THF adduct is presented in Fig. 10, and E–D and E–X distances for solid adducts are summarized in Table 10. The structure may be described as slightly distorted octahedral, deviation of the EX_4 unit from planarity is usually less than 5°.

2.2.8. Use of the structural characteristics of adducts in tensimetry studies

As can be seen from Table 1 and Tables 2–10, structural data for crystalline adducts are much more abundant than for gaseous ones. It is important to understand the difference and possibility of estimation of structural characteristics of gaseous species from the

Table 8
Selected structural properties of dimeric $[EX_4{\cdot}D]_2$ adducts.

Complex	*r*(E–D), Å	*r*(E–X_{term}), Å	*r*(E–X_{bridg}), Å	Ref.
$[TiCl_4{\cdot}POCl_3]_2$	2.10(2)	2.20–2.24(1)	2.44–2.54 (0.1)	[304]
$[TiCl_4{\cdot}CH_3NO_2]_2$	2.204(6)	2.202–2.206(4)	2.471–2.478(4)	[305]
$[TiCl_4{\cdot}CH_3COOC_2H_5]_2$	2.029(3)	2.222(2)	2.498(2)	[306]
$[TiCl_4{\cdot}C_2H_5OCOC_6H_4OCH_3]_2$	1.997(6)	2.233; 2.235; 2.252(3)	2.509; 2.498(2)	[307]
$[TiCl_4{\cdot}(2,6\text{-}Me_2C_6H_3NC)]_2$	2.235(6)	2.198(1); 2.214(2); 2.208(2)	2.485(2); 2.481(2)	[308]
$[TiCl_4{\cdot}THF]_2$	2.111(3)	2.212(1); 2.225(1); 2.224(1)	2.451(1); 2.521(1)	[309]
[$TiCl_4$·acetophenone]$_2$	1.9988(14)	2.2155(5) 2.2191(5) 2.2295(6)	2.4920(5); 2.5072(5)	[244]
[$TiCl_4$·hydrindone]$_2$	2.026(2)	2.2132(12); 2.2286(11); 2.2336(11)	2.4526(10) 2.5184(11)	[244]
[$TiCl_4$·benzoyl chloride]$_2$	2.1114(13)	2.1933(5); 2.2133(5); 2.2181(5)	2.4789(5); 2.4939(5)	[244]
[$TiCl_4$·*p*-toluoyl chloride]$_2$	2.1133(10)	2.1971(5); 2.2224(4); 2.2221(5)	2.4569(5); 2.4944(5)	[244]
[$TiCl_4$·fluorobenzoyl chloride]$_2$	2.1276(9)	2.1899(4); 2.2241(4); 2.2246(4)	2.4484(4) 2.5008(4)	[244]
$2TiCl_4$·MeSSMe	2.712(3); 2.742(3)	2.184–2.200(3)	2.450–2.482(3)	[310]
$[TiCl_4(MeCN)]_2$	2.189(3)	2.2096(9); 2.209(1)	2.4832(8)	[311]
$[TiCl_4(NTMSI)]_2$	2.131(2)	2.2013(7); 2.2251(7); 2.2601(6)	2.4625(7); 2.4857(7)	[312]
α-$[TiCl_4(N_4S_4)]_2$	2.246(2); 2.267(2)	2.219(1); 2.231(1)	2.262(1); 2.312(1)	[313]
β-$[TiCl_4(N_4S_4)]_2$	2.106(4); 2.110(4)	2.216(2); 2.242(1); 2.259(2); 2.223(2); 2.229(2); 2.255(2)	2.458(2); 2.513(1); 2.503(1); 2.514(2)	[313]
$[TiCl_4(OCMe_2)]_2$, acetone	2.061(1)	2.208(1); 2.222(1); 2.230(1)	2.489(1); 2.498(1)	[314]
$[TiCl_4(OCEt_2)]_2$, diethyl ketone	2.043(2)	2.2091(14); 2.2255(13); 2.243(2)	2.4720(13); 2.4931(14)	[134]
$[TiCl_4(OCMeSPh)]_2$	2.040(3)	2.212(1); 2.198(2); 2.230(2)	2.496(2); 2.481(1)	[314]
$[TiCl_4(OSON_2S_2)]_2$	2.144(2)	2.206(1); 2.234(1); 2.190(1)	2.444(1); 2.504(1)	[315]
$[TiCl_4(EtCOOEt)]_2$	2.030(6)	2.209(2); 2.237(4); 2.227(6)	2.490(5); 2.497(2)	[316]
$[TiCl_4(OC_6H_8)]_2$	2.004	2.214; 2.217; 2.231	2.447; 2.484	[317]
$[ZrCl_4{\cdot}CH_3CN]_2$	2.308(7)	2.344(3); 2.361(2); 2.333(2)	2.602(2); 2.603(2)	[323]
$[ZrCl_4(4\text{-}ClC_6H_4NH_2)]_2$, 4-chloroaniline	2.389(2)	2.3362(9); 2.3655(8); 2.3707(8)	2.5852(8); 2.6186(8)	[318]
$[ZrCl_4THF]_2$	2.206(2)	2.3511(8); 2.364(9); 2.3691(8)	2.5751(8); 2.6228(7)	[319]
$[ZrCl_4THF]_2$	2.205(2)	2.3712(9); 2.3718(11); 2.3772(9)	2.5838(8); 2.6249(10)	[320]
$[ZrCl_4(OCClCH_3{}^tBu)]_2$, *tert*-butylacetyl chloride	2.2065(12)	2.3439(5); 2.3517(4); 2.3624(5)	2.5815(4); 2.5868(4)	[244]
[$ZrCl_4$(hydrindone)]$_2$	2.090(3)	2.3500(16); 2.3766(19); 2.3834(18)	2.6016(19); 2.6313(15)	[244]
$[ZrCl_4(MeCOO(CH_2)_5Me)]_2$	2.111(9); 2.113(9)	2.329(4); 2.342(4); 2.337(5); 2.358(3); 2.355(4); 2.361(5)	2.574(3); 2.591(3); 2.594(3); 2.601(3)	[321]
$[ZrCl_4(MeCOOEt)]_2$	2.131(5)	2.362(3); 2.379(3)	2.608(3); 2.614(3)	[322]

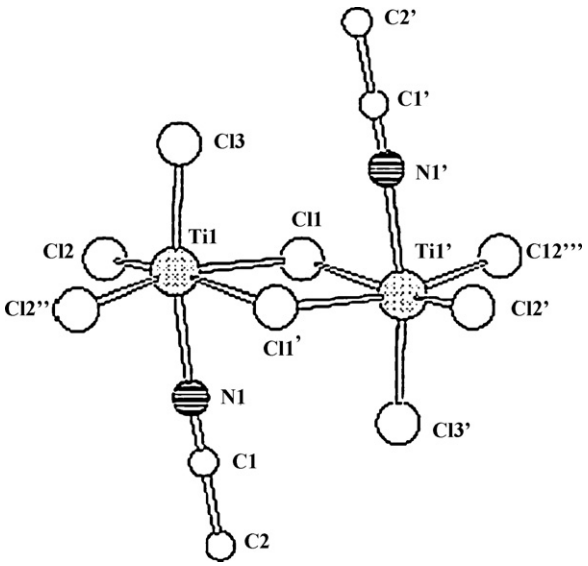

Fig. 8. Solid state structure of dimeric $[TiCl_4{\cdot}CH_3CN]_2$. Taken from Ref. [311].

structures of crystals. In studying the thermal behavior of molecular complex, structural data offer some help in interpretation of experimentally measured vapor pressure–temperature dependences.

In case of the molecular complexes (adducts) there are three major cases:

(1) Formation of crystal is based solely on Van der Waals interactions and the structure of the individual gaseous molecules is retained in the crystal. As can be seen from Table 3, the donor–acceptor bond length in crystal is by 4.3% shorter than in the gaseous adduct. In such a case the knowledge of the crystal structure of adduct allows to estimate the donor–acceptor bond length in the gas phase and (using for example ΔH–Δr correlation [28]) the possibility of adduct dissociation with donor–acceptor bond rupture.

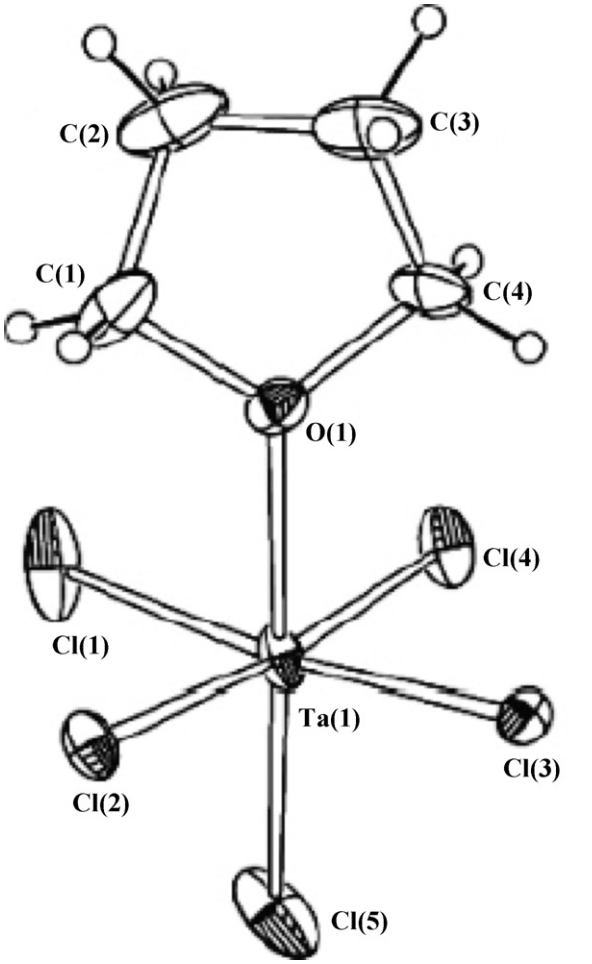

Fig. 10. Solid state structure of $TaCl_5{\cdot}THF$ adduct. Taken from Ref. [470].

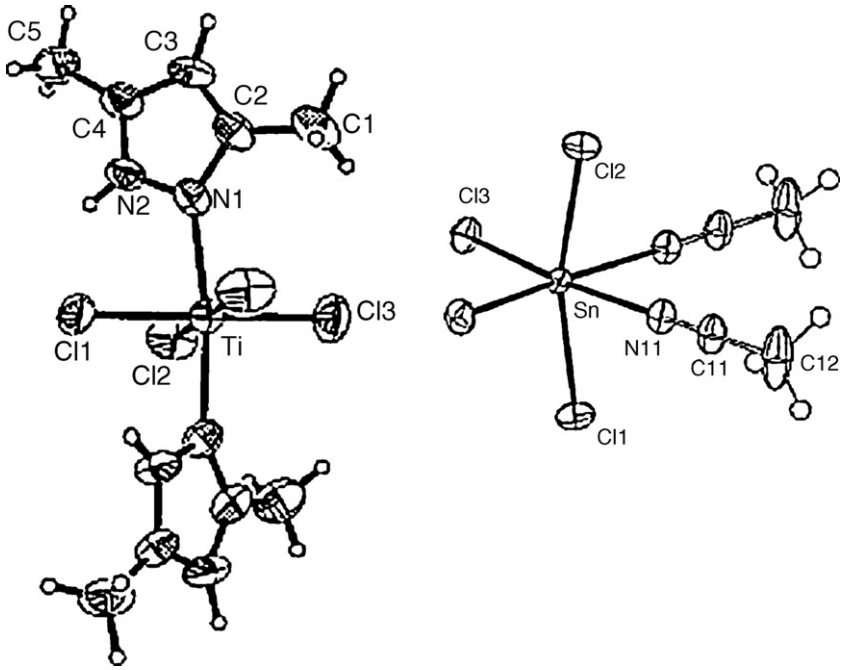

Fig. 9. Solid state structures of (a) *trans*-$TiCl_4{\cdot}2(3,5\text{-}Me_2C_3H_2N_2)$ and (b) *cis*-$SnCl_4{\cdot}2CH_3CN$. Taken from Refs. [413,365], respectively.

Table 9
Structural properties of $EX_4 \cdot 2D$ adducts.

Complex	r(E–D), Å	r(E–X_{eq}), Å	r(E–X_{ax}), Å	Ref
trans-$SiF_4 \cdot 2NH_3$	1.895(2)	1.662(2); 1.671(2)	–	[324]
trans-$SiF_4 \cdot 2NH_2Et$	1.9183(17)	1.6679(11); 1.6766(12)	–	[325]
trans-$SiF_4 \cdot 2py$	1.930(15)	1.640(15)		[326]
trans-$SiF_4 \cdot 2C[N(2,6\text{-}^iPr_2C_6H_3)CH]_2$	2.0088(14); 2.0109(15)	1.6465(17); 1.6648(17); 1.6539(17); 1.6628(16)	–	[31]
cis-$SiF_4 \cdot 2,2'\text{-bipy}$	1.972(4); 1.982(4)	1.629(3); 1.632(3)	1.654(3); 1.659(3)	[327]
cis-$SiF_4 \cdot$phen	1.9922(9)	1.6288(8)	1.6571(7)	[328]
trans-$SiCl_4 \cdot 2py$	1.976(9)	2.183(4)		[329]
trans-$SiCl_4 \cdot 2(4\text{-Me-py})$	1.9835(13)	2.2030(3)	–	[330]
trans-$SiCl_4 \cdot 2(O{=}P(NMe_2)_3)$	1.7696(11)	2.2102(5); 2.2173(6)	–	[331]
trans-$SiCl_4 \cdot 2(3,4\text{-}Me_2py)$	1.990(2)	2.2003(6)		[332]
trans-$SiBr_4 \cdot 2(3,4\text{-}Me_2py)$	1.991(3)	2.379(1)		[332]
trans-$SiBr_4 \cdot 2(4\text{-Me-py})$	1.979(4)	2.3835(3)	–	[330]
trans-$SiBr_4 \cdot 2py$	1.981(3)	2.3827(2)		[333]
trans-$SiBr_4 \cdot 2(3,5\text{-}Me_2py)$	2.005(5)	2.3763(6)		[333]
trans-$GeF_4 \cdot 2Py$	2.014(3)	1.7678(19); 1.7696(18)	–	[334]
trans-$GeF_4 \cdot 2Py$	2.011(4)	1.780(2); 1.782(3)	–	[335]
cis-$GeF_4 \cdot 2,2'\text{-bipy} \cdot CH_3NO_2$	2.023(4); 2.029(4)	1.757(3); 1.761(3)	1.777(2)	[327]
cis-$GeF_4 \cdot$phen	2.046(3)	1.753(2)	1.781(2)	[335]
cis-$GeF_4 \cdot$tmen	2.068(5); 2.087(3)	1.763(2); 1.756(4)	1.773(3); 1.774(4)	[335]
$[GeF_4\text{-}\{Ph_2P(CH_2)_2PPh_2\}]$	2.4636(7); 2.4822(7)	1.7731(14); 1.7692(14)	1.7987(14); 1.7829(13)	[336]
$[GeF_4\{o\text{-}C_6H_4(PMe_2)_2\}]$	2.4273(12); 2.4273(11)	1.772(2); 1.765(2)	1.815(2); 1.809(2)	[336]
$[GeF_4\{MeS(CH_2)_2SMe\}]$	2.4334(7); 2.4728(7)	1.7487(14); 1.7592(15)	1.7734(14); 1.7764(14)	[337]
$[GeF_4\{EtS(CH_2)_2SEt\}]$	2.4611(8); 2.4903(8)	1.7507(16); 1.7561(16)	1.7714(15); 1.7761(15)	[337]
trans-$GeF_4 \cdot 2(O{=}PMe_3)$	1.898(5)	1.772(4); 1.776(4)	–	[338]
trans-$GeF_4 \cdot 2(O{=}PEt_3)$	1.904(2)	1.770(2); 1.769(2)	–	[338]
trans-$GeF_4 \cdot 2(O{=}PPh_3)$	1.925(2)	1.774(1); 1.772(1)	–	[338]
trans-$GeF_4 \cdot 2Et_2O$	1.975(2)	1.754(2); 1.747(2)		[339]
trans-$GeCl_4 \cdot 2py$	2.02	2.27	–	[340]
cis-$GeCl_4 \cdot$phen	2.0716(17); 2.0759(17)	2.2232(6); 2.2244(6)	2.2619(6); 2.2799(6)	[335]
cis-$GeCl_4 \cdot 2,2'\text{-bipy}$	2.062(4); 2.068(4)	2.241(1); 2.246(1)	2.262(1); 2.272(1)	[341]
cis-$GeCl_4 \cdot$tmen	2.148(12); 2.156(10)	2.247(3); 2.236(4)	2.253(5); 2.248(4)	[342]
trans-$GeCl_4 \cdot 2(4\text{-Me-Py})$	2.057(2)	2.2670(6)	–	[343]
trans-$[GeCl_4(AsEt_3)_2]$	2.4904(9)	2.3296(19); 2.3233(19)	–	[336]
trans-$[GeCl_4(AsMe_3)_2]$	2.472(1)	2.307(4); 2.341(4)	–	[344]
cis-$GeBr_4 \cdot 2,2'\text{-bipy}$	2.070(3); 2.073(4)	2.4202(6); 2.4157(6)	2.4438(7); 2.428(7)	[335]
cis-$GeBr_4 \cdot$tmen	2.188(5); 2.192(5)	2.4388(10); 2.4372(10)	2.4587(10); 2.4506(11)	[335]
cis-$GeBr_4 \cdot$phen	2.069(7); 2.078(7)	2.3902(14); 2.3792(15)	2.4289(16); 2.4719(17)	[335]
trans-$GeBr_4 \cdot 2(3,5\text{-}Me_2\text{-Py})$	2.112(3)	2.458(4)	–	[345]
trans-$GeBr_4 \cdot 2(4\text{-Me-Py})$	2.083(3)	2.4425(4)	–	[346]
trans-$GeBr_4 \cdot 2(3,4\text{-}Me_2\text{-Py})$	2.101(5)	2.4392(5)	–	[346]
trans-$SnF_4 \cdot 2ND_3$ (neutron diffraction)	2.096(4)	1.994(5); 1.986(7)	–	[49]
cis-$SnF_4 \cdot 2,2'\text{-bipy}$	2.181(3); 2.183(3)	1.924(3); 1.925(3)	1.940(3); 1.948(3)	[327]
cis-$SnF_4 \cdot$phen	2.157(7)	1.860(8)	1.887(5)	[347]
trans-$SnF_4 \cdot 2PCy_3$	2.6538(11)	1.959(2); 1.980(2)	–	[347]
cis-$SnF_4 \cdot Et_2P(CH_2)_2PEt_2$	2.6058(9)	1.9532(16)	1.9863(17)	[347]
cis-$SnF_4 \cdot MeO(CH_2)_2OMe$	2.144(2); 2.1559(19)	1.9210(18); 1.9234(18)	1.9263(17); 1.9274(17)	[347]
trans-$SnF_4 \cdot 2O{=}PPh_3$	2.050(3)	1.928(3); 1.924(3)	–	[347]
trans-$SnF_4 \cdot 2O{=}PMe_3$	2.045(3)	1.937(2); 1.954(2)	–	[33]
cis-$[SnF_4\{EtS(CH_2)_2SEt\}]$	2.5849(6); 2.6028(6)	1.9298(13); 1.9352(12)	1.9540(12); 1.9490(12)	[337]
cis-$[SnF_4\{^iPrS(CH_2)_2S^iPr\}]$	2.5844(7)	1.9341(13)	1.9464(13)	[337]
$SnF_4 \cdot (o\text{-}C_6H_4(P(O)Ph_2)$	2.071(5); 2.088(5)	1.930(4); 1.940(4)	1.941(4); 1.951(4)	[33]
cis-$SnCl_4 \cdot 2,2'\text{-bipy}$	2.226(4); 2.247(4)	2.359(1); 2.371(1)	2.391(1); 2.408(1)	[348]
cis-$SnCl_4 \cdot$phen	2.234(2); 2.241(2)	2.3707(7); 2.3498(8)	2.3779(8); 2.3970(8)	[349]
cis-$SnCl_4 \cdot 2CH_3CN$	2.336(23); 2.326(25)	2.341(7); 2.356(7)	2.339(8); 2.355(7)	[350]
cis-$SnCl_4 \cdot 2POCl_3$	2.25(5); 2.30(4)	2.31(2); 2.36(2)	2.33(2)	[351]
cis-$SnCl_4 \cdot Et_2P(CH_2)_2PEt_2$	2.6481(17)	2.4084(14)	2.4529(14)	[347]
cis-$SnCl_4 \cdot$dppen	2.6537(5); 2.6780(5)	2.3745(6); 2.3812(6)	2.4102(6); 2.4138(5)	[352]
cis-$SnCl_4 \cdot$dppe	2.653(2); 2.679(2)	2.406(2); 2.408(2)	2.402(2); 2.447(2)	[379]
cis-$SnCl_4 \cdot 2OSMe_2$	2.110(7–8);	2.377(3); 2.406(3)	2.369(3); 2.396(3)	[372]
cis-$SnCl_4 \cdot 2O{=}PPh_3$	2.086(2)	2.3953(10)	2.3853(10)	[373]
trans-$SnCl_4 \cdot 2THF$	2.166(2)	2.3735(9); 2.3828(8)	–	[374]
trans-$SnCl_4 \cdot 2(EtCOOCH{=}CHPh)$	2.165	2.376; 2.379	–	[375]
cis-$SnCl_4 \cdot 2(4\text{-}^tBuC_6H_4CHO)$	2.168; 2.230	2.354; 2.355	2.356; 2.379	[376]
trans-$SnCl_4 \cdot 2$dppm	2.649	2.428; 2.450	–	[377]
$SnCl_4 \cdot (PhCO)_2$	2.204; 2.259	2.326; 2.329	2.365; 2.385	[378]
trans-$SnCl_4 \cdot 2NHMe_2$	2.224(6)	2.4045(18); 2.4256(18)	–	[364]
cis-$SnCl_4 \cdot 2NCMe$	2.259(2)	2.3635(7)	2.3518(10); 2.3641(10)	[365]
cis-$SnCl_4 \cdot 2NCMe$	2.2567(17)	2.3599(5)	2.3502(8); 2.3617(8)	[366]
cis-$SnCl_4 \cdot 2NCEt$	2.2388(18); 2.2508(18)	2.3634(6); 2.3653(6)	2.3609(6); 2.3699(6)	[365]
cis-$SnCl_4 \cdot 2NC^iPr$	2.255(4); 2.260(4); 2.256(4); 2.276(4)	2.3586(11); 2.3520(11); 2.3580(13);	2.3659(11); 2.3684(11); 2.3584(12); 2.3761(12)	[365]
cis-$SnCl_4 \cdot 2NC$cyclohexyl	2.257; 2.270; no errors	2.3620(4); 2.3682(5)	2.3488(5); 2.3732(5)	[365]
cis-$SnCl_4 \cdot 2NC(p\text{-Tol})$	2.2658(16); 2.2687(16)	2.3606(7); 2.3678(6)	2.3488(7); 2.3560(7)	[365]
trans-$SnCl_4 \cdot 2Ph_2PS_2N_3$	2.238	2.385; 2.418	–	[367]
trans-$SnCl_4 \cdot 2pyz$	2.246(1)	2.3883(4); 2.3980(4)	–	[368]

Table 9 (*Continued*)

Complex	r(E–D), Å	r(E–X_{eq}), Å	r(E–X_{ax}), Å	Ref
trans-$SnCl_4$·2(4-ClC_6H_4N=CHPh), N-benzyliden-4-chloroaniline	2.267(2)	2.390(1); 2.404(1)	–	[369]
cis-$SnCl_4$·phen	2.234; 2.251; 2.237; 2.251	2.363; 2.367; 2.367; 2.377	2.396; 2.410; 2.361; 2.390	[370]
cis-$SnCl_4$·phen	2.224(3); 2.238(3)	2.3333(12); 2.3708(10)	2.4095(10); 2.4480(10)	[371]
$SnCl_4$·$C_{16}H_6N_6$, dipyrido[f,h]quinoxaline-6,7-dicarbonitrile	2.237(3)	2.3556(10)	2.4200(12); 2.4223(13)	[35]
trans-$SnCl_4$·2Et_2O	2.191(3)	2.370(1); 2.373(1)	–	[353]
trans-$SnCl_4$·2O=P(NMe_2)$_3$	2.13(2)	2.40(1)	–	[354]
trans-$SnCl_4$·2O=C(NMe_2)$_2$	2.112(4)	2.388(1); 2.395(1)	–	[355]
cis-$SnCl_4$·(OCPh)$_2$NH	2.185(3)	2.342(2)	2.369(2); 2.375(2)	[356]
trans-$SnCl_4$·2PEt_3	2.615(5)	2.445(5); 2.465(5)	–	[357]
trans-$SnCl_4$·2$AsPh_3$	2.7623(3)	2.4153(8); 2.4239(7)	–	[8]
trans-$SnCl_4$·2SMe_2	2.6208(4)	2.4147(4); 2.4188(5)	–	[358]
trans-$SnCl_4$·2(1,5-dithiacyclooctane)	2.602(1)	2.414(1); 2.428(1)	–	[359]
cis-$SnCl_4$·MeS(CH_2)SMe	2.710(2) 2.647(2)	2.362(2); 2.343(2)	2.402(2); 2.390(2)	[360]
cis-$SnCl_4$·MeS(CH_2)$_2$SMe	2.619(4)	2.372(4)	2.413(3)	[361]
cis-$SnCl_4$·MeS(CH_2)$_3$SMe	2.667(2)	2.378(2)	2.409(2)	[361]
cis-$SnCl_4$·*o*-C_6H_4(SMe)$_2$	2.659(2); 2.677(2)	2.357(2); 2.357(2)	2.401(2); 2.383(2)	[361]
cis-$SnCl_4$·PhS(CH_2)$_3$SPh	2.724(5); 2.725(5)	2.379(6); 2.380(5)	2.385(5); 2.376(4)	[361]
cis-$SnCl_4$·2detu	2.49(l); 2.52(2)	2.51(2); 2.58(2)	2.55(3); 2.48(3)	[362]
cis-$SnCl_4$·2detu	2.494(1); 2.470(1)	2.521(8)[a]; 2.459(8)[a]	2.429(1); 2.427(1)	[363]
cis-$SnCl_4$·MeSe(CH_2)SeMe	2.782(1)	2.376(3)	2.406(4); 2.407(4)	[360]
trans-$SnBr_4$·2$NHMe_2$	2.244(3)	2.5707(12); 2.5867(11)	–	[477]
cis-$SnBr_4$·2,2′-bipy	2.23(1)	2.539(1); 2.541(1)	2.561(1); 2.568(1)	[348]
cis-$SnBr_4$·CH_2(C=ONHMe)$_2$	2.133(6); 2.151(6)	2.531(2); 2.532(2)	2.541(2); 2.553(2)	[385]
cis-$SnBr_4$·CH_2(C=ONH^{i}Pr)$_2$	2.158(7); 2.164(8)	2.511(2); 2.518(2)	2.511(2); 2.554(2)	[385]
trans-$SnBr_4$·2O=PPh_3	2.100(8); 2.102(9)	2.511(2); 2.558(2); 2.576(2); 2.584(2)	–	[382]
cis-$SnBr_4$·2O=PPh_3	2.080(8)	2.557(2)	2.537(1)	[380]
cis-$SnBr_4$·2OSMe_2	2.153(15); 2.205(15)	2.531(3); 2.549(3)	2.536(3); 2.548(3)	[381]
cis-$SnBr_4$·CH_2(C=SNH^{i}Pr)$_2$	2.576(4); 2.568(4)	2.569(2); 2.574(2)	2.582(3); 2.663(2)	[385]
trans-$SnBr_4$·2THF	2.200(3)	2.5307(5); 2.5427(5)	–	[374]
cis-$SnBr_4$·2deu	2.09(7); 2.36(9)	2.59(2); 2.55(l)	2.56(l) 2.56(l)	[362]
cis-$SnBr_4$·{MeC(CH_2AsMe_2)$_3$}	2.6932(5); 2.7095(6)	2.5479(5); 2.5708(6)	2.5807(5); 2.6340(5)	[347]
trans-$SnBr_4$·2O=P(NMe_2)$_3$	2.09(1)	2.56(1)	–	[354]
cis-$SnBr_4$·2O=SPh_2	2.128(11); 2.130(9)	2.496(1); 2.558(1)	2.555(1); 2.558(1)	[383]
$SnBr_4$·(OCPh)$_2$NH	2.174(6); 2.195(6)	2.473(2); 2.482(2)	2.528(2); 2.630(2)	[384]
trans-$SnBr_4$·2SMe_2	2.65(1)	2.554(3); 2.554(4)	–	[34]
cis-$SnBr_4$·2SMe_2	2.692(9) 2.692(8)	2.554(4); 2.532(4)	2.557(4) 2.539(4	[34]
cis-$SnBr_4$·MeS(CH_2)$_3$SMe	2.700(7)	2.533(3)	2.562(3)	[361]
trans-SnI_4·2O=P(^{p}Tol)$_3$	2.1590(15)	2.76735(17); 2.8158(2)	–	[388]
cis-SnI_4·2OSPh_2	2.189(6); 2.249(6)	2.773(1); 2.806(1)	2.776(1); 2.781(1)	[389]
cis-SnI_4·(*o*-C_6H_4(P(O)Ph_2)	2.12(1); 2.142(10)	2.772(2); 2.788(2)	2.780(2); 2.807(2)	[390]
cis-SnI_4·2{MeS(O)(CH_2)$_3$SMe}	2.18(1); 2.21(2)	2.788(2); 2.780(2)	2.762(2); 2.802(2)	[361]
cis-SnI_4·bipy	2.276(20); 2.277(19)	2.787(3); 2.788(2)	2.813(2); 2.819(2)	[386]
cis-SnI_4·2O=PPh_3	2.11(2); 2.15(2)	2.783(2); 2.811(2)	2.781(2); 2.816(2)	[387]
trans-SnI_4·2P^nPr_3	2.69(1)	2.872(3); 2.863(3)	–	[34]
cis-TiF_4·2O=PPh_3	2.055(6)	1.813(4)	1.822(4)	[391]
cis-TiF_4·2Me_2SO	1.99(3)	1.745(15)	1.80(2)	[391]
cis-TiF_4·2Me_2SO	1.96(8); 2.02(2); 2.05	1.73(2); 1.76(2)	1.78(2); 1.82(2)	[392]
trans-TiF_4·2L^{Me}	2.255(4)	1.831(3); 1.835(2)	–	[393]
trans-TiF_4·2L^{iPr}	2.2812 (12); 2.2781(12)	1.8337(8)–1.8409(7)	–	[393]
trans-$TiCl_4$·2py	2.208;; 2.235	2.396; 2.407; 2.365; 2.446	–	[408]
cis-$TiCl_4$·2NCMe	2.187(4)	2.228(2)	2.269(2); 2.288(2)	[409]
cis-$TiCl_4$·2$PhCN_4H$	2.265(5); 2.279(5)	2.216(2); 2.231(2)	2.271(2); 2.275(2);	[410]
trans-$TiCl_4$·2(3,4-$Me_2C_5H_3N$)	2.193(2)	2.2971(5)	–	[411]
trans-$TiCl_4$·2(4-MeC_5H_4N)	2.191(4)	2.2976(10)	–	[411]
cis-$TiCl_4$·2N_3NHCPh	2.265(5); 2.279(5)	2.216(2); 2.231(2)	2.271(2); 2.275(2)	[177]
cis-$TiCl_4$·2NCC_6H_4(2-$SiMe_3$)$_2$	2.212(10)	2.210(4)	2.271(3)	[412]
trans-$TiCl_4$·2(3,5-$Me_2C_3H_2N_2$)	2.146(5)	2.254(3); 2.297(2); 2.303(3)	–	[413]
cis-$TiCl_4$·2(4-$IC_3H_3N_2$)	2.235(7)	2.265(2)	2.280(2)	[413]
$TiCl_4$·tmen	2.279(7); 2.304(7)	2.254(2); 2.256(3)	2.259(3); 2.280(3)	[414]
cis-$TiCl_4$·2Et_2O	2.056(20); 2.118(14)	2.197(13); 2.256(8)	2.268(7); 2.273(7)	[415]
cis-$TiCl_4$·2THF	2.116(3); 2.118(3)	2.242(2); 2.248(2)	2.283(2); 2.285(2)	[416]
trans-$TiCl_4$·2THF	2.050(4)	2.293(2)	–	[416]
trans-$TiCl_4$·2(2,4-$Me_2C_5H_3N$)	2.257(3)	2.281(1); 2.295(1)		[297]
cis-$TiCl_4$·2CH_3CN	2.21	2.216	2.264	[394,395]
cis-$TiCl_4$·2^{t}BuNC	2.240(8); 2.256(6)	2.244(3), 2.218(2)	2.287(3); 2.286(3)	[396]
trans-$TiCl_4$·2Py	2.20	2.29	–	[397]
cis-$TiCl_4$·2$POCl_3$				[398]
cis-$TiCl_4$·2Et_2O	2.21	2.256	2.282	[399]
cis-$TiCl_4$·2Et_2O	2.120(6); 2.158(5)	2.250(2); 2.262(3)		[399]
cis-$TiCl_4$·MeO(C_2H_4)OMe	2.1714(16)	2.2307(7)	2.2978(7)	[400]
cis-$TiCl_4$(SC_4H_8)$_2$, tetrahydrothiophen	2.625(7); 2.626(7)	2.232(8); 2.233(8)	2.280(4); 2.280(4)	[310]
cis-$TiCl_4$·2SHC_6H_{11}	2.663(2); 2.646(2)	2.221(2); 2.226(2)	2.263(2) 2.300(2)	[401]
$TiCl_4$·C_6H_4($OCOC_2H_5$)$_2$	2.068(3)	2.235(2)	2.295; 2.289(2)	[402]
cis-[$TiCl_4${MeS(CH_2)$_2$SMe}]	2.6106(9); 2.6010(8)	2.2358(8); 2.2253(9)	2.2907(8); 2.2926(8)	[403]
cis-[$TiCl_4${MeS(CH_2)$_3$SMe}]	2.644(2)	2.235(2)	2.285(2)	[403]

Table 9 (*Continued*)

Complex	r(E–D), Å	r(E–X_{eq}), Å	r(E–X_{ax}), Å	Ref
cis-[$TiCl_4${$MeSe(CH_2)_3SeMe$}]	2.755(3)	2.247(4)	2.278(3)	[403]
cis-[$TiCl_4${*o*-C_6H_4-$(SeMe)_2$}]	2.727(1); 2.744(1)	2.239(2); 2.231(2)	2.267(2); 2.308(2)	[403]
trans-$TiCl_4$·2($PHCy_2$)	2.6372(8)	2.2892(8); 2.2837(8)	–	[9]
cis-$TiCl_4$·dppe	2.660(2); 2.640(2)	2.265(2); 2.251(2)	2.265(2); 2.296(2)	[9]
cis-$TiCl_4$·dmpe	2.582(2); 2.577(2)	2.273(2); 2.288(2)	2.307(2); 2.293(2)	[404]
cis-$TiCl_4$·depe	2.5981(9)	2.2758(8)	2.3050(7)	[405]
[$TiCl_4${*o*-$C_6H_4(PMe_2)_2$}]	2.5733(13); 2.5600(12)	2.2748(12); 2.253(1)	2.2975(13); 2.2938(13)	[84]
trans-$TiCl_4$·2O=PPh_3	1.9229(15)	2.3283(6); 2.3336(6)	–	[417]
trans-$TiCl_4$·2O=$P(NMe_2)_3$	1.945(3)	2.3224(14); 2.333(2)	–	[418]
trans-$TiCl_4$·2O=$P(NC_5H_{10})_3$	1.923(3)	2.341(1); 2.343(1)	–	[32]
trans-$TiCl_4$·2O=$AsPh_3$	1.895	2.335; 2.368	–	[419]
cis-$TiCl_4$·2OCHMes, Mes = 2,4,6-$Me_3C_6H_2$	2.091(2); 2.100(3)	2.244(1); 2.231(1)	2.293(1); 2.308(1)	[314]
trans-$TiCl_4$·2^{i}PrHNCMe=CHCMe=O	1.916(2)	2.3726(9); 2.378(1)	–	[420]
trans-$TiCl_4$·2^{i}PrC_6H_3NH=CC_6H_4O (N-(2,6-diisopropylphenyl)salicylimine)	1.895(1)	2.340(1); 2.373(1)	–	[421]
$TiCl_4$·$(OCMe)_2$O	2.162	2.213	2.267; 2.318	[422]
$TiCl_4$·$O_3C_8H_{12}$	2.109(3); 2.136(3)	2.222; 2.227	2.277; 2.321	[423]
$TiCl_4$·$(OCMe)_2CMe_2$, 3,3-dimethyl-2,4-pentanedione	2.077(3); 2.086(3)	2.213(1); 2.229(1)	2.264(1); 2.300(1)	[424]
$TiCl_4$·*o*-$C_6H_4(CO^iBu)_2$	2.093(7); 2.113(7)	2.238(3)	2.282(3); 2.305(3)	[425]
$TiCl_4$·$(COOEt)_2CH_2$, diethyl malonate	2.109(3); 2.136(3)	2.225(2); 2.239(2)	2.273(2); 2.304(2)	[426]
$TiCl_4$·$(COOEt)_2CH_2$, diethyl malonate	2.102(4); 2.112(4)	2.219(2); 2.233(2)	2.262(2); 2.293(2)	[427]
$TiCl_4$·$(COOEt)_2C$=CMe_2, diethyl isopropylidenemalonate	2.099(4); 2.118(3)	2.242(2); 2.245(2)	2.298(2); 2.302(2)	[426]
cis-$TiCl_4$·$(COOEt)_2CEt_2$, diethyl diethylmalonate	2.092(8); 2.119(7)	2.218(4); 2.242(4)	2.285(4); 2.317(4)	[426]
$TiCl_4$·$(COOEt)_2C_2H_2$, diethyl maleate	2.087(4); 2.098(4)	2.232(3); 2.239(3)	2.276(3); 2.283(3)	[426]
$TiCl_4$·$(COOEt)_2CHCMe$, diethyl citraconate	2.068(10); 2.097(9)	2.238(5); 2.242(6)	2.265(5); 2.310(5)	[426]
$TiCl_4$·*o*-$C_6H_4(COOMe)_2$, diethyl phthalate	2.091(3)	2.226(2)	2.290(2); 2.303(2)	[426]
cis-$TiCl_4$·1,2-$C_6H_{10}(CO^iBu)_2$, cis-1,2-diisobuthylcyclohexanoate	2.090(12); 2.098(13); 2.062(15); 2.065(14)	2.220(6); 2.234(6); 2.214(6); 2.226(6)	2.303(6); 2.305(6); 2.307(6); 2.308(7)	[426]
cis-$TiCl_4$·$(^nPrOCHPh)_2$	2.087(18); 2.140(16)	2.111(9); 2.223(10)	2.274(9); 2.297(9)	[428]
cis-$TiCl_4$·$(PhOC_2H_4COO)_2C_2H_4$, bis(2-phenoxoethyl) succinate	2.088(5); 2.113(5)	2.197(2); 2.211(2)	2.284(2); 2.293(2)	[427]
cis-$TiCl_4$·$CH(COOEt)_3$, triethyl methanetricarboxylate	2.122(2); 2.144(2)	2.208(1); 2.214(1)	2.260(1); 2.271(1)	[210]
$TiCl_4$·$(PhCO)_2$, dibenzoyl	2.146(3); 2.186(3)	2.197(2)	2.281(2); 2.299(2)	[308]
$TiCl_4$·$O_2C_{12}H_6$, acenaphthenedione	2.194; 2.272	2.199; 2.206	2.262; 2.271	[378]
[$TiBr_4${$MeC(CH_2AsMe_2)_3$}]	2.680(3); 2.688(3)	2.407(3); 2.403(3)	2.471(3) 2.445(3)	[84]
cis-$TiBr_4$·2CH_3CN	2.208(16)	2.390(4)	2.403(6); 2.489(6)	[406]
cis-$ZrCl_4$·2CH_3CN	2.340(3); 2.324(9)	2.365(3); 2.366(3)	2.417(3); 2.395(3)	[407]
cis-$ZrCl_4$·bipy	2.297(9); 2.301(9)	2.383(3); 2.390(3)	2.401(3); 2.410(3)	[429]
cis-$ZrCl_4$·phen	2.35; 2.37	2.359; 2.372	2.410; 2.418	[430]
trans-$ZrCl_4$·2DMFA	2.052(8)	2.443(4); 2.445(3)	–	[431]
trans-$ZrCl_4$·2(1,3-diisopropylimidazol-2-ylidene)	2.432(3)	2.439(1); 2.437(1)	–	[432]
trans-$ZrCl_4$·2[1-methyl-3-(1-methylpropyl)-imidazol-2-ylidene]	2.456(3)	2.436(1); 2.428(1)	–	[432]
trans-$ZrCl_4$·2[1-methyl-3-(2,4,6-trimethylbenzyl)imidazol-2-ylidene]	2.448(3)	2.431(1); 2.436(1)	–	[432]
cis-[$ZrCl_4(Me_2S)_2$]	2.754(3); 2.788(2)	2.361(2); 2.425(2);	2.386(2); 2.386(3)	[83]
trans-$ZrCl_4$·2Et_2O	2.186(1)	2.4263(5); 2.4278(5)	–	[433]
trans-$ZrCl_4$·2py	2.366(12)	2.457(3)	–	[434]
cis-$ZrCl_4$·2NCMe	2.319; 2.333	2.370; 2.372	2.398; 2.424	[435]
$ZrCl_4$·tmeda, tmeda-N,N,N′,N′-tetramethylethylenediamine	2.4319(17); 2.4337(19)	2.4066(7); 2.4111(5)	2.4281(6); 2.4298(6)	[436]
$ZrCl_4$·DAD, DAD = 1,4-diaza-1,3-diene	2.360(2); 2.365(2)	2.3566(8); 2.3724(10)	2.4092(7); 2.4246(7)	[437]
cis-$ZrCl_4$·2THF	2.229(10); 2.237(13)	2.389(11); 2.398(8)	2.422(8); 2.425(8)	[438]
cis-$ZrCl_4$·2Me_2SO_2	2.173(6); 2.175(6)	2.367(3); 2.378(2)	2.405(3); 2.422(3)	[163]
cis-$ZrCl_4$·2OCMe^{t}Bu, pinacolone	2.1838(19); 2.1984(19)	2.2855(7); 2.3960(8)	2.4080(6); 2.4414(6)	[439]
trans-$ZrCl_4$·2^{i}PrHNCMe=CHCMe=O	2.052(1)	2.464(1); 2.468(1)	–	[420]
$ZrCl_4$·$N_2S_2C_8H_{12}$ 2,2′-bi-2-thiazine	2.292(7); 2.301(7); 2.293(7); 2.314(7)	2.370(3); 2.378(3); 2.374(3); 2.381(2)	2.374(3); 2.431(3); 2.408(3); 2.430(3)	[440]
cis-$ZrBr_4$·2CH_3CN	2.29(3); 2.37(3)	2.509(7); 2.525(7)	2.555(7); 2.562(6)	[441]
trans-ZrI_4·2(PMe_2Ph)	2.774(3)	2.7787(6); 2.7902(7)	–	[442]
cis-[$HfCl_4${$MeSe(CH_2)_2SeMe$}]	2.844(2); 2.848(2)	2.348(6); 2.364(6)	2.396(6); 2.397(5)	[83]
trans-$HfCl_4$·2(1,3-diisopropylimidazol-2-ylidene)	2.401(2)	2.421(1); 2.419(1)	–	[432]

[a] Average Sn–S(Cl) distance due to disorder.

(2) If the acceptor atom in adduct is coordinationally unsaturated, formation of crystal may lead to increase of the coordination number due to dimerization (polymerization) of individual adduct molecules. As can be seen from Table 8, dimerization in the solid state is very common for adducts of group 4 and 14 element halides MX_4·D. In such a case upon adduct vaporization several concurrent processes are expected:

(a) vaporization in form of dimeric molecules $(MX_4·D)_2$.

Table 10
Structural properties of $EX_5 \cdot D$ adducts.

Complex	r(E–D), Å	r(E–X_{ax}), Å	r(E–X_{eq}), Å	Ref.
PF_5·4,5-dichloro-1,3-dimesitylimidazol-2-ylidene	1.898(3)	1.592; 1.596	1.600; 1.589	[142]
AsF_5·4,5-dichloro-1,3-dimesitylimidazol-2-ylidene	1.991(6); 2.006(5)	1.709; 1.716	1.726; 1.710	[142]
$SbF_5 \cdot pyz \cdot SbF_5$	2.172(5)	1.861(3)	1.858(4); 1.863(3); 1.870(3); 1.866(3)	[443]
SbF_5·4,5-dichloro-1,3-dimesitylimidazol-2-ylidene	2.175(5)	1.863	1.866	[142]
$SbF_5 \cdot NCCN$	2.213(5)	1.837(4)	1.814(4); 1.859(5)	[444]
$SbCl_5 \cdot NCMe$	2.23(4)	2.35(2)	2.33(2); 2.40(2)	[445]
$SbCl_5 \cdot NCCl$	2.286(5)	2.322(2)	2.336(1)	[446]
$SbCl_5 \cdot NCCN \cdot SbCl_5$	2.663	2.272(1)	2.336(2)	[446]
$SbCl_5 \cdot NCN^iPr_2$	2.14(1)	2.329(4)	2.341–2.361(5)	[447]
$SbCl_5 \cdot POCl_3$	2.17(2)	2.32(1)	2.33–2.35(1)	[448]
$SbCl_5 \cdot POMe_3$	1.94(4)	2.34(2)	2.33–2.35(2)	[448]
$SbCl_5 \cdot O{=}CO_2C_2Cl_4$	2.400(20)	2.280(10)	2.300–2.330(10)	[449]
$SbCl_5 \cdot C_6H_5COCl$	2.317(5)	2.318(2)	2.323(1); 2.317(1)	[450]
$SbCl_5 \cdot m\text{-}CH_3C_6H_4COCl$	2.295(3)	2.304(1)	2.324(1); 2.329(1)	[450]
$SbCl_5 \cdot p\text{-}CH_3C_6H_4COCl$	2.253(6)	2.305(2)	2.323(3); 2.314(2)	[451]
$SbCl_5 \cdot O{=}CPhCH_2Br$	2.168(5)			[452]
$SbCl_5$·(+)-3-endo-bromocamphor	2.23(1)			[452]
$SbCl_5 \cdot OSClMe$	2.151(3)	2.320(2)	2.325(2); 2.338(2); 2.347(2); 2.355(2)	[453]
$SbCl_5 \cdot OSPh_2$	2.091	2.314	2.319; 2.333; 2.346; 2.344	[454]
$SbCl_5 \cdot O{=}PPh_3$	2.039; 2.035	2.363; 2.356	2.322; 2.334; 2.345; 2.371; 2.328; 2.337; 2.344; 2.346	[455]
$SbCl_5 \cdot C_{17}H_{21}Cl_5NO_2$	1.948(4)	2.344(3)	2.341; 2.350; 2.351; 2.354(3)	[456]
$SbCl_5$·benzoyl chloride	2.270(2)	2.3014(7)	2.3252(5); 2.3256(5)	[244]
$SbCl_5 \cdot HCON(CH_3)_2$	2.048(6)	2.330(3)	2.336; 2.343; 2.353; 2.332(3)	[457]
$SbCl_5$·DMSO	2.05(5); 2.10(4)	2.29(2)	2.33–2.37(1)	[458]
$SbCl_5 \cdot ONNMe_2$	2.113(3)	2.344(1)	2.346(1); 2.350(1); 2.345(1); 2.364(1)	[459]
$2SbCl_5 \cdot COClCH_2CH_2COCl$	2.428(7)	2.298 (3)	2.322(3); 2.319(3); 2.325(3); 2.303 (3)	[460]
$SbCl_5 \cdot O{=}SeCl_2$	2.042(25); 2.122(23)	2.318(10); 2.346(9)	2.326–2.356(14)	[461]
$NbCl_5 \cdot O{=}PCl_3$	2.16(2)	2.25(1)	2.29–2.35(1)	[448]
$NbCl_5 \cdot CH_3CN$	2.236(4)	2.249(2)	2.317(1); 2.293(1); 2.286(2); 2.319(2)	[462]
$NbCl_5 \cdot [NC(CH_2)_2S(CH_2)_2CN]$	2.259(3)	2.2490(9)	2 2.3148(9); 2.3152(9); 2.3178(8); 2.3347(8)	[463]
$NbCl_5 \cdot NCCH_2C_6H_5$	2.279(3)	2.258(1)	2.310(1); 2.314(1); 2.316(1); 2.317(1)	[464]
$NbCl_5 \cdot NCCCl_3$	2.343	2.246(3)	2.291(2); 2.301(3); 2.308(3)	[465]
$NbCl_5 \cdot NC(CH_2)_5CN \cdot NbCl_5$	2.258(6); 2.264(6)	2.252(2); 2.247(2)	2.296(2); 2.306(2); 2.328(2); 2.328(2); 2.308(2); 2.320(2); 2.320(2); 2.326(2)	[466]
$NbCl_5 \cdot (m\text{-}CF_3)C_6H_4CN$	2.262(6)	2.2499(17)	2.2866(16); 2.3098(16); 2.3187(16); 2.3182(18)	[467]
$NbCl_5$·EtCN	2.228(10)	2.225(3)	2.273(12); 2.278(14); 2.315(2); 2.320(3)	[468]
$NbCl_5 \cdot HCN$	2.306(3)	2.243(1)	2.315(1); 2.312(1)	[469]
$NbCl_5$·diox	2.206(4)	2.2637(15)	2.3237(14)–2.3265(15)	[470]
$NbCl_5$·TEU	1.9596(12)	2.3375(5)	2.3531(4); 2.3407(4); 2.3488(5); 2.3597(5)	[471]
$NbCl_5$·DMF	2.018(10)	2.297(4)	2.331(4); 2.337(3); 2.350(4); 2.366(3)	[471]
$NbCl_5 \cdot PMe_2Ph$	2.673(5)	2.405(5)	2.366(10); 2.362(10); 2.360(10); 2.394(10)	[472]
$NbCl_5 \cdot S{=}PPh_3$	2.6159(8)	2.2952(8)	2.3030(9); 2.3234(9); 2.3386(9); 2.3584(9)	[473]
$2NbCl_5$·1,4,8,11-tetrathiacyclotetradecane	2.713(8)	2.252(8)	2.314(10); 2.299(10); 2.311(11); 2.328(11)	[474]
$TaCl_5$·DMF	2.000(12)	2.302(5)	2.329(6); 2.362(4); 2.336(6); 2.338(4)	[471]
$TaCl_5$·PhA	2.007(2); 1.991(2)	2.2872(8); 2.3041(8)	2.3597(8); 2.3848(8); 2.3843(9) 2.3314(9); 2.3186(9); 2.3145(8) 2.3184(9); 2.3548(9)	[471]
$TaCl_5 \cdot O{=}PPh_3$	2.016(12); 2.017(13)	2.325(5); 2.339(5)	2.319(5); 2.333(5); 2.341(5); 2.328(5); 2.365(5); 2.335(5); 2.326(5); 2.342(5)	[471]
$TaCl_5$·THF	2.146(4); 2.149(4)	2.2727(19); 2.2866(15)	2.3155–2.3324(18)	[470]
$TaCl_5 \cdot Ph_2C{=}O$	2.0108(18)	2.3059(6)	2.3304–2.3466(7)	[475]
$TaCl_5$·EtCN	2.21(2)	2.228(5)	2.24(3); 2.290(13); 2.314(4); 2.320(4)	[468]
$TaCl_5 \cdot [NC(CH_2)_2S(CH_2)_2CN]$	2.239(6)	2.257(2)	2.313(2); 2.318(2); 2.320(2); 2.332(2)	[463]
$[TaCl_5\{(2,4,6\text{-}^iPr_3)C_6H_2CN\}]$	2.207(2)	2.2668(6)	2.3196(6); 2.3348(6); 2.3393(6); 2.3315(6)	[476]
$TaBr_5 \cdot PhA$	1.999(8)	2.4451(15)	2.5380(16); 2.4736(17); 2.4635(17); 2.4756(17)	[471]

(b) destruction of the coordination lattice and vaporization in form of $MX_4 \cdot D$.
(c) dissociation of $MX_4 \cdot D$ into gaseous MX_4 and D.
(d) disproportionation of the solid adduct: $2MX_4 \cdot D = MX_4 \cdot 2D + MX_4$.

It should be taken into account that new compounds $MX_4 \cdot 2D$, $MX_4 \cdot D$ may exist only in the gaseous or both in the gaseous and solid states.

(3) For many adducts of group 13 element halides (especially Al and Ga) with excess donor molecules L, transformation from the molecular $MX_3 \cdot nL$ to the ionic form $[ML_6]^{3+}\ 3[MX_4]^-$ becomes prominent. In such a case prognosis of the thermal behavior of adduct is not possible. Since ionic lattices are in general more thermally stable than the molecular ones, adducts with ionic structure should have lower volatility. Thus, the knowledge of the crystal structure of adduct allows one to plan its experimental study by tensimetry methods.

3. Description of the experimental method

3.1. Tensimetric methods and their capabilities

Tensimetry methods allow to measure or determine pressure both in homo and heterogeneous systems in wide temperature and pressure range [478–480]. Modern tensimetry methods operate in very wide pressure range from 10^{-6} Pa (10^{-8} Torr) to 10^7 Pa

(100 atm). Upper limits of the temperature range are determined by thermal and chemical resistance of the apparatus materials and may reach 2000 K. Tensimetry allows to measure the total pressure P_{total}; obtain composition of saturated and unsaturated vapor above the individual substances and calculate on this basis enthalpies and entropies of sublimation and vaporization; obtain equilibrium constants and thermodynamic characteristics of gaseous species.

On the basis of tensimetric data one can make a conclusion about congruent or incongruent character of the vaporization process, in other words about stability of the substance upon vaporization. Obtained information is used for understanding chemical processes which occur in the system in wide temperature range and may serve as a basis for the thermodynamic description of studied system. For the complete description of the system not only the total vapor pressure should be measured, but the true molecular vapor composition must be known. Depending on the complexity of vapor composition, the task of its determination can be solved either by tensimetry method alone, or with the help of one or several auxiliary methods which study properties of the system, quantitatively related to the partial pressure of molecular forms. For example, spectral methods, such as electronic, UV, Raman, IR spectroscopy may be used to establish equilibrium constants for complex composition in vapors [44,55,481,482].

In situation when several processes occur simultaneously, carefully conducted tensimetry investigation allows, without using auxiliary spectral methods, to determine the partial pressures of 2–3 molecular forms and to compute equilibrium constants of 1–2 equations. If several equilibria exist in the system simultaneously, some of them could be studied beforehand in simple systems, and obtained equilibrium constants could be afterwards used as parameters when studying more complicated systems. For example, when the dissociation of complex of group 13 metal trihalide is accompanied by the dimerization of the acceptor molecule (group 13 metal trihalides readily form M_2X_6 dimers at low temperatures), the dimerization constant of the equilibrium $2MX_{3(g)} = M_2X_{6(g)}$ can be measured separately in the tensimetric study of the pure metal trihalide [483,484] and then used as a known parameter.

In practice, the vapor pressure–temperature dependence is usually measured over the pure adduct, or, alternatively, in the systems containing acceptor A and donor D molecules in different A/D ratio. Obtained information permits to establish the nature of the primary process which occurs upon heating of adduct and to determine its thermodynamic characteristics. In particular, the enthalpy of the homogeneous gas phase dissociation of adduct into the donor and acceptor molecules (which determines the energy of the donor–acceptor bond) can be determined by this approach.

In the present review we will exclusively focus on the results obtained by the static tensimetric method with membrane null-manometer developed in our laboratory.

3.2. Static method

Static method is a direct method of pressure measurement. The principal basis of the all variants of static method is very simple. The studied system is placed in a closed volume, the pressure in which by some means is transferred to the measuring manometer. There are three variants of a static method:

(1) direct method, in which studied system is placed directly in the manometer knee;
(2) isoteniscope method, in which volume with studied substance ("working volume") is separated from the measuring manometer by small liquid null-manometer;
(3) membrane method, in which working volume is separated from the measuring manometer by null-manometer with elastic membrane. Null-manometer indicates equality of pressures in the working volume and in the measuring manometer.

The lower limit of measured pressure is determined either by the sensitivity of measuring manometer or, much more frequently, by the sensitivity of null-manometer. In most experimental works the lower limit equals to 0.5–1.0 Torr [486]. Using special techniques it can be reduced to 0.1–0.3 Torr [484]. The upper limit is determined by the mechanical stability of the apparatus and reaches hundreds of atmospheres. However, since vapor composition is usually computed using the ideal gas model, the total pressure in the system should not exceed 1–2 atm.

In contrast to other methods, such as well-known and widely used Knudsen [478–480,485] and transpiration (flow) [478–480] methods, in which true equilibrium between the vapor and condensed phase is not achievable in principle, the static method allows to obtain results which correspond to the true equilibrium state. Since the studied system is kept in the closed volume, time of the establishing of the equilibrium is practically unlimited. Moreover, in some cases static method allows to study the pressure changes upon establishing of the equilibrium.

Besides direct measurements of pressure and its dependence from temperature (or from time) the static method in many cases allows to obtain additional information about transformations (chemical reactions) which occur in the studied system upon temperature increase. In particular, information about the reversible/irreversible character of the chemical process can be easily obtained. The temperature, at which irreversible changes occur, can also be identified. Static method also allows one to explore homogeneous processes which occur after the complete vaporization of the sample. The mean molecular mass of vapor can be easily obtained and conclusions about the molecular forms existing in vapors can be made [486]. In addition, static method permits to study the equilibrium gas phase dissociation of the complex and to determine the dissociation enthalpies of the donor–acceptor bond in the gas phase.

It should be noted, that the static method is the only tensimetry method which allows one to study equilibria in the homogeneous gaseous systems.

3.3. Static method with membrane null-manometer

All results reported in the present review were obtained by static method with membrane null-manometer. In this variant the experimental device is wholly made from glass or quartz; the studied substance contacts only with these chemically inert materials. Glass apparatus may be used up to 400–600 °C (depending on the glass type), quartz apparatus—up to 900–1100 °C. There are many types of elastic membrane elements: spiral, bellows, spoon-type, and plane membranes [478]. One of the variants is a plane membrane null-manometer which was developed in our laboratory by Novikov and Suvorov [478], and is also widely used elsewhere [487–491].

Construction details of one of the variants of the apparatus are schematically shown in Fig. 11. Thin glass membrane (1) separates a working volume (2) from the compensation volume (3). Fused to the membrane (1) is the system of two glass rods (4) and (5) which ends by thin glass needle (6). Upon change of pressure in the membrane chamber (2) the glass needle (6) changes its placement relative to the static indicator of null position (7). The positions of glass needle (6) and indicator of null position (7) are projected on the screen (11) using an optical projection system (10) with about 30th-fold magnification. Compensation volume (3) via branch (8) is connected to the measuring stand. Measuring stand consists of the system of faucets with which pressure in "working" and "compensating" volumes is equalized, and mercury manometer, with

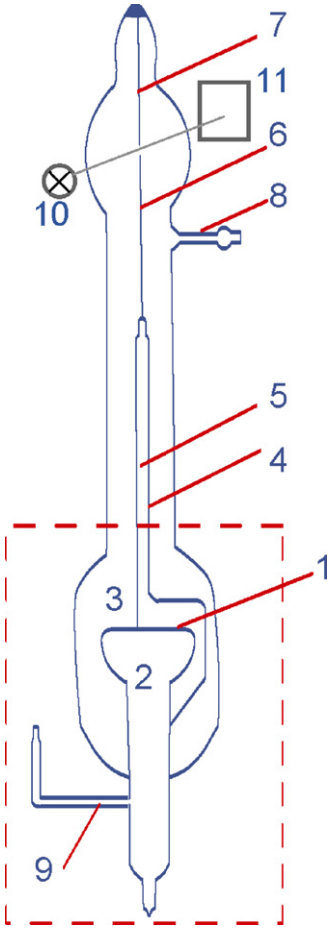

Fig. 11. One of the variants of a static tensimetric method with membrane null-manometer. (1) Thin glass membrane; (2) working volume; (3) compensation volume; (4) and (5) glass rods; (6) thin glass needle; (7) static indicator of null position; (8) branch to the measuring stand; (9) branches for introduction (or removal) of additional substances; (10) an optical system; (11) screen.

which pressure in the compensating volume is measured. Thermostatic zone is showed by broken line. Additional substances can be introduced into (or removed from) the "working volume" via one or several branches (9). Size of the working volume can be varied in wide limits; its maximal value is limited by the thermostat dimensions, and the minimal value can be made as small as 0.5–1.0 ml. The volume is determined by the mass difference between water filled and empty apparatus. In addition, the volume of the vapor phase can be lowered up to the desired minimum, for example 0.01 ml. Amount of substance, which is necessary for conducting experiments with membrane null-manometer, is small. Depending on the task of the experiment it varies from several milligrams to several grams.

Possibility of the separate introduction (or removal) of substances in the "working volume" via branches (9) allows to study relatively complex systems. Volume of the branches is usually calibrated beforehand, by this allowing adjustment of the working volume after the sealing off the branches (9). Construction of apparatus allows one to introduce/remove substances under high vacuum, which completely eliminates any contact of the studied substance with air. Before the introduction of the substances, whole apparatus is degassed under high vacuum ($\sim 10^{-4}$ Torr) at elevated temperatures for several hours. This procedure efficiently eliminates residual or "parasitic" pressure (which without such treatment appears at higher temperatures due to air and moisture desorption from the walls of the apparatus). In a typical measurement run with a glass apparatus, the system is placed in the furnace and heated with a rate of about 1 °C per minute. This heating rate is usually sufficient for establishing of the equilibria for the fast homogeneous gaseous reactions. For studying heterogeneous (gas–solid) processes with slow equilibration, apparatus may be thermostated at a desired temperature for a long (in principle infinite) period of time, which allows one to control the achievement of the equilibrium state. Temperature is controlled by means of two chromel–alumel thermocouples, placed in upper and lower parts of the working volume. The temperature gradient in the system which heated with speed of 1 °C per minute is usually about 1–2 °C; it is much less for the thermostated system.

4. Primary processes upon vaporization of the complex

4.1. General considerations

It is important to note the following:

1. According to the thermodynamic analysis, in *homogeneous gas phase system* at the equilibrium conditions the measured vapor pressure could only *increase* with temperature increase.
2. If a static method with membrane null-manometer is used, then the total mass m of the substances in the working volume V is constant. Therefore, if all processes in the studied system are reversible (the true equilibrium state is achieved), the *measured pressure is one-to-one function of the temperature*, regardless of the real variance of the system.
3. Change of the phase composition is always accompanied by a distinct point on the vapor pressure–temperature dependence curve.

Thermodynamic analysis of complexes of group 13 metal halides with pyridine, carried out by Sevastianova and Suvorov [27], reveals that $EX_3{\cdot}3Py$ and $EX_3{\cdot}2Py$ complexes should not exist in vapors due to the fact that their sublimation enthalpies are larger than the enthalpy of the donor–acceptor bond dissociation. Upon heating, these adducts evolve the excess of donor molecules and form complexes of 1:1 composition $EX_3{\cdot}Py$. This conclusion can be generalized to other $EX_m{\cdot}nD$ adducts.

It is convenient to represent results, obtained by the static method, in the graphical form. In general case the $P=f(T)$ dependence for the adduct AD of 1:1 composition is shown in Fig. 12. The vapor pressure–temperature dependence curve may be dissected (splitted) into several zones, number and appearance of which are dependent on the nature of the occurred process and on the m/V ratio (m – mass of the substance; V – volume of membrane chamber ("working volume")).

Zone 1 corresponds to the vapor-condensed phase equilibrium. If during the experiment the chemical composition in the condensed phase remains constant, then a vapor pressure at a given temperature does not depend on the mass of the substance, introduced into the working volume. In such a case, upon temperature increase the measured pressure increases according to the exponential law:

$$\ln\left(\frac{P}{P^\circ}\right) = \frac{-\Delta_{vap}H^\circ}{RT} + \frac{\Delta_{vap}S^\circ}{R}$$

This zone 1 is named "saturated vapor pressure range." If m/V ratio is large enough, then only saturated vapor pressure is measured in the experiment. Strictly speaking, zone 1 corresponds to some monovariant equilibrium, for which dependence of the vapor pressure from temperature is given by equation of the general type $\ln(P/P^\circ) = -A/T + B$. At the same time, the static method alone cannot provide full information about the nature (detailed type) of this monovariant equilibrium. Such information can be derived on

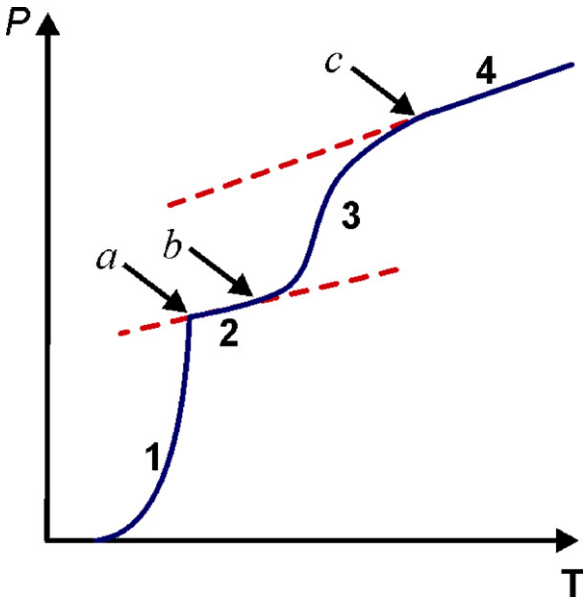

Fig. 12. General $P=f(T)$ dependence for the donor–acceptor complex. See text for details.

the basis of the analysis of all chemical and physico-chemical data known for the studied substance or system.

In case when m/V ratio is small, the substance can completely vaporize upon heating and condensed phase disappears. In such a case zone 2 appears, which is named "unsaturated vapor pressure range". The moment of disappearance of the condensed phase corresponds to the break on the exponential P–T dependence curve (point a). Coordinates of this break point are called "point of exit (or transformation) into the unsaturated vapor region". If transformation into unsaturated vapor occurs at $P<1$ atm and $T>400$ K, vapor behaves as an ideal gas. In this case in unsaturated vapor region (zone 2) vapor pressure upon subsequent temperature increase changes according to the law $P_1/T_1 = P_2/T_2 = \text{const}$. In other words, in such a case unsaturated vapor pressure corresponds to the thermal expansion line. Value of the P/T constant can be calculated if mass of the substance m, its molar mass M and working volume V are known. Then $P/T = \text{const} = (m/MV)R$. From the comparison between experimentally measured P/T and computed $(m/MV)R$ one can made definitive conclusion about the correspondence between the molecular mass of the compound in the condensed phase and molecular weight of its vapor in the studied temperature range. It should be noted, that if in some temperature interval unsaturated vapor pressure changes according to the thermal expansion line ($P/T = \text{const}$), this definitely evidences absence of the processes which are accompanied by the change of number of gaseous moles.

If, upon temperature increase, the process, which is accompanied by the increase of the number of gaseous moles, occurs in vapor, S-shaped zone 3 appears. Strictly speaking, this section corresponds to some bivariant equilibrium. The process "starts" when the deviation of measured pressure from the thermal expansion line becomes *greater* than the experimental error (point b), and "ends" when deviation of the measured pressure from the new thermal expansion line (zone 4) becomes *smaller* than the experimental error (point c). The difference between the initial and the final thermal expansion lines 2 and 4 is strictly determined by the change of the number of gaseous moles in the equilibrium process. However, similar to the case of zone 1, information about the detailed type of this bivariant equilibrium may be obtained only on the basis of the analysis of all chemical and physico-chemical data known for the studied substance or system.

Since only the variance of the corresponding equilibria determines the appearance of the zones shown in Fig. 12, the general type and the sequence of the segments (zones) on the $P=f(T)$ dependence diagram remains the same for the large number of chemical systems. Any thermodynamic investigation starts with identification of the equilibrium, which establishes in the system, and thermodynamic characteristics of which are necessary to determine. Often word "equilibrium" is substituted by word "process", under which one understands reversible process which leads to establishing of the equilibrium in the system.

Present review is devoted to the problem of thermal stability of molecular complexes or adducts AD_x. In general case one can consider $P=f(T)$ dependence which includes two primary processes: vaporization of adduct and its dissociation into components in the gas phase. As a rule, general features of the $P=f(T)$ dependence remain the same regardless of the chemical nature of the studied complex. Of course, in the real system these two major processes may be accompanied by others, such as polymerization (dimerization) of the acceptor molecules A, formation of the solutions of the dissociation products in the melt of the complex, or irreversible pyrolysis of the organic ligand D. Carefully conducted tensimetry investigation can either avoid or take into account undesired processes in the system.

4.2. Concurrence between vaporization and dissociation on the example of the adduct of 1:1 composition

Let us consider two principal processes: vaporization of the condensed (solid or liquid) adduct AD (process 1) and its dissociation in the gas phase (process 2):

$$\mathrm{AD_{(cond)}} = \mathrm{AD_{(gas)}}, \qquad K_1 = P_{\mathrm{AD}} \tag{1}$$

$$\mathrm{AD_{(gas)}} = \mathrm{A_{(gas)}} + \mathrm{D_{(gas)}}, \qquad K_2 = \frac{P_{\mathrm{A}} \times P_{\mathrm{D}}}{P_{\mathrm{AD}}} \tag{2}$$

Relative overlap of these processes in the temperature range is determined by values of the respective Gibbs free energies:

$$\Delta_{(1)}G^\circ = \Delta_{(1)}H^\circ - T\Delta_{(1)}S^\circ$$

$$\Delta_{(2)}G^\circ = \Delta_{(2)}H^\circ - T\Delta_{(2)}S^\circ$$

For the following analysis let us make several assumptions:

(1) Since each process is accompanied by 1 mole gas increase, for the simplicity let us assume that $\Delta_{(1)}S^\circ = \Delta_{(2)}S^\circ$.
(2) Let us assume that if value of $K_2 \leq 10^{-6}$ then dissociation of the gaseous adduct AD is negligible and only $\mathrm{AD_{(gas)}}$ exists in vapors. Accordingly, if $K_2 \geq 10^{+6}$ then adduct dissociation is complete and vapor consists only from the molecules of the dissociation products $\mathrm{A_{(gas)}}$ and $\mathrm{D_{(gas)}}$.
(3) Note that P_{AD} is the partial pressure of the saturated vapor of the adduct AD and it is in general not equal to the measured total pressure in the system P_{total}.

Thermodynamic characteristics of processes (1) and (2) are independent from each other, since these processes are governed by different forces: vaporization is determined by intermolecular interactions, while gas phase dissociation strongly depends on the intramolecular donor–acceptor interaction (energy of the donor–acceptor bond). Therefore, in general, superposition of the vaporization and dissociation processes may occur in different ways. Since for the simplicity reasons in this analysis entropy changes are assumed to be equal ($\Delta_{(1)}S^\circ = \Delta_{(2)}S^\circ$), concurrence between processes is determined by values of their respective enthalpies $\Delta_{(1)}H^\circ$ and $\Delta_{(2)}H^\circ$. Let us analyze four different scenaria, which are dependent on relative values of $\Delta_{(1)}H^\circ$ and $\Delta_{(2)}H^\circ$.

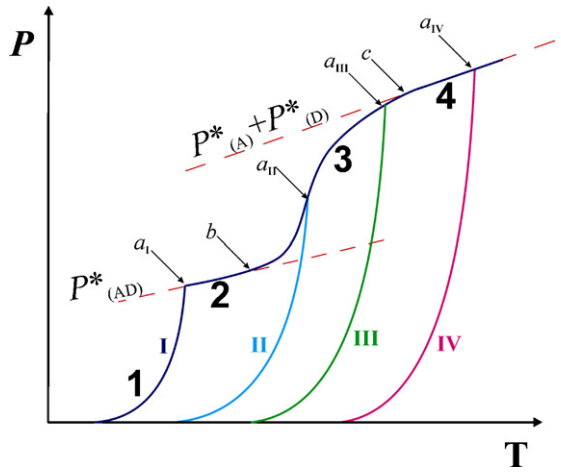

Fig. 13. Schematic $P=f(T)$ dependence for the vaporization and gas phase dissociation of the molecular complex AD. Different $P=f(T)$ dependence lines I, II, III, IV represent cases of concurrence between vaporization and dissociation. I. $\Delta_{(1)}H^\circ \ll \Delta_{(2)}H^\circ$; adduct AD vaporizes without dissociation. II. $\Delta_{(1)}H^\circ = \Delta_{(2)}H^\circ$; adduct AD vaporizes with noticeable dissociation into components. III. $\Delta_{(1)}H^\circ > \Delta_{(2)}H^\circ$; upon vaporization adduct AD dissociates considerably, but not completely. IV. $\Delta_{(1)}H^\circ \gg \Delta_{(2)}H^\circ$; adduct AD completely dissociates into components upon vaporization. a_I, a_{II}, a_{III}, a_{IV} – respective points of exit into unsaturated vapor region. b – start temperature for the measurable equilibrium dissociation of the adduct. c – end temperature for the measurable equilibrium dissociation of the adduct.

I. In the first scenario $\Delta_{(1)}H^\circ \ll \Delta_{(2)}H^\circ$ and adduct AD will vaporize without decomposition.

For example, if at boiling point of the adduct ($K_1 = P^\circ_{AD} = 1$) we assume that $K_2 = 10^{-6}$, we obtain

$$\frac{-\Delta_{(1)}H^\circ}{RT} + \frac{\Delta_{(1)}S^\circ}{R} = 0, \quad \frac{-\Delta_{(2)}H^\circ}{RT} + \frac{\Delta_{(2)}S^\circ}{R} = -13.8$$

Taking into account our assumption that $\Delta_{(1)}S^\circ = \Delta_{(2)}S^\circ$, we find:

$$\Delta_{(2)}H^\circ - \Delta_{(1)}H^\circ = 13.8RT,$$

where T – the boiling point of adduct.

It should be noted, that if the boiling point of adduct equals 500 K, then value of $13.8RT \approx 57.4$ kJ mol^{-1}. Taking into account that in the real systems the value of the dissociation entropy $\Delta_{(2)}S^\circ$ is generally larger than that of the vaporization entropy $\Delta_{(1)}S^\circ$, for the adducts which are *vaporized without dissociation into components*, vaporization (sublimation) enthalpy must be by about *60* kJ mol^{-1} *smaller* than the enthalpy of complex dissociation into components in the gas phase.

Curve I in Fig. 13 corresponds to the vaporization of the small amount of pure adduct without decomposition (saturated vapor region, zone 1). At low temperatures, after the exit of the system into the unsaturated vapor region at point "a_I", the dissociation of adduct is practically absent ($K_2 \leq 10^{-6}$) and vapor pressure initially follows the thermal expansion line $P^*_{(AD)}$ (zone 2). The crossing point "a_I" is easily obtained by the extrapolation of small parts of $\ln(P/P^\circ) = f(1/T)$ curves in saturated and unsaturated vapor regions. With a temperature increase value of the dissociation constant K_2 increases and at some temperature it becomes greater than 10^{-6} (point "b"). At this point, vapor pressure of the dissociation products becomes larger than the experimental error of pressure measurement, and measured total pressure P_{total} starts to deviate upwards from the thermal expansion line P^*_{AD}. As a result, S-shaped zone 3 appears, which represents vapor pressure–temperature dependence for the gas phase dissociation of adduct according to Eq. (2). At some temperature value of K_2 becomes equal to one, and then the partial pressures of adduct AD and its dissociation products A, D are comparable to each other (of the same order of magnitude). As the temperature increases, the equilibrium (2) of the dissociation of adduct more and more shifts to the right side. Above point "c" $K_2 \geq 10^{+6}$, the partial pressure of adduct P_{AD} approaches zero and the total pressure approaches the thermal expansion line of the dissociation products (zone 4), $P_{total} = P^*_A + P^*_D$, where P^*_A and P^*_D – vapor pressures of the ideal gases A and D.

II. In second scenario, let us assume that enthalpies of vaporization and gas phase dissociation of the adduct are equal, $\Delta_{(1)}H^\circ = \Delta_{(2)}H^\circ$. Then $\Delta_{(1)}G^\circ{}_T = \Delta_{(2)}G^\circ{}_T$ and since at the boiling point of adduct $K_1 = 1$ and $\Delta_{(1)}G^\circ{}_T = 0$, then $\Delta_{(2)}G^\circ{}_T$ also equals zero, $K_2 = 1$, and dissociation degree $\alpha = 50\%$. In this case, after the point of exit into unsaturated vapor (point a_{II}), vapor pressure continue to grow steeply and determination of the temperature of the point of exit into unsaturated vapor from the $P=f(T)$ curve is not straightforward. More precisely coordinates of point "a_{II}" are determined by the break of the line on the logarithmic graph $\ln(P/P^\circ) = f(1/T)$.

III. In third scenario, let us consider the situation when upon reaching the point of exit into unsaturated vapor region the adduct dissociates considerably, but not completely ($\Delta_{(1)}H^\circ > \Delta_{(2)}H^\circ$). This case is represented in Fig. 13, curve **III**. In unsaturated vapor region, curve in zone 3 approaches the thermal expansion line of the dissociation products $P^*_A + P^*_D$. The shape of the measured $P=f(T)$ dependence clearly indicates the end part of the S-shaped dissociation curve, indicating final stages of the adduct dissociation.

IV. Finally, as last scenario, $\Delta_{(1)}H^\circ \gg \Delta_{(2)}H^\circ$. Assuming that at the boiling point of adduct $K_2 = 10^{+6}$, we obtain:

$$\Delta_{(1)}H^\circ - \Delta_{(2)}H^\circ = = 13.8RT$$

where T – the boiling point of the adduct.

At 500 K, $\Delta_{(1)}H^\circ > \Delta_{(2)}H^\circ$ by 57 kJ mol^{-1}. In this case, upon vaporization there are no gaseous molecules of the adduct present in the gas phase, adduct completely dissociates into gaseous components $A_{(gas)}$ and $D_{(gas)}$. After the exit into the unsaturated vapor region (point "a_{IV}"), measured vapor pressure follows the sum of thermal expansion lines of individual components $P^*_A + P^*_D$. The crossing point "a_{IV}" is easily obtained by the extrapolation of small parts of $P=f(T)$ curves in saturated and unsaturated vapor region.

Usually, the experimentally measured unsaturated vapor region has rather small temperature range (it is often limited by side processes, such as thermal destruction of ligands). In practice, one or maximum two unsaturated vapor pressure zones can be completely measured in a single experiment (either zones 2 and 3 or zones 3 and 4). Therefore, it is hard to distinguish the case of the vaporization of adduct without dissociation from vaporization with complete dissociation into components by just looking on the $P=f(T)$ dependence alone, since in both cases in the unsaturated vapor region pressure follows the thermal expansion line. To distinguish between those cases, information about mass of the sample m and volume of the measuring chamber V is needed. One can find out if thermal expansion line corresponds to P^*_{AD} or $P^*_A + P^*_D$ by computing the mean molecular weight of vapor from the m/V ratio, since molecular mass of the adduct M_{AD} and mean molecular mass of the donor and acceptor components $M_{(A+D)} = 0.5\,(M_A + M_D)$ are significantly different.

From our thermodynamic analysis it follows that if the gas phase dissociation enthalpy is by 60 kJ mol^{-1} less than vaporization enthalpy, the adduct content in vapors will be negligible.

In the next chapter, we will discuss in more detail several illustrative examples of the tensimetric investigation of donor–acceptor complexes.

5. Illustrative examples

Several important case studies, illustrating different cases of behavior of complex compounds upon heating will be presented below in detail. A summary of all studied systems and determined thermodynamic characteristics of various processes involving Donor–acceptor complexes will be presented in Section 6 of present review.

5.1. Vaporization without dissociation and subsequent thermal dissociation and pyrolysis of the AlI_3·Py complex

The possibility of vaporization of the complex without dissociation into components is primarily determined by the strength of the donor–acceptor bond. Complexes with strong bonds have higher probability to exist in vapors. Aluminum–nitrogen bond is one of the strongest donor–acceptor bonds, and due to this strength the molecular complexes of aluminum trihalides with thermally stable amines do vaporize without decomposition and exist in vapors in wide temperature range (it can reach 100°) without noticeable dissociation into components. One of such complexes is AlI_3·Py, which vaporization was studied by static method [492].

Preliminary experiments showed that complex AlI_3·Py is sublimable in vacuum without noticeable decomposition and only above 200 °C has vapor pressure, measurable by the static method. Since the melting point of complex is 110 °C [493,494], the static method can be used to study liquid–vapor equilibrium and to obtain thermodynamic characteristics of the vaporization process.

First, vapor composition over the complex should be determined and possibility of thermal dissociation into components in the gas phase should be checked. To this end, measurements with small amount of the complex (to obtain unsaturated vapor range) have been carried out. Obtained results for the several heating/cooling runs of the series 2 are given in Fig. 14. In addition, the thermal expansion line $P^*_{AlI_3\cdot Py}$, computed from mass of the complex and the volume of the system, is given in Fig. 14:

$$P^*_{AlI_3\cdot Py} = \left(\frac{m}{V}\right)\left(\frac{R}{M}\right)T$$

where m, mass of the complex; V, volume of the measuring chamber, M, molar mass of complex, R, universal gas constant, T, absolute temperature.

It can be seen, that after the transition into the "unsaturated vapor range" at 315 °C (Fig. 14, point *a*), experimentally measured pressure P_{total} follows the thermal expansion line $P^*_{AlI_3\cdot Py}$ until 410–415 °C. From this follows, that:

(1) Mean molar mass of vapor equals to the molar mass of the complex AlI_3·Py.
(2) In 315–415 °C temperature range, there are no processes which lead to change of the mean number of gaseous moles in the system.

Therefore, at such conditions complex AlI_3·Py is stable and exist in vapors in monomeric form. Process of thermal dissociation of the complex into components is noticeable above 415 °C. Starting from this temperature the measured pressure P_{total} is greater than pressure computed according to the thermal expansion line $P^*_{AlI_3\cdot Py}$. As follows from good agreement between heating and cooling runs, dissociation process is reversible up to 470 °C. Subsequent prolonged heating above 470 °C results in irreversible growth of the total pressure due to thermal decomposition (pyrolysis) of the Py ligand (Fig. 14, runs 3–5). Therefore, determination of the thermodynamic characteristics of the reversible homogeneous gas phase dissociation is possible only for the narrow temperature interval (415–470 °C).

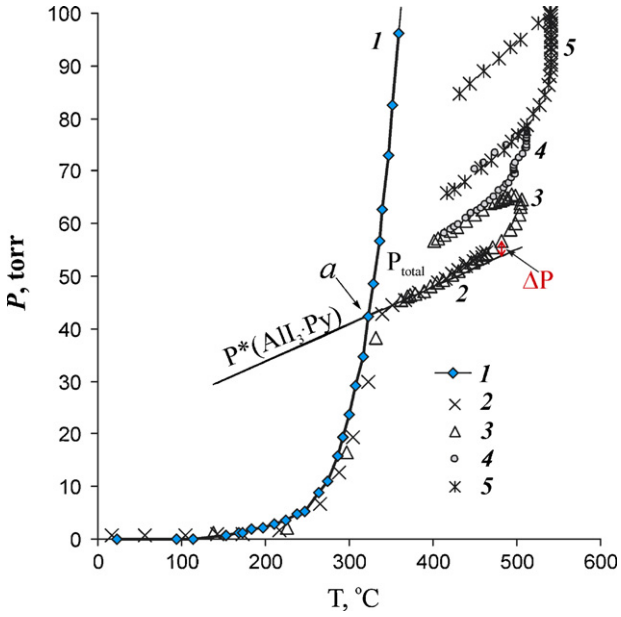

Fig. 14. Vapor pressure–temperature dependence for the complex AlI_3·Py.

In this interval, adduct reversibly dissociates into gaseous components according to equilibrium:

$$AlI_3 \cdot Py_{(gas)} = AlI_{3(gas)} + Py_{(gas)}$$

We must note that peculiarity of the system, such as very narrow temperature range and small dissociation degree of the complex at these conditions (dissociation pressure does not exceed 6 Torr) does not allow to obtain trustworthy results on the gas phase dissociation of AlI_3·$Py_{(gas)}$. Our estimated values are $\Delta_{diss}H^\circ_{709} = (156 \pm 7)$ kJ mol^{-1}, $\Delta_{diss}S^\circ_{709} = (146 \pm 9)$ J mol^{-1} k^{-1}.

From the fact that dissociation of the complex starts only after 415 °C, it follows that vapor pressure over the liquid complex is determined only by its vaporization:

$$AlI_3 \cdot Py_{(liquid)} = AlI_3 \cdot Py_{(gas)}$$

For the determination of thermodynamic characteristics of vaporization process, two sets of experiments have been carried out. Data obtained in series 1 (with large amount of the complex, ~400–500 mg) are more reliable since they are measured in wide temperature (200–405 °C) and pressure (2–280 Torr) range.

Table 11
Thermodynamic characteristics of vaporization process of AlI_3·Py [492].

Series	m, mg	Temperature range, K	$\ln(P/P^\circ) = -A/T + B$		T_{mean}, K	$\Delta_{vap}H^\circ_T$, kJ mol^{-1}	$\Delta_{vap}S^\circ_T$, J mol^{-1} K^{-1}	$T_{b.p.}$, K
			A	B				
1	>400	506–688 (96 points)	7976 ± 88	10.643 ± 0.088	598	66.3 ± 0.7	88.5 ± 1.2	749
2	57.55	516–658 (62 points)	8296 ± 113	11.110 ± 0.115	587	69.0 ± 0.9	92.4 ± 1.5	747

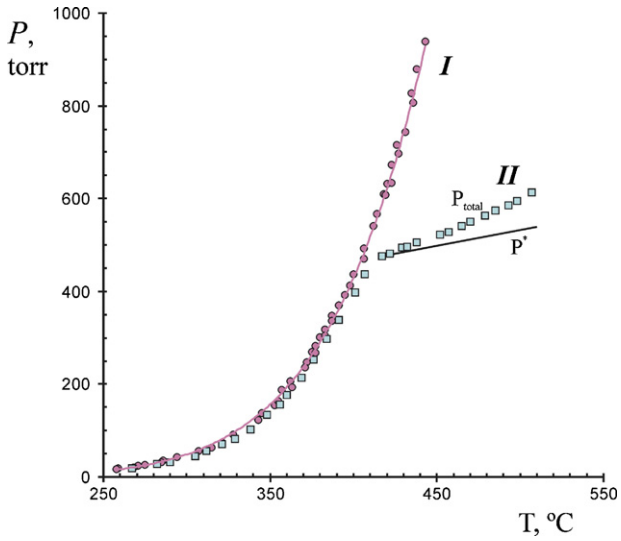

Fig. 15. Vapor pressure over the complex $GaCl_3{\cdot}NH_3$.

Vapor pressure of the complex, obtained on the basis of 96 experimental points, is given by the equation:

$$\ln\left(\frac{P}{P^\circ}\right) = \frac{-(7976 \pm 88)}{T} + (10.643 \pm 0.088)$$

Thermodynamic characteristics of vaporization process are given in Table 11. Comparison of A and B coefficients in $\ln(P/P^\circ) = f(1/T)$ dependence, enthalpies and entropies of vaporization, boiling temperature of the complex (obtained by extrapolation of $\ln(P/P^\circ) = f(1/T)$ equation on $P = 1$ atm) shows good agreement between first and second series, but results from series 1 are taken as reference values.

It should be noted, that monitoring the irreversible thermal pyrolysis of the complex with formation of carbon on the walls of the system in the temperature range 498–512 °C (Fig. 14, runs 3–5) allowed to estimate activation energy of pyrolytic process as 210 kJ mol^{-1} [492], which is significantly less than activation energy of free Py pyrolysis (439 ± 8 kJ mol^{-1}) [495].

5.2. Vaporization of the complex which is accompanied by the partial gas phase dissociation. $GaCl_3{\cdot}NH_3$ complex

Thermal behavior of $GaCl_3{\cdot}NH_3$ complex has been studied [496] up to 510 °C, since above this temperature the irreversible ammonolysis process starts [497]. First, an excess amount of $GaCl_3{\cdot}NH_3$ was introduced into apparatus and its saturated vapor pressure was measured up to 938 Torr (curve I, Fig. 15). After that, some (unknown) amount of complex was condensed in one of the parts of the measuring chamber and sealed off. Vapor pressure of saturated and unsaturated vapor was measured (curve II, Fig. 15). For the identification of the process upon vaporization of the complex let us consider results obtained for the unsaturated vapor range first.

5.2.1. Unsaturated vapor range

Unsaturated vapor pressure has been measured in temperature range 400–510 °C. Measured total pressure P_{total} in the unsaturated vapor range (Fig. 15, zone II) deviates from the thermal expansion line P^* which indicates adduct dissociation. The shape of the curve allows to conclude that this is a beginning of the dissociation process. Preliminary experiments showed that the partial pressure of the Ga_2Cl_6 dimer formed by complex dissociation in the studied temperature range is less than 0.5 Torr, which is less than

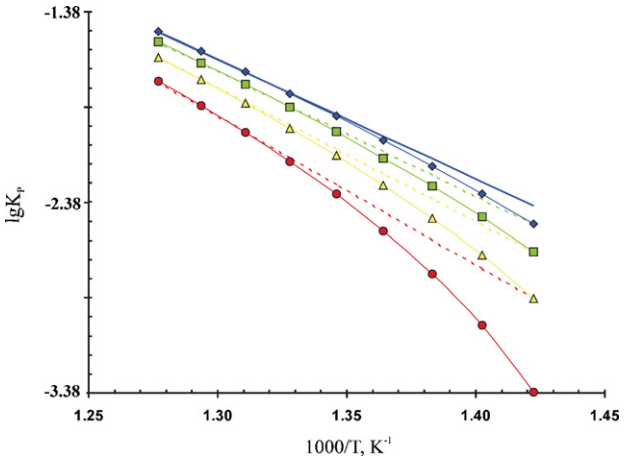

Fig. 16. Illustration of method of self-consistent approximations on the dependence of the lg K_P versus $1/T$ for $GaCl_3{\cdot}NH_3$.

experimental uncertainty (1–2 Torr). This allows one to completely neglect dimerization of $GaCl_3$ and compute vapor composition by solving the system of following equations:

$$\begin{cases} P_{total} = P_{GaCl_3{\cdot}NH_3} + P_{GaCl_3} + P_{NH_3} \\ P^*_{GaCl_3} = P_{GaCl_3{\cdot}NH_3} + P_{GaCl_3} \\ P^*_{NH_3} = P_{GaCl_3{\cdot}NH_3} + P_{NH_3} \end{cases} \quad (3)$$

where P_{total} – measured total pressure; $P_{GaCl_3{\cdot}NH_3}$, P_{GaCl_3}, P_{NH_3} – partial pressures of $GaCl_3{\cdot}NH_3$, $GaCl_3$ and NH_3, respectively; $P^*_{GaCl_3}$ and $P^*_{NH_3}$ – hypothetical pressures of non-interacting components (net composition of $GaCl_3$ and NH_3, respectively).

For the individual complex $GaCl_3{\cdot}NH_3$ due to the stoichiometric reasons $P^*_{GaCl_3} = P^*_{NH_3}$ and the system of Eq. (3) can be rewritten as (4):

$$\begin{cases} P_{total} = P_{GaCl_3{\cdot}NH_3} + P_{GaCl_3} + P_{NH_3} \\ P_{GaCl_3} = P_{total} - P^*_{GaCl_3{\cdot}NH_3} \\ P_{GaCl_3} = P_{NH_3} \end{cases} \quad (4)$$

where $P^*_{GaCl_3{\cdot}NH_3}$ – hypothetical vapor pressure of non-dissociated adduct, computed according to the thermal expansion line drawn throughout the point of exit into unsaturated vapor range.

Values of the partial pressures and equilibrium constants for the process:

$$GaCl_3 \cdot NH_{3(gas)} = GaCl_{3(gas)} + NH_{3(gas)},$$

$$K_P = \frac{P_{GaCl_3}P_{NH_3}}{P_{GaCl_3{\cdot}NH_3}} = \frac{(P_{total} - P^*_{GaCl_3{\cdot}NH_3})^2}{2P^*_{GaCl_3{\cdot}NH_3} - P_{total}}$$

are given in Table 12 and lg $K = f(1/T)$ dependence is shown in Fig. 16.

As can be seen, initial data points (series 1a) cannot be approximated by the straight line. Evidently, assuming that adduct is not dissociated at the first point of the unsaturated vapor region, we introduced a systematic error. The influence of this error is smaller in the region of larger dissociation degree, i.e. error is minimal for the high temperature points. In such situation, finding of the real values of K_P is possible by method of consequent approximations. Assuming that at last two points of series 1a values of K_P are closest to the true values, we extrapolate K_P up to the point with the lowest temperature $K_{P(703\,K)} = 0.98$ and find the corrected value of $P'^*_{GaCl_3{\cdot}NH_3}$ corresponding to the breaking point:

$$P'^*_{GaCl_3{\cdot}NH_3} = (P_{total} + K_P) - \sqrt{K_P(P_{total} + K_P)}$$

Table 12
Unsaturated vapor composition and dissociation constants of $GaCl_3{\cdot}NH_3$ adduct.

T, K	P_{total}, Torr	Initial ("zero") approximation			Third approximation		
		$P_{GaCl_3} = P_{NH_3}$, Torr	$P_{GaCl_3{\cdot}NH_3}$, Torr	$K_P \times 10^3$	$P_{GaCl_3} = P_{NH_3}$, Torr	$P_{GaCl_3{\cdot}NH_3}$, Torr	$K_P \times 10^3$
703	494.2	12.2	469.8	0.417	28.0	438.2	2.354
713	507.2	18.4	470.5	0.947	34.3	438.6	3.529
723	520.8	25.1	470.6	1.761	41.3	438.2	5.122
733	535.0	32.5	470.1	2.956	48.9	437.2	7.197
743	549.9	40.5	468.9	4.603	57.1	435.7	9.846
753	565.4	49.1	467.1	6.791	66.0	433.4	13.23
763	581.5	58.4	464.7	9.657	75.5	430.5	17.42
773	598.4	68.4	461.5	13.34	85.7	427.0	22.63
783	615.9	79.1	457.7	17.99	96.6	422.7	29.05

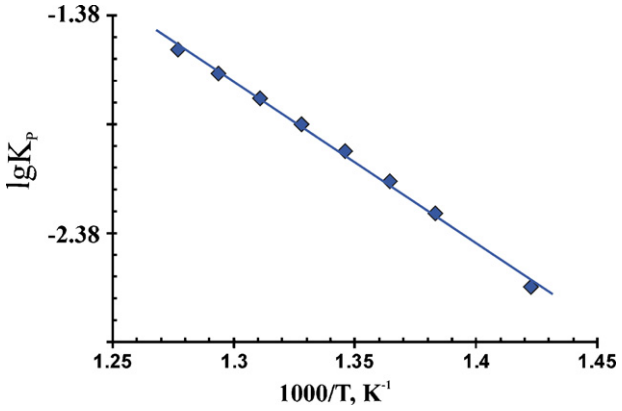

Fig. 17. Temperature dependence of the logarithm of dissociation constant $\lg K_P$ versus $1/T$ for gaseous $GaCl_3{\cdot}NH_3$.

Then for 703 K we obtain $P'^*_{GaCl_3{\cdot}NH_3} = 473.2$ Torr (original value $P^*_{GaCl_3{\cdot}NH_3} = 482.0$ Torr). Repeating all computations with a new $P'^*_{GaCl_3{\cdot}NH_3}$ value, we find values of $\lg K_P = f(1/T)$ in the first approximation (line 1, Fig. 16). Deviation from linearity in this case is considerably smaller compared to "zero" approximation (curve 1a), but still noticeable. Therefore, we performed computations in second and third approximations with $P''^*_{GaCl_3{\cdot}NH_3} = 469.1$ and $P'''^*_{GaCl_3{\cdot}NH_3} = 466.2$ (lines 2 and 3, respectively). For the fourth approximation obtained value within experimental error agrees with that of the third approximation, therefore self-consistence is achieved and one can use results of the third approximation. Note, that as a result of performed approximations, the original value of $P^*_{GaCl_3{\cdot}NH_3}$ changes from 482.0 to 466 Torr (only by 16 Torr or ~3%). Therefore, method of consequent self-consistent approximations indeed corrects the absolute value of $P^*_{GaCl_3{\cdot}NH_3}$ but does not contradict original assumption about small dissociation degree of $GaCl_3{\cdot}NH_3$ in unsaturated vapor region. Thus, dissociation degree $\alpha = P_{GaCl_3}/P_{total}$ at 703 K equals 5.7%. Table 12 summarize final results, and dependence of $\lg K$ from $1/T$ is shown in Fig. 17. Least squares method (LSM) treatment yields the following equation:

$$\ln K_P = (17.96 \pm 0.20) - \frac{16809 \pm 92}{T} (T = 703 - 783\,\mathrm{K}) \quad (5)$$

$$\Delta_{diss}H^\circ_{743} = (134.3 \pm 0.8)\,\mathrm{kJ\,mol^{-1}},$$

$$\Delta_{diss}S^\circ_{743} = (141.4 \pm 2.5)\,\mathrm{J\,mol^{-1}K^{-1}}$$

We must point out, that in this particular experiment neither mass m of the $GaCl_3{\cdot}NH_3$ adduct nor volume V of the system have been used to derive thermodynamic characteristics of the dissociation process.

5.2.2. Saturated vapor range

Now let us turn our attention to the saturated vapor range. Complex $GaCl_3{\cdot}NH_3$ melts at 124 °C [498], therefore vapor pressure measurements in the experiment correspond to the vaporization of the liquid complex. Taking the total pressure as $P_{GaCl_3{\cdot}NH_3}$ (neglecting dissociation of the complex) from $\ln(P/P^\circ) = f(1/T)$ one should obtain values of vaporization enthalpy and entropy. However, such treatment does not take into account the adduct dissociation. At the highest temperature 443 °C dissociation degree of $GaCl_3{\cdot}NH_3$ adduct equals 6.5%, which is considerable. Using determined earlier characteristics of the dissociation of the gaseous adduct (Eq. (5)), equilibrium dissociation of the complex in the saturated vapor region has been taken into account. Partial pressure of the pure (non-dissociated) adduct in the saturated vapor region can be found using the system of following equations:

$$\begin{cases} P_{total} = P_{GaCl_3{\cdot}NH_3} + P_{GaCl_3} + P_{NH_3} \\ K_P = \dfrac{P_{GaCl_3} P_{NH_3}}{P_{GaCl_3{\cdot}NH_3}} \\ P_{GaCl_3} = P_{NH_3} \end{cases}$$

from which $P_{GaCl_3{\cdot}NH_3} = (P_{total} + 2K_P) - 2\sqrt{K_P(P_{total} + K_P)}$

Selected results are given in Table 13 and Fig. 18. As can be seen from Table 13, at the highest temperatures of the saturated vapor region the difference between total pressure and partial pressure

Table 13
Vapor composition of the saturated vapors taking into account equilibrium dissociation of the $GaCl_3{\cdot}NH_3$ complex.

T, K	P_{total}, Torr	$P_{GaCl_3} = P_{NH_3}$, Torr	$P_{GaCl_3{\cdot}NH_3}$, Torr	$\ln(P_{GaCl_3{\cdot}NH_3}/P^\circ)$
532	18	0.1	17.7	−3.76
559	35	0.4	34.2	−3.10
580	55	0.8	53.4	−2.66
618	138	3.1	131.8	−1.75
645	248	7.3	233.3	−1.18
664	369	12.9	343.2	−0.80
673	436	16.6	402.9	−0.63
693	632	28.4	575.2	−0.28
708	828	41.7	744.5	−0.02
716	938	50.5	836.9	0.10

Table 14
Thermodynamic characteristics of adduct vaporization computed from the total pressure P_{total} and partial pressure of $GaCl_3{\cdot}NH_3$ adduct $P_{GaCl_3{\cdot}NH_3}$ over the $GaCl_3{\cdot}NH_3$ melt.

Source pressure for computation	$\ln(P/P^\circ) = -A/T + B$		ΔH°_T, kJ mol^{-1}	ΔS°_T, J K^{-1} mol^{-1}	$T_{b.p.}$, K
	A	B			
P_{total}	8444 ± 55	11.97 ± 0.07	70.0 ± 0.5	99.3 ± 0.5	705
$P_{GaCl_3{\cdot}NH_3}$	8241 ± 51	11.60 ± 0.05	68.4 ± 0.4	96.3 ± 0.4	710

of the $GaCl_3{\cdot}NH_3$ adduct is considerable (about 100 Torr). This difference also affects thermodynamic characteristics of vaporization process (Table 14). Our final recommended values for the vaporization enthalpy and entropy of the $GaCl_3{\cdot}NH_3$ complex are:

$$\Delta_{vap}H^\circ_{624} = (68.4 \pm 0.4)\,\text{kJ mol}^{-1},$$

$$\Delta_{vap}S^\circ_{624} = (96.3 \pm 0.4),\ \text{J mol}^{-1}\text{K}^{-1}$$

5.3. Vaporization of complex which is accompanied by the significant dissociation in the gas phase. Vaporization and equilibrium dissociation of $GaI_3{\cdot}Py$ adduct

In many cases dissociation of adduct is already significant in the saturated vapor pressure region. Therefore, at the point of exit into the unsaturated vapor region, comparable quantities of AD and its dissociation products are present in vapors. In such a case determination of the P^*_{AD} from the $P = f(T)$ dependence alone (as may be performed for the $AlI_3{\cdot}Py$ adduct, Section 5.1, Fig. 14) is not possible. Correction of P^*_{AD} by method of self-consistent approximations (described in Section 5.2 on the example of $GaCl_3{\cdot}NH_3$ adduct) is also not possible, since it assumes that adduct dissociation in vapor phase is very small. In such a situation, knowledge of the mass and volume of vapor is required for the determination of the P^*_{AD} via equation:

$$P^*_{AD} = \left(\frac{m}{M}\right)\left(\frac{RT}{V}\right) \quad (6)$$

where m – mass of vapor, V – volume of the system, M – molecular mass of the adduct, T – temperature and R – gas constant.

The error in P^*_{AD} is primarily determined by the experimental error in determination of mass of the adduct m. On the one hand, mass of the adduct should be small in order to achieve the exit into the unsaturated vapor region, on the other hand the small value of m is determined with large experimental error. This problem is specific for the group 13 metal trihalide complexes, which are highly hydrolysable and must be handled in wholeglass systems under vacuum. In order to obtain more reliable values of the equilibrium constants, additional experiments should be performed, which are carried out with excess of one of the components. Introduction of the additional Donor or Acceptor component shifts the equilibrium in favor of complex formation and allows one to confirm the independence of the equilibrium constant from the chemical composition of the system.

Let us in more detail consider results obtained for the GaI_3–Py system [499]. Thermal behavior was studied up to 422 °C. Four independent experiments have been carried out, which differ by component ratio $n(GaI_3)/n(Py)$ and m/V ratio (mass of the substance to the volume of measuring chamber). Both saturated and unsaturated vapor pressure regions have been measured. The summary of performed experiments is given in Table 15, and selected results are shown in Fig. 19.

In series 1, small amount of the complex was introduced into the measuring chamber and vapor pressure–temperature dependence has been measured (curve 1, Fig. 19). Regions of saturated and unsaturated vapor are clearly distinguishable.

5.3.1. Unsaturated vapor region

Since mass of the complex and volume of the measuring chamber is known, hypothetical vapor pressure of the non-dissociated adduct $P^*_{GaI_3{\cdot}Py}$ can be computed according to Eq. (6). In Fig. 19 this line is denoted $P^*(GaI_3{\cdot}Py)$. The difference between total pressure P_{total} and P^* equals to the vapor pressure of one of dissociation products and will be denoted ΔP:

$$\Delta P = P_{total} - P^*_{GaI_3{\cdot}Py}$$

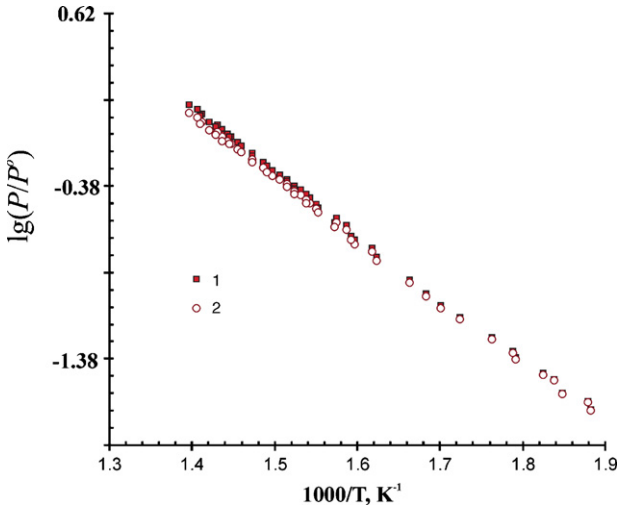

Fig. 18. Logarithmic dependence of the saturated vapor pressure over $GaCl_3{\cdot}NH_3$ versus $1/T$. 1 – total pressure; 2 – partial pressure of the $GaCl_3{\cdot}NH_3$ adduct.

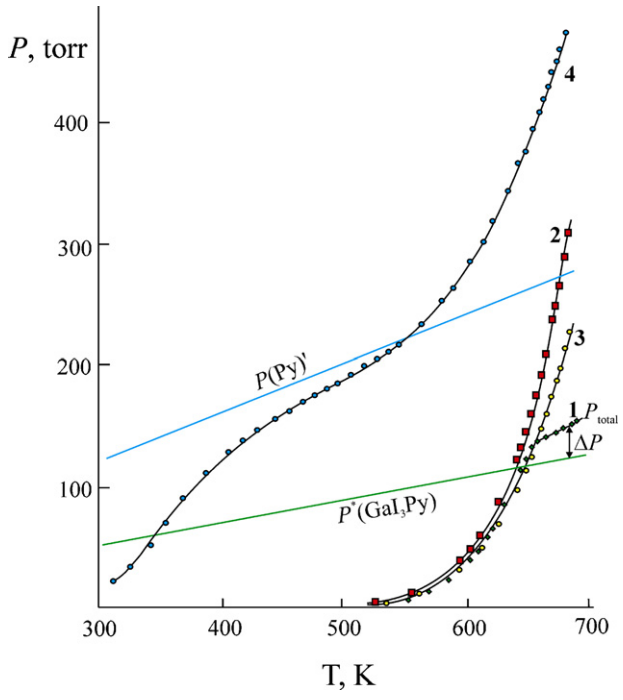

Fig. 19. Vapor pressure–temperature dependence for $GaI_3{\cdot}Py$ system.

Table 15
Summary of the performed experiments in GaI_3·Py system.

Series	Temperature interval, K	m, mg	n(Py)/n(GaI_3)	V, ml	Comment
1	293–639	49 (GaI_3·Py)	1:1	32.77	Unsaturated vapor
2	293–693	5.75 (Py) 29.2 (GaI_3)	1.12:1	27.34	Unsaturated vapor
3	293–683	170 (GaI_3·Py)	1:1	–[a]	Saturated vapor
4	293–693	31.6 (Py) 81.6 (GaI_3)	2.29:1	34.13	Saturated vapor

[a] Volume was not measured.

Table 16
Computations of vapor composition and equilibrium dissociation constant in GaI_3·Py system (series 1).

T, K	P_{total}, Torr	$P^*_{(adduct)}$, Torr	$P_{GaI_3} = P_{Py}$, Torr	$P_{GaI_3\cdot Py}$, Torr	$K_P \times 10^3$
653.4	132.1	115.1	17.0	98.1	3.88
661.3	136.2	116.5	19.7	96.8	5.28
667.7	139.2	117.6	21.6	96.1	6.39
671.3	141.0	118.3	22.7	95.5	7.10
676.2	143.5	119.1	24.4	94.8	8.26
680.8	145.6	119.9	25.7	94.3	9.22
684.3	147.8	120.6	27.2	93.3	10.43
687.8	150.1	121.2	28.9	92.3	11.91
691.1	151.4	121.8	29.6	92.1	12.52

At point of exit into the unsaturated vapor $\Delta P = 17$ Torr which amounts more than 12% from the total pressure. This shows noticeable adduct dissociation. It is well known that gallium trihalides form dimeric molecules in the gas phase. Comparison of P_{total} and P^* shows, that at 690 K dissociation degree amounts to 30%, and partial pressures of GaI_3 and Py are about ~30 Torr each. Using dimerization constant from [500], computed vapor pressure of the Ga_2I_6 dimer at these conditions is only 0.06 Torr, which is considerably less than experimental error of the vapor pressure measurements. At lower temperatures $P_{Ga_2I_6}$ will be even smaller. Therefore, in further considerations vapor pressure of Ga_2I_6 was assumed negligible and it was assumed that gallium triiodide exists only in monomeric form GaI_3. Computation of the unsaturated vapor composition is carried out according to the system of the equations, which is analogous to system (5) from the previous chapter. Results are presented in Table 16.

For the determination of more reliable equilibrium constant, and confirmation of its independence on the vapor composition, a second experiment was carried out with small excess of Py (ratio n(Py)/n(GaI_3) = 1.12:1). At such ratio of the components P^* is the sum of the hypothetical vapor pressures of undissociated adduct $P^*_{GaI_3\cdot Py}$ and excess Py ($P^*_{Py'}$):

$$P^* = P^*_{GaI_3\cdot Py} + P^*_{Py'}$$

Since masses of the components and volume of the system (volume of vapor) are known, values of $P^*_{GaI_3\cdot Py}$ and $P^*_{Py'}$ may be computed at any given temperature:

$$P^*_{GaI_3\cdot Py} = \left(\frac{n_{GaI_3\cdot Py}}{V}\right) RT \quad \text{and} \quad P^*_{Py'} = \left(\frac{n'_{Py}}{V}\right) RT$$

where n'_{Py} corresponds to the excess Py with respect to complex of 1:1 composition.

Computation of the equilibrium constant of the gas phase dissociation process in this case:

$$GaI_3 \cdot Py_{(gas)} = GaI_{3(gas)} + Py_{(gas)} \qquad (7)$$

was carried out according to formulae:

$$K_P^{diss} = \frac{P_{GaI_3} P_{Py}}{P_{GaI_3\cdot Py}} = \frac{(P_{total} - P^*)(P_{total} - P^* + P^*_{Py'})}{2P^* - P_{total} - P^*_{Py'}}$$

Results of computations of vapor composition and equilibrium constant are given in Table 17.

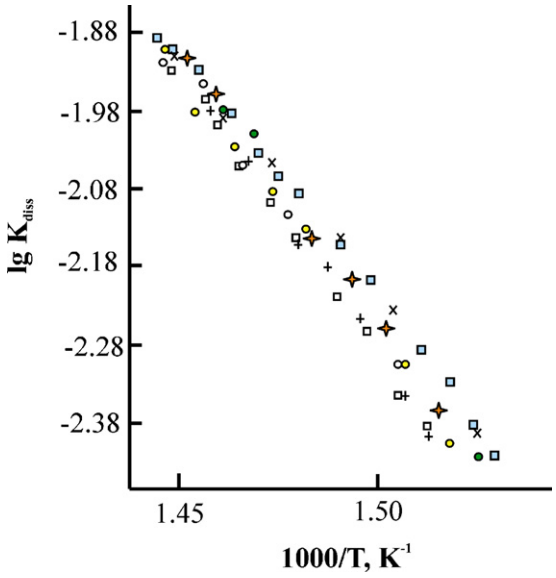

Fig. 20. $\lg K = f(1/T)$ dependence for the dissociation of the GaI_3·Py adduct.

All data on the equilibrium constants of the process (7), obtained in experiments 1 and 2, are given in Fig. 20 as $\lg K^{diss} = f(1/T)$ dependence. Data for several heating and cooling runs of both experiments are presented (more than 50 independent experimental data points in total). Data of individual runs are slightly different from each other, but the difference is not systematic and caused by statistical errors of the experiment. For the equation $\ln K^{diss} = -A/T + B$, A and B coefficients have been computed using LSM separately for the each experiment and for all experimental data points. They are summarized in Table 18. From these data thermodynamic characteristics of the GaI_3·Py adduct dissociation have been obtained.

5.3.2. Saturated vapor region

Now, when $\ln K^{diss} = f(1/T)$ dependence for the gas phase dissociation of the adduct is known, lets turn our attention to the saturated vapor pressure region. Melting point of the GaI_3·Py complex is 98 °C [501]. For the determination of vaporization characteristics, a special experiment with larger (by 3.5 times more than in experiment 1) amount of complex was carried out. The measured vapor pres-

Table 17
Computations of vapor composition and equilibrium dissociation constant in GaI_3·Py system (series 2).

T, K	P_{total}, Torr	P^*, Torr	P_{Py}, Torr	P_{GaI_3}, Torr	$P_{GaI_3\cdot Py}$, Torr	$K_P \times 10^3$
658.4	120.5	109.2	23.1	11.3	86.1	3.99
663.7	123.2	110.1	25.0	13.1	85.1	5.06
675.1	128.5	112.0	28.6	16.5	83.4	7.45
679.1	130.2	112.7	29.7	17.5	82.9	8.25
683.5	143.5	113.4	31.1	18.8	82.3	9.35
688.2	134.2	114.2	32.4	20.0	81.8	10.42
692.4	137.1	114.9	34.7	22.2	80.2	12.64
685.0	133.6	113.6	32.3	20.0	81.4	10.44
681.2	129.4	113.0	28.6	16.4	84.4	7.31

Table 18
Thermodynamic characteristics of the GaI_3·Py adduct dissociation.

Series	Temperature range, K	$\ln K_P = -A/T + B$		T_{mean}, K	$\Delta_{diss}H^\circ$, kJ mol^{-1}	$\Delta_{diss}S^\circ$, J mol^{-1} K^{-1}
		A	B			
1	655–695	15,658 ± 345	18.28	675	130 ± 2.9	151.7
2	655–695	14,552 ± 553	16.65	675	121 ± 4.7	138.1
All points		14,944 ± 668	17.22	675	124 ± 5.0	143.0

sure – temperature dependence is given in Fig. 19, curve 2. Vapor pressure is noticeable above 200 °C and corresponds to vaporization of the complex. Compared to the AlI_3·Py adduct, which was stable in the saturated vapor pressure range, GaI_3·Py is dissociated in vapors (dissociation degree is about 30% at 690 K), and the measured vapor pressure in the saturated vapor region P_{total} is the sum of partial pressures of the adduct and its dissociation products. Dissociation should be taken into account for the determination of the saturated vapor pressure of the pure adduct. Temperatures, at which dissociation of the complex is significant, are close to the critical temperature of pyridine (620 K) [502], therefore pyridine solvation in the melt of the complex can be neglected.

Vapor pressure–temperature dependence for the vapor pressure of pure (undissociated) GaI_3·Py complex is given in Fig. 19, curve 3. Results of one of the heating are given in Table 19. LSM treatment of all data points yielded the following equation:

$$\ln \frac{P}{P^\circ} = (13.38 \pm 0.40) - \frac{9878 \pm 322}{T} \quad (465 - 695\ \mathrm{K})$$

and thermodynamic characteristics of the vaporization of the adduct:

$$\Delta_{vap}H^\circ_{580} = (82.0 \pm 2.7)\ \mathrm{kJ\,mol^{-1}},$$

$$\Delta_{vap}S^\circ_{580} = (111.1 \pm 3.3)\ \mathrm{J\,mol^{-1}\,K^{-1}}$$

In order to suppress the dissociation of the complex, experiment 4 with twofold excess of Py was carried out (curve 4, Fig. 19). From the initial part of the curve one can see interaction of excess of Py with the melt of the complex. However, at temperatures when vapor pressure of the complex is noticeable, full amount of the excess Py exists in the gaseous phase. Additional amount of Py suppress dissociation of the complex, and the saturated vapor pressure of undissociated adduct can be obtained from the difference between the measured vapor pressure and the vapor pressure of thermal expansion of pyridine excess, denoted as $P(\mathrm{Py})'$.

At 600 K the saturated vapor pressure of undissociated adduct is ~40 Torr, and the value of equilibrium dissociation constant is 0.4 (Table 19). At excess vapor pressure of Py (240 Torr) the vapor pressure of dissociation product of the complex (GaI_3) is only ~0.1 Torr. At maximal temperature 680 K the vapor pressure of dissociation products increases to 4 Torr, which is still considerably less than the saturated vapor pressure of GaI_3·Py adduct (~180 Torr).

For this experiment the following system of equations was used for computing vapor composition:

$$\begin{cases} P_{total} = P_{GaI_3\cdot Py} + P_{GaI_3} + P_{Py} \\ P^*_{GaI_3} = P^*_{GaI_3\cdot Py} = \dfrac{n_{GaI_3}RT}{V} = P_{GaI_3\cdot Py} + P_{GaI_3} \\ P^*_{Py} = P^*_{GaI_3\cdot Py} + P^*_{Py'} = \dfrac{n_{Py}RT}{V} = P_{GaI_3\cdot Py} + P_{Py} \end{cases}$$

Results are given in Table 20. The comparison of obtained vapor pressures of the undissociated adduct with values shown in Table 19 gives reasonable agreement between the two experiments, but not the exact match. Introduction of highly hydrolyzed substances in the measuring volume is a complicated task. In most of the cases the mass of substance is obtained as a difference between masses of a glass capillary with and without a substance. The mean error in determination of the mass of the substance is about ±0.5 mg. As a result, a systematic error is introduced into the value of P^*, and therefore, ΔP which affects the computed on its basis equilibrium partial pressures. For the analysis of this factor computations of partial pressures have been performed on the basis of two extreme values of mass of Py: (m_{Py} = 31.65 mg и m_{Py} = 32.95 mg), which differ only by 1.3 mg. However, this small mass difference significantly change the line of thermal expansion of the excess pyridine $P^*_{Py'}$, computed on its basis ratio $P^*_{Py'}/T$ changes from 0.4003 to 0.4288 (about 7% increase). As a result, computed partial pressures change significantly (Table 20), which seriously affects determined thermodynamic characteristics. Therefore, data from experiment 4 should be used only as a confirmation of the thermodynamic values of vaporization of GaI_3·Py adduct, obtained in experiment 3 (Table 19). Thus, the error in determination of the thermodynamic characteristics for GaI_3·Py adduct primarily depends on the error in determination of P^*/T, which for this particular system can be obtained only with use of the mass of the substance. More accurate value of P^*/T is determined directly from the tensimetric data (provided that there is a range with constant P^*/T), as was shown for AlI_3·Py adduct (Section 5.1). Another example of the successful use of this approach will be discussed in the following chapter.

5.4. Vaporization with congruent dissociation of the solid adduct into gaseous products. System $SnCl_4$–dioxan

Investigation of the $SnCl_4$–dioxan system exemplifies the use of tensimetric method for the solution of the following problems:

Table 19
Computation of the vapor composition for series 3 and 4 in GaI_3–Py system.

T, K	P_{total}, Torr	$K_P \times 10^3$	P_{GaI_3}, Torr	$P_{GaI_3 \cdot Py}$, Torr
Series 3				
476.5	1.3	0.0007	–[a]	1.3
524.2	5.9	0.013	0.4	5.1
553.1	12.2	0.055	0.7	10.8
592.0	36.6	0.33	2.8	31.0
602.4	46.3	0.51	3.85	38.6
615.1	64.6	0.85	5.85	52.9
657.8	172.2	4.11	20.25	131.7
661.9	188.2	4.72	22.65	142.9
665.7	204.9	5.37	25.15	154.6
674.5	246.4	7.20	31.65	183.1
678.2	262.2	8.12	34.55	193.1
682.3	286.7	9.28	36.1	214.5
684.8	301.4	10.03	40.9	219.6

T, K	P_{total}, Torr	m(Py) = 31.65 mg		m(Py) = 32.95 mg	
		$P_{Py'}$, Torr	$P_{GaI_3 \cdot Py}$, Torr	$P_{py'}$, Torr	$P_{GaI_3 \cdot Py}$, Torr
Series 4					
590.15	261.1	236.3	24.9	253.1	8.0
604.6	281.8	242.0	40.0	259.2	22.6
616.1	299.9	246.6	53.3	264.1	35.8
624.2	314.8	249.9	64.9	267.7	47.1
658.0	387.7	263.4	124.3	282.2	105.5
663.4	401.1	265.6	135.5	284.5	116.6
675.2	434.8	270.3	164.5	289.5	145.3
678.1	443.6	271.5	172.1	290.8	152.8
681.7	454.1	272.9	181.2	292.3	161.8
686.4	466.4	274.8	191.6	294.3	172.1
691.4	476.9	275.5	194.6	295.1	175.0

[a] Less than experimental error.

1. Determination of the number of complexes formed in the system $SnCl_4$–dioxane and their chemical composition.
2. Determination the principal character of the process upon heating of adducts.
3. Determination of thermodynamic characteristics of this process.

Data on complex formation between $SnCl_4$ and bidentate oxygen-containing donor dioxan (DO–$C_4H_8O_2$) are controversial. According to Rheinboldt [503] product of interaction has $SnCl_4 \cdot 2DO$ composition; however cryoscopy titration of $SnCl_4$ by dioxan in benzene indicates formation of adduct of $SnCl_4 \cdot DO$ composition [504]. Tensimetric method allows one to determine both the number of complexes and their chemical composition. To this end, two series of experiments have been carried out [505]. Vapor pressure–temperature dependence measurements were carried out from 25 to 250 °C. At higher temperatures irreversible thermal destruction of dioxan was evident. Measured vapor pressures varied from 1 to 790 Torr.

The sequence of experimental measurements will be considered on the example of series 1, where measurements on pure DO and then on its mixture with $SnCl_4$ were carried out. Initially, 0.0209 g of DO was introduced into the measuring chamber (V = 30.19 ml) and its saturated and unsaturated vapor pressures have been measured. Good agreement with literature data indicates purity of the substance.

In the unsaturated vapor region (temperatures 60–180 °C, pressures 150–200 Torr) vapor pressure of DO follows the thermal expansion line. This line is characterized by the constant ratio P/T, which in turn connected with m/V ratio:

$$\frac{P}{T} = \left(\frac{m}{V}\right)\left(\frac{R}{M}\right)$$

If values of P/T and $(m/V)(R/M)$ are not in agreement with each other, and the difference is greater than the experimental error, this indicates systematic error on the mass of the substance. Measured P_{DO}/T for pure DO is 0.4761 ± 0.0019 and it is constant within whole temperature range. This confirms the absence of association of DO molecules in vapors, absence of significant adsorption of DO on the surface of apparatus and the absence of chemical interaction with material of apparatus. From P/T ratio one can obtain the amount of substance in known volume of the measuring chamber $n_{DO} = (P/T)(V/R) = 2.303 \times 10^{-4}$ mol. The amount of DO in the apparatus, obtained from the mass of the sample, equals 2.375×10^{-4} mol. The difference between values amounts 3%, which upon converting to mass of dioxan equals 0.6 mg, which can be attributed to weighting error (see previous chapter). Amount of DO obtained from P/T ratio in unsaturated vapor range is more trustable and will be used in the following analysis. Thus, the first experiment in series I allowed to confirm the purity and precisely determine quantity of dioxan in the system.

After that small amount of $SnCl_4$ was introduced into the apparatus via special compartment. Amount of $SnCl_4$ was chosen so, that part of dioxane will be in excess with respect to the complex of 1:1 composition. Upon introduction of $SnCl_4$, the volume of measured

Table 20
Thermodynamic characteristics of adduct vaporization computed from the partial pressure of $GaI_3 \cdot Py$ adduct over the $GaI_3 \cdot Py$ melt.

Series	Temperature range, K	$\ln(P/P^\circ) = -A/T + B$		T_{mean}, K	$\Delta_{vap}H^\circ$, kJ mol^{-1}	$\Delta_{vap}S^\circ$, J mol^{-1} K^{-1}
		A	B			
3	465–695	9878 ± 322	13.38 ± 0.40	580	82 ± 2.7	111.1 ± 3.3
4	565–695	9487 ± 415	12.53	630	78.8 ± 3.5	103.8

Table 21
Details of experiments for the determination of complex composition in system $SnCl_4$–dioxan.

Series	P_1/T	P_{excess}/T	P_{total}/T	$P_1/T - P_{excess}/T = n_1$	$P_{total}/T - P_1/T = n_2$	Complex composition n_2/n_1
1[a]	0.4826 ± 0.0040	0.2179 ± 0.0048	0.7530 ± 0.0040	0.2647	0.2704	1.022
2[b]	0.5203 ± 0.0030	0.3037 ± 0.0052	0.7379 ± 0.0023	0.2166	0.2176	1.005

[a] In series 1, first component DO, second – $SnCl_4$.
[b] In series 2, first component $SnCl_4$, second – DO.

chamber lowers due to sealing off some branches, and P_{DO}/T ratio changes accordingly to 0.4826 ± 0.0040 and will be denoted later as P_1/T (Table 21).

Immediately after the introduction of $SnCl_4$ into the measurement chamber, the reaction between DO and $SnCl_4$ starts. As a result, white solid substance is formed, and some amount of colorless liquid remains. *A priori*, one can assume three possible cases:

(1) Interaction leads to formation of complex of 1:1 composition, which in excess of DO partially forms $SnCl_4 \cdot 2DO$ complex. Presence of the liquid phase after the interaction allows to dismiss this case immediately.
(2) Complex of 1:1 composition is formed and excess of DO remains as a liquid phase.
(3) Complex $SnCl_4 \cdot 2DO$ is formed, and the liquid phase corresponds to $SnCl_4$.

For the correct choice between cases 2 and 3, additional experimental data are necessary. After the mixing of components, apparatus was heated in order to achieve equilibrium and then vapor pressure–temperature dependence was measured. Obtained data are shown in Fig. 21 (curve 1). In this curve four regions can be identified. Region "*a*" coincides with saturated vapor curve of pure DO and lies very far off from the saturated vapor pressure of $SnCl_4$. That confirms case 2—formation of the solid $SnCl_4 \cdot DO$ adduct which is not soluble in excess of dioxane. Region "*b*" corresponds to the unsaturated vapor pressure of DO excess. From the P/T ratio in this region, the exact amount of DO excess is given by equation $P_{excess}/T = 0.2179 \pm 0.0048$, which allows to compute vapor pressure of DO excess at any given temperature.

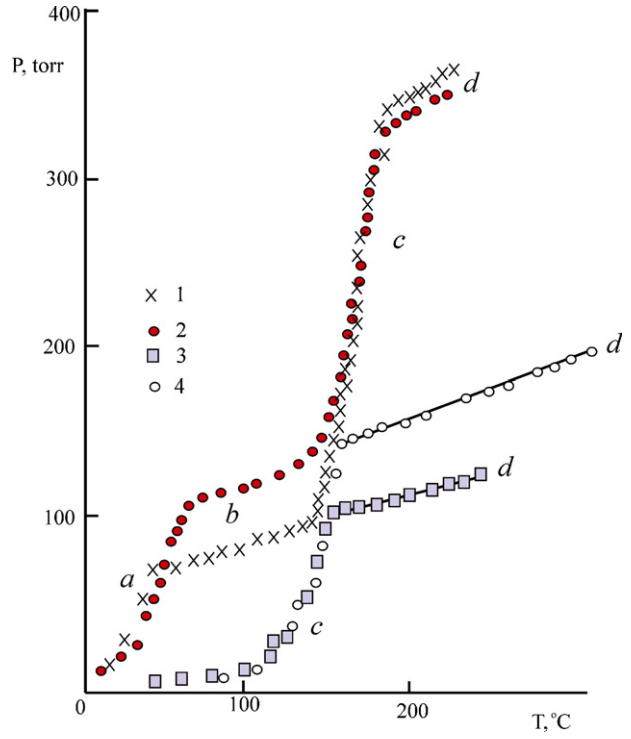

Fig. 21. Vapor pressure temperature dependence in $SnCl_4$–dioxan system.

In region "*c*" the vapor pressure of complex is measured. Finally, a region "*d*" (from 184 to 216 °C) corresponds to the total transition of system into the homogeneous gaseous state (pressure follows the thermal expansion line, ratio $P_{total}/T = 0.7530 \pm 0.0040$ (Table 21).

At the end of first series, the following values have been measured: P_1/T – total amount of DO in the system, P_{total}/T – total amount of all gaseous substances in the system, P_{excess}/T – amount of excess (not complexed) DO (Table 21).

Difference $P_{total}/T - P_1/T = P_2/T$ allows to determine quantity of second introduced component ($SnCl_4$) and establish the ratio of components in first series: 35.9% (molar percent) $SnCl_4$ and 64.1% (molar percent) DO. Difference $P_1/T - P_{excess}/T = n_1$ gives amount of *complexed* DO, while $P_{total}/T - P_1/T = n_2$ gives amount of *complexed* $SnCl_4$. Ratio n_2/n_1 describes complex composition (ratio of the components in the complex).

Series 2, represented by curve 2 in Fig. 21, was carried out analogously to series 1, but $SnCl_4$ was introduced first. Excess of $SnCl_4$ was used in series 2; its amount in the system was 68.61% molar percent. Values of P/T for this series are also listed in Table 21. The ratio of amounts of reacted compounds definitely establishes the complex composition as 1:1. No other species are formed under experimental conditions, and excess components vaporize separately from the complex.

For the determination of the main character of the process upon complex vaporization, series 3 and 4 with small amounts of specially prepared complex have been studied. Obtained $P = f(T)$ dependences are shown in Fig. 21 (curves 3 and 4). Each of these curves is composed from two regions: the region "*c*" corresponds to vapor pressure of the solid complex, and the region "*d*" corresponds to the unsaturated vapor (homogeneous gas phase system). For the region "*c*" vapor pressures in series 3 and 4 are in good agreement with each other. Points of exit into the unsaturated vapor are sharp and very well defined. In series 3 the unsaturated vapor region exists from 157 to 250 °C, in series 4—from 160 to 310 °C. Ratios of P/T are constant within 1–2% for these temperature ranges, which indicates the absence of processes in the gas phase which are accompanied by the change of number of gaseous moles. This is possible in two cases: either the gaseous complex is stable and does not dissociate in this temperature range or the complex is completely dissociated and only donor and acceptor molecules are present in the gas phase.

For the determination of vapor composition for the unsaturated vapor range the values of mean molecular mass of vapor have been computed $M_{exp} = (m/V)R/(P/T)$ (Table 22). In the last column the theoretical values of molecular mass of vapor (M_{theor}) are given. They are computed for the two extreme cases: (1) for the total dissociation of the complex upon vaporization ($M_{theor}(SnCl_4 + DO) = 174.3$); and (2) assuming the sublimation of complex ($M_{theor}(SnCl_4 \cdot DO) = 348.6$). Comparison with the experimentally obtained value $M_{exp} = 175 \pm 3$ in series 3, 4 confirms the complete dissociation of complex into components upon vaporization. The mean molecular masses of vapor for the experiments 1 and 2 with non-stoichiometric ratio of components are also in

Table 22
Determination of mean molecular mass of vapor in the system $SnCl_4$–dioxan.

Series	Amount[a], g	V, ml	P/T	M_{exp}	M_{theor}	
					For dissociation	For sublimation
3	0.0194	28.95	0.2387 ± 0.0039	175 ± 3	174.3	348.6
4	0.0140	14.9	0.3333 ± 0.0032	176 ± 2	174.3	348.6
1	0.0519	30.2	0.7530 ± 0.0040	150 ± 1	147.5	
2	0.0807	32.5	0.7379 ± 0.0023	206 ± 1	206.4	

[a] Total mass of introduced substances.

good agreement with theoretically predicted values, computed on the basis of the assumption of complete dissociation of complex in the gas phase. This allows us to conclude, that upon heating of the solid $SnCl_4$·DO complex, dissociation process occurs:

$$SnCl_4 \cdot DO_{(solid)} = SnCl_{4(gas)} + DO_{(gas)} \quad (8)$$

For the determination of its thermodynamic characteristics, a special experiment was carried out, in which the vapor pressure–temperature dependence was measured over the large (about 3 g) amount of solid $SnCl_4$·DO complex. The use of large amount extends the saturated vapor region up to the atmospheric pressure (in this particular experiment the maximal measured vapor pressure was 790 Torr) and also lowers the influence of changes in the composition of condensed phase. For a given temperature, the equilibrium constant of Eq. (8) was computed as

$$K^{diss} = \left(\frac{P_{total}}{2}\right)^2$$

From the experiments 1 and 2 with non-stoichiometric amounts of components, the equilibrium constant was computed using the following formulae:

$$K^{diss} = \frac{(P_{total} - P_{excess})(P_{total} + P_{excess})}{4}$$

where P_{excess} – pressure of the excess component.

The data points from different series in 100–190 °C temperature range are well approximated by the single equation $\ln K^{diss} = -(17684 \pm 5.7)/T + 36.82 \pm 0.78$, which suggests validity of the used model. Thermodynamic characteristics of process (8) have been obtained:

$$\Delta_{(8)}H_T^\circ = 149.79 \pm 0.13\ kJ\ mol^{-1};$$

$$\Delta_{(8)}S_T^\circ = 311.6 \pm 5.0\ J\ mol^{-1}\ K^{-1}$$

The total pressure over the solid complex $SnCl_4$·DO in 100–190 °C temperature range can be computed using the equilibrium constant K^{diss}, since $\ln(P_{total}/P^\circ) = 1/2\ \ln K^{diss} + \ln 2$. The total pressure over the solid complex is given by the equation:

$$\ln\left(\frac{P_{total}}{P^\circ}\right) = -\left(\frac{8842.05 \pm 2.86}{T}\right) + 19.10 \pm 0.40$$

It should be specially pointed out, that the solid $SnCl_4$·DO complex is insoluble both in excess of liquid $SnCl_4$ and in excess of liquid dioxane. It is exactly this fact that allowed the trustful determination of the amount of the excess component from the experimentally measured thermal expansion lines.

5.5. Subsequent ligand dissociation from the solid adduct. Alumazene–pyridine system

In previous chapters, the thermal behavior of complexes of 1:1 composition has been considered. In the present chapter the thermal dissociation of complex of 1:3 composition will be discussed. Trimeric iminoalane 1,3,5-trimethyl-2,4,6-tris(2,6-diisopropylphenyl)alumazene [2,6-(*i*-Pr)$_2$C$_6$H$_3$NAlMe]$_3$ (**AZ**) is also known as an "inorganic benzene" [506–508]. It is a Lewis acid which forms mono, bis, and tris adducts with Lewis bases [509,510]. Bis and tris adducts with pyridine (Py) were synthesized and structurally characterized by NMR spectroscopy, X-ray diffraction analysis and quantum chemical computations [511]. The melting point of alumazene is 272 °C, and both complexes **AZ**(Py)$_2$ and **AZ**(Py)$_3$ melt at 251 °C. The thermodynamics of complex formation has been investigated experimentally by the static tensimetric method [511]. Complexes with excess donor ligands usually undergo subsequent dissociation to form complex of 1:1 composition. Thermodynamic characteristics of the **AZ**(Py)$_x$ (x = 2, 3) complex dissociation in the temperature range 25–200 °C have been derived from the vapor pressure–temperature dependence measurements.

In all experiments, the following efficient measurements scheme has been employed. First, an approximately known amount of Py was introduced in the system of the known volume V. The small sealed ampoule of calibrated volume containing the known mass of **AZ** was placed inside the working volume beforehand. The thermal expansion of Py in the unsaturated vapor range has been measured at least two times. From the $P/T = (m/M)(R/V)$ equation the amount of introduced pyridine has been determined with high accuracy. After that, the ampoule with **AZ** was mechanically broken inside the working volume. Yellow coloring was observed immediately after breaking of the ampoule. After the overnight equilibration at room temperature, the vapor pressure–temperature dependence measurements have been performed.

In the experiment with excess of alumazene (volume of the system 27.18 ml, mass of alumazene 171.2 mg, the mass of pyridine (from the P/T value) 9.33 mg, **AZ**:Py ratio 2.23:1) it was shown that introduced Py interacts with solid **AZ** (yellow color). Py almost completely binds with **AZ**, even at 100 °C (the measured residual vapor pressure at 100 °C is less than 5 Torr, as compared to 100 Torr for the unsaturated vapor pressure of introduced amount of Py). Subsequent heating up to 200 °C revealed the irreversible pressure increase which was accompanied by green discoloring of the system and was attributed to the irreversible thermal decomposition. Thus, it was not possible to measure the equilibrium thermal dissociation of the solid monoadduct **AZ**(Py) due to side pyrolytic processes. Nevertheless, our experiments show that the monoadduct is quite stable with respect to the equilibrium dissociation into **AZ** and Py (at least up to 200 °C) and it is more stable compared to bis and tris adducts (vide infra).

Three series of measurements were performed with excess of Py with respect to **AZ**. The alumazene-to-pyridine **AZ**:Py ratios are: 1:20.8 in series 1; 1:3.3 in series 2; and 1:5.5 in series 3. The vapor pressure–temperature dependences for all series are given in Fig. 22. Details of the measurements for the series 3 are illustrated in Fig. 23 as P/T dependence from the temperature. In a typical run, the vapor pressure of pure pyridine was measured first in saturated and unsaturated vapor pressure regions (solid circles). Then the ampoule with alumazene was mechanically broken (yellow coloring was observed immediately); the system was allowed to stay overnight. Then measuring the vapor pressure–temperature dependence was performed by repeating heating/cooling cycles

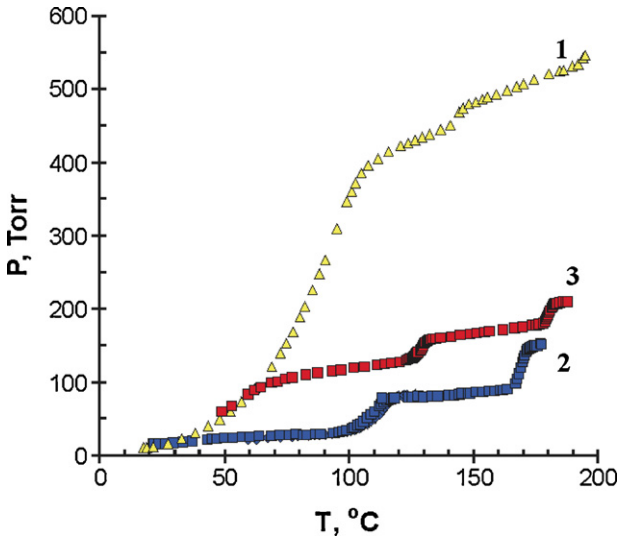

Fig. 22. Vapor pressure–temperature dependence in alumazene–pyridine system. Only heating data points are given. Yellow points – first series (**AZ**/Py ratio 1:20.8), blue points – second series (**AZ**/Py ratio 1:3.3), red points – third series (**AZ**/Py ratio 1:5.5). (For interpretation of the references to color in this figure legend, the reader is referred to the web version of the article.)

several times. At first heating (red triangles), the thermal expansion of Py occurred at much lower pressures, indicating that Py has complexed with alumazene. Taking the differences in thermal expansion lines of Py before and after complexation, formation of solid **AZ**$(Py)_3$ was confirmed. At about 400 K the first exponential increase of pressure has occurred, followed by another thermal expansion line. We attribute this exponential increase to the release of the first mole of gaseous Py from the solid **AZ**$(Py)_3$, and formation of the solid **AZ**$(Py)_2$. Note that at cooling, the exponential pressure decrease was absent and the pressure followed along the thermal expansion line. This indicates that gaseous pyridine does not readily react with solid **AZ**$(Py)_2$. We attribute the difference between the heating and cooling data points to the fact, that establishing of the equilibrium between gaseous pyridine and solid **AZ**$(Py)_2$ is kinetically limited due to the slow diffusion of pyridine vapors into the solid sample. The similar situation was observed for the dehydration of $MnCl_2{\cdot}H_2O$ complex, where establishing the equilibrium from above (on cooling) proceeds 10–15 times slower than establishing the equilibrium from below (on heating) [490]. However, after the overnight stay at room temperature, the second heating/cooling run (white rhombs) showed good reproducibility with the first one. This observation indicates that liquid pyridine reacts with **AZ**$(Py)_2$ overnight, which dovetails with the fact that tris-adduct is formed only in mother liquor solution containing the excess of liquid Py. At the second heating/cooling run, in addition to the reproducible first exponential increase of pressure, the second exponential increase of pressure was observed about 450 K, followed by another thermal expansion line. We attribute this second exponential increase of pressure to the release of one gaseous mole of Py from the solid **AZ**$(Py)_2$. On cooling, data points are systematically higher due to the slow reaction between gaseous Py and the solid **AZ**(Py). Differences between measured thermal expansion lines agree well with each other and confirm formation of the tris-adduct.

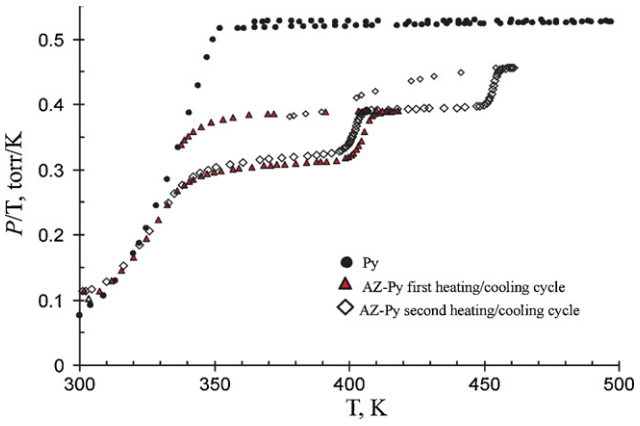

Fig. 23. P/T – temperature dependence for the first two heating-cooling runs for the third series of experiments (**AZ**/Py ratio 1:5.5).

Obtained results for all three series with different alumazene-pyridine ratios are presented in Fig. 22. For the sake of clarity, only data for selected heating runs are given.

Due to the fact that prolonged heating at temperatures about 200 °C results in slow irreversible decomposition of the compound (seen by the loss of reproducibility of the subsequent heating/cooling runs and the dark green discoloring of the sample), for the thermodynamic analysis data for the few first heating runs only were used in the each series. The following processes were attributed to the exponential pressure increase:

$$\mathbf{AZ}(Py)_{3(solid)} = \mathbf{AZ}(Py)_{2(solid)} + Py_{(gas)}, \quad K_{(9)} = P_{Py} \tag{9}$$

$$\mathbf{AZ}(Py)_{2(solid)} = \mathbf{AZ}(Py)_{(solid)} + Py_{(gas)}, \quad K_{(10)} = P_{Py} \tag{10}$$

For both equilibria, the equilibrium constant K is equal to the partial pressure of pyridine. Plot of $\lg K$ versus $1000/T$ for both processes is given in Fig. 24 and clearly indicates consistence between the different experimental series. The pyridine excess shifts the dissociation of the complex to higher temperatures, therefore in series 1 only couple of points correspond to the exponential zone of complex dissociation, while more points appear in series 3. The most number of points was obtained in series 2, but they correspond to very narrow temperature interval. Since results of all series satisfactory agree with each other, this confirms the proposed model (reactions (9) and (10)) and allows to determine the thermodynamic properties of corresponding processes (Table 23).

The experimentally observed increase of the complex stability from tris to bis adducts in the solid state dovetails both with the decrease of Al–N(Py) donor–acceptor bond distance found by X-ray

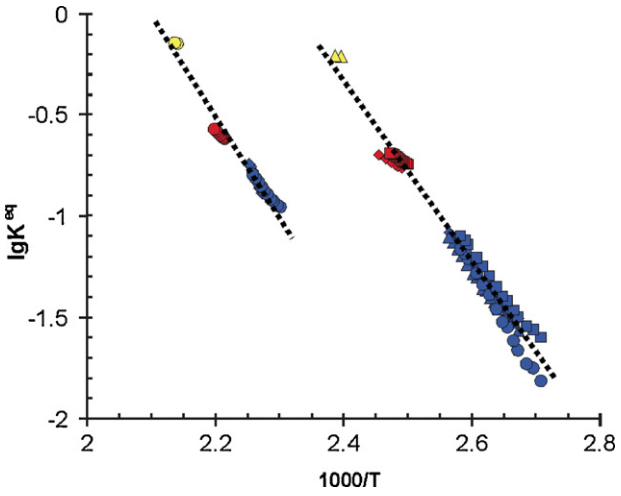

Fig. 24. Logarithm of the equilibrium constant versus reverse temperature. Yellow points – data of the first series, blue points – second series, red points – third series. (For interpretation of the references to color in this figure legend, the reader is referred to the web version of the article.)

Table 23
Thermodynamic characteristics of dissociation process of complexes of alumazene with pyridine.

Process	Temperature range, K	Mean temperature, *T*, K	ΔH°_{T}, kJ mol^{-1}	ΔS°_{T}, J mol^{-1} K^{-1}
AZ$(Py)_{3(solid)}$ = **AZ**$(Py)_{2(solid)}$ + $Py_{(gas)}$	369–419	394	78 ± 3	180 ± 8
AZ$(Py)_{2(solid)}$ = **AZ**$(Py)_{(solid)}$ + $Py_{(gas)}$	435–468	451	91 ± 3	191 ± 7

analysis and with the theoretical trend of complex stability found by DFT computations [511].

5.6. System $ZrCl_4$–$POCl_3$

The system $ZrCl_4$–$POCl_3$ was studied in the condensed phase [512–514]. Although the liquid–vapor phase diagram has not been studied in detail, the distilled product is an azeotrope of $3ZrCl_4{\cdot}2POCl_3$ composition [515,516] with boiling point 360 °C [515]. The molecular mass of the azeotrope at 370–400 °C is about 450 [516], which is considerably higher than the mean molecular mass for the mixture of non-interacting $ZrCl_4$ and $POCl_3$ in 3:2 composition (M = 201), but twice as low as for the hypothetical complex $3ZrCl_4{\cdot}2POCl_3$ (M = 1007). Authors [516] assume that azeotrope is a mixture of complexes formed between $ZrCl_4$ and $POCl_3$.

Vapor pressure–temperature dependence in the system was measured for five different compositions in the temperature range 20–500 °C and pressures up to 800 Torr [517–519]. Depending on the ratio of the components, at room temperature the following phases exist:

Amount of $ZrCl_4$, molar percent	Condensed phase composition
0–33.3%	$POCl_3$; crystals of $ZrCl_4{\cdot}2POCl_3$ and its solution in $POCl_3$
33.3–50%	Crystals of $ZrCl_4{\cdot}POCl_3$ and $ZrCl_4{\cdot}2POCl_3$
50–100%	Crystals of $ZrCl_4$ and $ZrCl_4{\cdot}POCl_3$

Special attention was paid to the unsaturated vapor region. Experiments were carried out in the following way. The known amounts of the component (in series 1, 2, and 5 – $POCl_3$, in series 3 and 4 – $ZrCl_4$) has been placed into the membrane chamber and the vapor-pressure temperature dependence was measured in the saturated and unsaturated vapor regions. For both components the transition into the unsaturated vapor is marked by the distinct break point on the curve $P = f(T)$. In the unsaturated vapor region vapor pressure follows the thermal expansion line, which agrees with the known fact of the stability of source components in the studied temperature range. Using the average P_1/T value from the unsaturated vapor range and the known volume of working chamber, the exact amount of the first component was established. After that a known mass of the second component was introduced in the apparatus, and its exact amount was refined from the difference between P_{total}/T and P_1/T.

As an example let us consider the vapor pressure–temperature dependence for two compositions: with excess of $ZrCl_4$ (experiment 5, 62.8% $ZrCl_4$) and $ZrCl_4{\cdot}2POCl_3$ with excess of $POCl_3$ (experiment 2, 21.7% $ZrCl_4$).

In Fig. 25 the $P = f(T)$ dependence is given for pure $POCl_3$ (curve 1) and mixtures of 62.8 and 21.7% $ZrCl_4$ (curves 2, and 3, respectively). As can be seen from Fig. 25, in case of pure $POCl_3$ the transition from saturated (I) into unsaturated (II) vapor is marked by the distinct temperature point (52 °C), above which vapor pressure follows the thermal expansion line. In contrast, curves 2 and 3 exhibit smooth vapor pressure–temperature dependence both in the saturated and unsaturated vapor pressure regions and do not have distinct break points on the $P = f(T)$ curves.

For the composition of 62.8% $ZrCl_4$ the noticeable saturated vapor pressure appears only after the melting (which, according to the phase diagram, occurs about 200 °C). With the further temperature increase the melt is enriched by low-volatile $ZrCl_4$, until the azeotrope of the $3ZrCl_4{\cdot}2POCl_3$ composition is formed [515,516], which vaporizes without changing the composition of the liquid phase.

To establish the "exit point" of the transition into the unsaturated vapor region, literature values about the saturated vapor pressure above the azeotrope were used [515]. Evidently, if at a given temperature the measured vapor pressure is lower compared to the saturated vapor pressure of azeotrope, the system belongs to the unsaturated vapor region. This is illustrated in Fig. 26, where graphs of $\lg P = f(1/T)$ are given for the saturated vapor of $ZrCl_4$ and azeotrope (lines 1 and 2, respectively) and the total vapor pressure in the system with 62.8% $ZrCl_4$ (curve 3). At first, the measured vapor pressure is close to the saturated vapor pressure of $ZrCl_4$, after that it is close to the vapor pressure of azeotrope and finally system transforms into the unsaturated vapor region.

For the composition of 21.7% $ZrCl_4$ (Fig. 25, curve 3) the excess of $POCl_3$ vaporizes first in the saturated vapor region (I) and after that solid $ZrCl_4{\cdot}2POCl_3$ dissociates into the gaseous $POCl_3$ and solid $ZrCl_4{\cdot}POCl_3$. Due to the large excess of $POCl_3$, decomposition of the adduct occurs at higher temperature (compared to the reported by Larsen et al. [512]). After the melting of the solid phase at circa 200 °C the composition of the liquid phase changes until azeotrope composition is reached.

In the unsaturated vapor region (Fig. 25, zone II on curves 2 and 3) for both compositions the total pressure is significantly less than

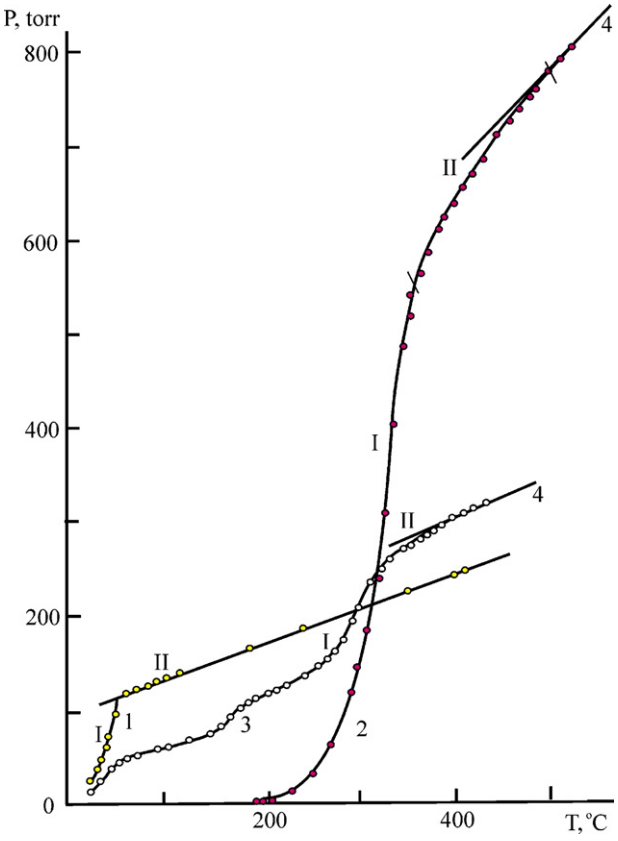

Fig. 25. Vapor pressure–temperature dependence for $ZrCl_4$–$POCl_3$ system. I – saturated vapor region; II – unsaturated vapor region. 1 – $POCl_3$; 2 – 62.8 mol% $ZrCl_4$; 3 – 21.7 mol% $ZrCl_4$; 4 – thermal expansion lines.

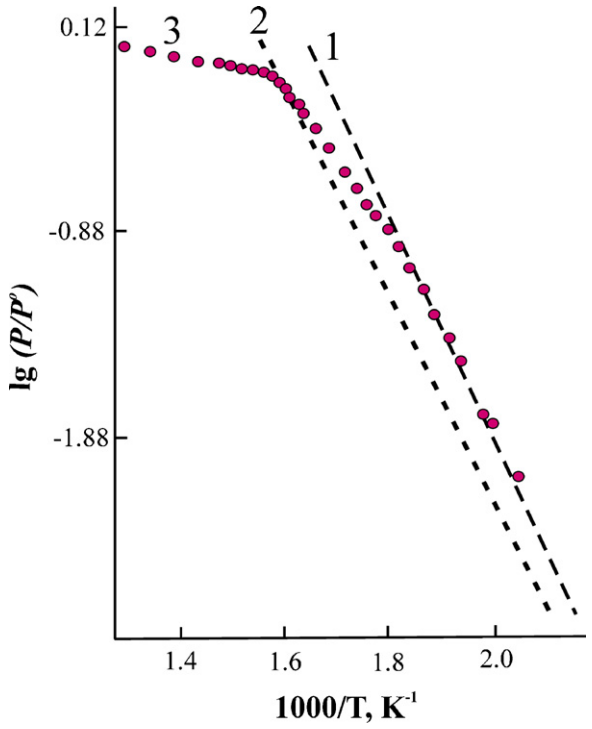

Fig. 26. $\lg P = f(1/T)$ dependence for $ZrCl_4POCl_3$ system. 1 – $ZrCl_4$; 2 – azeotrope mixture; 3 – 62.8 mol% $ZrCl_4$.

the sum of the partial pressures of non-interacting components (curve 4). However, with the temperature increase, both curves 2 and 3 smoothly approach respective lines 4 and overlap with them at temperatures 450–500 °C.

Vapor pressure–temperature dependences for other experiments with different $ZrCl_4/POCl_3$ compositions are similar to that of described above. For all experiments, the mean molecular mass of vapor, M_{mean}, computed for the unsaturated vapor region is larger compared to M_{theor}, computed on the basis of non-interacting components (Table 24).

Thus, the mean molecular mass of vapor in the system $ZrCl_4$–$POCl_3$ definitely points out on the interaction between $ZrCl_4$ and $POCl_3$ in the gas phase. It is interesting to note, that in experiment 5 a mixture of the composition close to azeotrope has been studied. In this case at 372 °C and 578 Torr the mean molecular mass M_{mean} equals 225, which is more than M_{theor} = 203 but twice as less as 450, determined by Niselson et al. at 370–400 °C [516]. *A priori*, one can assume formation of gaseous complex compounds with general formulae $xZrCl_4{\cdot}yPOCl_3$.

The tensimetric study, carried out in wide temperature and composition range, allows to estimate the complex composition (x, y) in vapors. The criterion of the correctness of the derived complex composition is the independence of equilibrium constant of complex dissociation from the composition of the system. The computation of vapor composition in the system formed by three compounds can be carried out using three independent equations, which connect partial pressures with the experimentally studied characteristics. For the studied system, the following system of equations can be written:

$$\begin{cases} P_{total} = P_{ZrCl_4} + P_{POCl_3} + P_{xZrCl_4{\cdot}yPOCl_3} \\ P^*_{ZrCl_4} = P_{ZrCl_4} + xP_{xZrCl_4{\cdot}yPOCl_3} \\ P^*_{POCl_3} = P_{POCl_3} + yP_{xZrCl_4{\cdot}yPOCl_3} \end{cases}$$

where P_{total} – total pressure; P_{ZrCl_4}, P_{POCl_3}, $P_{xZrCl_4{\cdot}yPOCl_3}$ – partial pressures of $ZrCl_4$, $POCl_3$ and complex respectively; $P^*_{ZrCl_4}$ and $P^*_{POCl_3}$ – hypothetical partial pressures of non-interacting components.

Solution of this system with respect to $P_{xZrCl_4{\cdot}yPOCl_3}$ yields:

$$P_{xZrCl_4{\cdot}yPOCl_3} = \frac{(P^*_{ZrCl_4} + P^*_{POCl_3}) - P_{total}}{x + y - 1} = \frac{\Delta P}{x + y - 1}$$

If $x = y = 1$, $P_{xZrCl_4{\cdot}yPOCl_3} = \Delta P$, and if $x = 1$, $y = 2$ or if $x = 2$, $y = 1$, then $P_{xZrCl_4{\cdot}yPOCl_3} = \Delta P/2$.

Comparison of A and B coefficients in equation $\ln K^{diss} = -A/T + B$ for series 1 and 5 (which are the most different in chemical composition) is given in Table 24.

The error in determination of each coefficient is about 5–6% and it is evident, that the complex of 1:2 composition can be ruled out. However, the choice between 1:1 and 2:1 complexes cannot be made on the obtained data alone. Complex 2:1 was ruled out due to the absence of dimerization of $ZrCl_4$ and due to the monodentate nature of $POCl_3$. Mass-spectrometric study of vapor composition over the complex $ZrCl_4{\cdot}POCl_3$ showed absence of ions which correspond to other compositions. Therefore, in the following treatment it was assumed that only one complex, $ZrCl_4{\cdot}POCl_3$, is formed in the vapor phase.

The computation of partial pressures and equilibrium constants was carried out in the temperature interval 320–500 °C according to the following dissociation process:

$$ZrCl_4{\cdot}POCl_3(g) = ZrCl_4(g) + POCl_3(g)$$

$$K^{diss} = \frac{P_{ZrCl_4} P_{POCl_3}}{P_{ZrCl_4{\cdot}POCl_3}}$$

Results are given in Table 25. On the basis of the data obtained, A and B coefficients in the equation $\ln K^{diss} = -A/T + B$ have been computed and respective thermodynamic characteristics of the complex dissociation process in the gas phase have been derived (Table 26). Results obtained for the different stoichiometric ratios are in good agreement with each other (Table 26).

Obtained thermodynamic characteristics were corrected to the standard conditions. To this end, heat capacities of $ZrCl_4$ and $POCl_3$ have been taken from [520], and the heat capacity of the gaseous complex has been estimated using Kelley rules [521,522]. Estimated value for the process of gas phase dissociation of the complex $\Delta C_p(gas) = 8\ J\ mol^{-1}\ K^{-1}$.

Dissociation of the solid $ZrCl_4{\cdot}POCl_{3(s)}$ was not studied, since the vapor pressure over the solid compound is small and cannot be measured by the static method. Vapor pressure becomes noticeable only at temperatures higher than the melting point of the adduct. In such situation, due to partial dissociation and different solubility of the dissociation products in the melt of the complex, determination of the equilibrium constant of gas phase processes over the melt of the complex is not straightforward. Vapor composition strongly depends on the composition of the liquid phase. Since our primary goal was determination of thermodynamic characteristics of the individual complexes, vapor pressures over the melt were not studied.

In contrast, the solid complex $ZrCl_4{\cdot}2POCl_3$ has significant vapor pressure, which allowed to study its dissociation. As a result of the

Table 24
Comparison of different models of complex composition in system $ZrCl_4$–$POCl_3$.

Series	Complex 1:1		Complex 1:2		Complex 2:1	
	A	*B*	*A*	*B*	*A*	*B*
1	12,358	19.8	12,093	19.3	14,976	21.9
5	13,118	20.5	14,693	22.3	13,832	21.6
Difference	760	0.7	2600	3.0	1144	0.3

Table 25
Vapor pressures, composition and mean molecular mass of unsaturated vapor in system $ZrCl_4$–$POCl_3$.

Series	Experimental details	$ZrCl_4$, molar%	T, K	P_{total}, Torr	P_{ZrCl_4}, Torr	P_{POCl_3}, Torr	$P_{ZrCl_4 \cdot POCl_3}$, Torr	M_{mean}
1	$P^*_{ZrCl_4} = 0.098 \cdot T$, $P^*_{POCl_3} = 0.540 \cdot T$, $V = 25.3$ ml, $M_{theor} = 165$	15.4	602	358	33	299	26	178
			628	385	46	324	15	172
			651	404	52	341	11	170
			673	423	60	357	6	168
			707	448	65	379	3	166
2	$P^*_{ZrCl_4} = 0.101 \cdot T$, $P^*_{POCl_3} = 0.366 \cdot T$, $V = 26.7$ ml, $M_{theor} = 170$	21.7	597	256	38	196	23	185
			614	271	46	209	16	181
			637	288	55	223	10	176
			654	298	59	232	7	174
			687	319	67	248	3	172
3	$P^*_{ZrCl_4} = 0.344 \cdot T$, $P^*_{POCl_3} = 0.460 \cdot T$, $V = 24.7$ ml, $M_T = 188$	42.7	630	445	153	228	62	213
			655	489	187	263	38	202
			674	515	205	283	27	197
			689	535	218	298	19	194
			711	560	234	315	12	191
4	$P^*_{ZrCl_4} = 0.649 \cdot T$, $P^*_{POCl_3} = 0.502 \cdot T$, $V = 26.2$ ml, $M_{theor} = 198$	56.3	644	685	361	267	57	215
			663	728	395	297	36	208
			679	756	415	315	26	205
			698	786	435	333	18	203
			716	812	452	347	13	201
5	$P^*_{ZrCl_4} = 0.624 \cdot T$, $P^*_{POCl_3} = 0.370 \cdot T$, $V = 26.4$ ml, $M_{theor} = 203$	62.8	645	578	339	175	64	225
			663	617	372	203	42	217
			685	654	401	226	27	212
			713	693	429	248	16	208
			749	737	460	269	8	205

Table 26
Thermodynamic characteristics of the $ZrCl_4 \cdot POCl_3$ complex in the gas phase.

Experiment	Mol% $ZrCl_4$	Temperature range, K	$\ln K_P^{diss} = -A/T + B$		ΔH°_T, kJ mol^{-1}	ΔS°_T, J mol^{-1} K^{-1}
			A	B		
1	15.4	602–707	12,158	19.526	101.3 ± 5.9	162.3 ± 11.3
2	21.7	591–687	12,273	19.779	102.1 ± 4.2	164.4 ± 6.7
3	42.7	630–711	12,549	19.733	104.2 ± 3.8	164.0 ± 5.9
4	56.3	641–711	12,066	19.641	100.4 ± 5.0	163.2 ± 7.9
5	62.8	645–749	12,618	19.894	104.6 ± 2.5	165.3 ± 3.3
Mean value		673	12,342	19.710	102.5 ± 4.2	164.0 ± 7.1
Standard value		298			98.7 ± 4.6	157.3 ± 7.9

Table 27
Thermodynamic characteristics of the dissociation of solid $ZrCl_4 \cdot 2POCl_3$.

Experiment	Temperature range, K	$\ln K = -A/T + B$		ΔH°_T, kJ mol^{-1}	ΔS°_T, J mol^{-1} K^{-1}
		A	B		
1	378–452	7576	15.29	62.8 ± 1.3	126.8 ± 2.5
2	378–452	6724	13.35	56.1 ± 1.3	110.9 ± 2.5
Mean value	415			59.5 ± 3.4	118.9 ± 8.0
Standard value	298			67 ± 8	138 ± 21

partial dissociation of $ZrCl_4 \cdot 2POCl_3$, a mixture of 1:1 and 1:2 complexes is formed. As follows from the $ZrCl_4$–$POCl_3$ phase diagram, this mixture melts in the temperature range between eutectic and the melting point of adduct. For $ZrCl_4 \cdot 2POCl_3$ melting occurs at 179 °C, which determines the upper temperature for the measurements. At this temperature both the vapor pressure of the individual $ZrCl_4$ and its complex of 1:1 composition is less than 1–2 Torr, while the vapor pressure of dissociation of the solid $ZrCl_4 \cdot 2POCl_3$ amounts to 180–220 Torr. From this follows, that the total vapor pressure in this system essentially equals to the partial vapor pressure of $POCl_3$.

Therefore, in considered temperature range the process of dissociation occurs:

$$ZrCl_4 \cdot 2POCl_{3(solid)} = ZrCl_4 \cdot POCl_{3(solid)} + POCl_{3(gas)} \quad K = P_{POCl_3} = P_{total}$$

Computed coefficients A and B in equation $\ln K^{diss} = -A/T + B$, and thermodynamic characteristics of $ZrCl_4 \cdot 2POCl_3$ dissociation, are given in Table 27. The standard values of thermodynamic characteristics of the process of adduct dissociation were obtained by using estimated change in heat capacity (vide supra). Thus, conducted tensimetric study allowed to establish both the complex composition and obtain thermodynamic characteristics of its dissociation.

6. Summary of the studied systems and obtained thermodynamic characteristics

Thermodynamic characteristics of various processes obtained with the static method are summarized in Table 28. They are grouped according to the process nature. In Table 29 we sum-

Table 28
Summary of the thermodynamic characteristics obtained by static method.

Process	Temperature range, K	Mean temperature, K	ΔH_T°, kJ mol^{-1}	ΔS_T°, J mol^{-1} K^{-1}	Ref.
Homogeneous gas phase dissociation					
$AlCl_3{\cdot}NH_3$ (g) = $AlCl_3$ (g) + NH_3 (g)	663–815	739	137.2 ± 3.8	120.5 ± 9.2	[549]
$AlBr_3{\cdot}NH_3$ (g) = $AlBr_3$ (g) + NH_3 (g)	705–783	744	143.9 ± 4.6	141.0 ± 6.3	[525]
$GaCl_3{\cdot}NH_3$ (g) = $GaCl_3$ (g) + NH_3 (g)	673–783	728	134.3 ± 0.8	141.4 ± 2.5	[496]
$GaBr_3{\cdot}NH_3$ (g) = $GaBr_3$ (g) + NH_3 (g)	675–783	729	137.2 ± 0.8	157.7 ± 2.5	[496]
$InCl_3{\cdot}NH_3$ (g) = $InCl_3$ (g) + NH_3 (g)	723–803	763	112.1 ± 5.4	117.6 ± 7.1	[526]
$InBr_3{\cdot}NH_3$ (g) = $InBr_3$ (g) + NH_3 (g)	715–803	759	114.2 ± 6.3	129.7 ± 8.4	[526]
$AlI_3{\cdot}$py (g) = AlI_3 (g) + py (g)	671–747	709	156 ± 7	146 ± 9	[492]
$GaI_3{\cdot}$py (g) = GaI_3 (g) + py (g)	655–695	675	124 ± 5	143	[499]
$GaCl_3{\cdot}$pyz (g) = $GaCl_3$ (g) + pyz (g)	559–692	625	124.2 ± 2.8	133.6 ± 2.6	[527]
$GaCl_3{\cdot}$pyz$\cdot GaCl_3$ (g) = $GaCl_3{\cdot}$pyz (g) + pyz (g)	627–736	667	98.4 ± 3.3[a]	141.7[a]	[527]
$AlCl_3{\cdot}POCl_3$ (g) = $AlCl_3$ (g) + $POCl_3$ (g)	630–818	724	188.8 ± 3.3	128.0 ± 5.4	[528]
$GaCl_3{\cdot}POCl_3$ (g) = $GaCl_3$ (g) + $POCl_3$ (g)	578–758	668	90.0 ± 1.3	130.5 ± 0.8	[529]
$FeCl_3{\cdot}POCl_3$ (g) = $FeCl_3$ (g) + $POCl_3$ (g)	573–808	691	119.2 ± 2.5	114.2 ± 4.2	[549]
$GeBr_4{\cdot}POCl_3$ (g) = $GeBr_4$ (g) + $POCl_3$ (g)	410–562	486	43.1 ± 6.3	118.4 ± 6.3	[530]
$TiBr_4{\cdot}POCl_3$ (g) = $TiBr_4$ (g) + $POCl_3$ (g)	448–653	551	56.5 ± 2.1	126.8 ± 4.2	[531]
$ZrCl_4{\cdot}POCl_3$ (g) = $ZrCl_4$ (g) + $POCl_3$ (g)	591–749	670	102.5 ± 4.2	164.0 ± 7.1	[519]
$HfCl_4{\cdot}POCl_3$ (g) = $HfCl_4$ (g) + $POCl_3$ (g)	629–756	693	91.2 ± 3.8	150.6 ± 6.3	[519]
$SbCl_5{\cdot}POCl_3$ (g) = $SbCl_5$ (g) + $POCl_3$ (g)			(50)	(126)	[532]
$NbCl_5{\cdot}POCl_3$ (g) = $NbCl_5$ (g) + $POCl_3$ (g)	533–685	609	64.9 ± 3.8	123.4 ± 4	[533]
$TaCl_5{\cdot}POCl_3$ (g) = $TaCl_5$ (g) + $POCl_3$ (g)			71 ± 4	130 ± 4	[534]
$SnBr_4{\cdot}POBr_3$ (g) = $SnBr_4$ (g) + $POBr_3$ (g)	443–581	512	53.6 ± 6.3	137.7 ± 6.3	[535]
$ZrBr_4{\cdot}POBr_3$ (g) = $ZrBr_4$ (g) + $POBr_3$ (g)[a]	623–673	648	(86)[a]	(134)[a]	[536]
$AlCl_3{\cdot}PCl_5$ (g) = (1/2)Al_2Cl_6 (g) + PCl_3 (g) + Cl_2 (g)	926	926	142	(188)	[549]
$FeCl_3{\cdot}PCl_5$ (g) = (1/2)Fe_2Cl_6 (g) + PCl_3 (g) + Cl_2 (g)	744–903	824	176 ± 59	243 ± 79	[549]
$AlBr_3{\cdot}PBr_3$ (g) = (1/2)Al_2Br_6 (g) + PBr_3 (g)	483–549	516	36.8 ± 6.3	75 ± 12	[106]
$GaCl_3{\cdot}SbCl_3$ (g) = $GaCl_3$ (g) + $SbCl_3$ (g)	483–529	506	64 ± 3	129 ± 6	[107]
$AlBr_3{\cdot}SbBr_3$ (g) = (1/2)Al_2Br_6 (g) + $SbBr_3$ (g)	525–620	573	34.3 ± 6.3	63.2 ± 12	[106]
Dissociation of liquid adduct					
$BiCl_3{\cdot}2POCl_3$ (l) = $BiCl_3$ (g) + 2$POCl_3$ (g)			78.7	192.5	[532]
$TiCl_4{\cdot}POCl_3$ (l) = $TiCl_4$ (g) + $POCl_3$ (g)	379–418	399	97.5 ± 4	220.1 ± 4	[524]
			100.4 ± 2.9	229.3 ± 6.3	[519]
$SbCl_5{\cdot}POCl_3$ (l) = $SbCl_5$ (g) + $POCl_3$ (g)		273	119.2	(243)	[532]
$AlCl_3{\cdot}PCl_5$ (l) = (1/2)Al_2Cl_6 (g) + PCl_3 (g) + Cl_2 (g)	627–655	641	192 ± 13	226 ± 21	[549]
$AlBr_3{\cdot}PBr_3$ (l) = (1/2)Al_2Br_6 (g) + PBr_3 (g)	483–549	516	36.8 ± 6.3	75 ± 12	[106]
Dissociation of the solid adduct					
$GaCl_3{\cdot}NH_3$ (s) = $GaCl_3$ (g) + NH_3 (g)	624–743	684	(222)	(280)	[537]
$AlBr_3{\cdot}NH_3$ (s) = $AlBr_3$ (g) + NH_3 (g)	609–747	678	(234)	(285)	[537]
$TiCl_4{\cdot}2CH_3CN$ (s) = $TiCl_4$ (g) + 2CH_3CN (g)	328–443	386	210 ± 2	464 ± 3	[538]
$SiCl_4{\cdot}$2py (s) = $SiCl_4$ (g) + 2py (g)	333–393	363	217 ± 3	523 ± 7	[539]
$TiCl_4{\cdot}$2py (s) = $TiCl_4$ (g) + 2py (g)	478–543	511	268 ± 3	460 ± 6	[540]
$SiCl_4{\cdot}$bipy (s) = $SiCl_4$ (g) + bipy (g)	473–513	493	170 ± 7	315 ± 15	[541]
$GeCl_4{\cdot}$bipy (s) = $GeCl_4$ (g) + bipy (g)	473–553	513	171 ± 7	307 ± 15	[542]
$TiCl_4{\cdot}$bipy (s) = $TiCl_4$ (g) + bipy (g)	573–663	618	203 ± 21	259 ± 33	[543]
$BCl_3{\cdot}POCl_3$ (s) = BCl_3 (g) + $POCl_3$ (g)	293–341	317	104.2 ± 5.0	290 ± 13	[544]
$BBr_3{\cdot}POCl_3$ (s) = BBr_3 (g) + $POCl_3$ (g)	313–378	346	84.5 ± 3.3	193.7 ± 6.3	[537]
$GaCl_3{\cdot}POCl_3$ (s) = $GaCl_3$ (g) + $POCl_3$ (g)	298–273	298	160.7	283.7	[537]
$SnCl_4{\cdot}2POCl_3$ (s) = $SnCl_4$ (g) + 2$POCl_3$ (g)	288–328	308	197.9 ± 4.6	528 ± 10	[545]
$TiCl_4{\cdot}POCl_3$ (s) = $TiCl_4$ (g) + $POCl_3$ (g)			136.7 ± 4	324.0 ± 4	[524]
	323–379	351	141.0 ± 3.3	336.8 ± 8.4	[519]
$TiCl_4{\cdot}2POCl_3$ (s) = $TiCl_4$ (g) + 2$POCl_3$ (g)	308–378	343	199.2 ± 4.2	479.9 ± 12.1	[545]
$TiBr_4{\cdot}2POCl_3$ (s) = $TiBr_4$ (g) + 2$POCl_3$ (g)			180	(351)	[536]
$SbCl_5{\cdot}POCl_3$ (s) = $SbCl_5$ (g) + $POCl_3$ (g)			158.2	(343)	[532]
$NbCl_5{\cdot}POCl_3$ (s) = $NbCl_5$ (g) + $POCl_3$ (g)			199.9	(335)	[532]
$TaCl_5{\cdot}POCl_3$ (s) = $TaCl_5$ (g) + $POCl_3$ (g)			(230)	(368)	[532]
$SnCl_4{\cdot}C_4H_8O_2$ (s) = $SnCl_4$ (g) + $C_4H_8O_2$ (g)	373–463	418	149.79 ± 0.13	311.6 ± 5.0	[505]
$SnCl_4{\cdot}C_4H_{10}O_2$(s) = $SnCl_4$ (g) + $C_4H_{10}O_2$ (g)	373–473	423	166 ± 3	346 ± 8	[505]
$AlCl_3{\cdot}PCl_5$ (s) = (1/2)Al_2Cl_6 (g) + PCl_3 (g) + Cl_2 (g)	531–627	579	268 ± 13	347 ± 21	[549]
$GaCl_3{\cdot}PCl_5$ (s) = $GaCl_3$ (g) + PCl_3 (g) + Cl_2 (g)	573–643	608	307.5 ± 41.8	416.7 ± 46.0	[546]
$TiCl_4{\cdot}PCl_5$ (s) = $TiCl_4$ (g) + PCl_5 (g)	370–500	435	148.5 ± 2.9	275.7 ± 5.9	[547]
Subsequent dissociation of the complex					
$NH_4[AlCl_4]$(s) = $AlCl_3{\cdot}NH_3$ (s) + HCl (g)	451–574	513	77.4	115.1	[549]
$AlCl_3{\cdot}NH_4Cl$ (l) = $AlCl_3{\cdot}NH_3$ (solut.) + HCl (g)	581–690	636	65.7	77.4	[549]
AZ(Py)$_3$ (s) = AZ(Py)$_2$ (s) + Py (g)	369–422	396	78 ± 3	180 ± 8	[511]
AZ(Py)$_2$ (s) = AZ(Py) (s) + Py (g)	435–468	452	91 ± 3	191 ± 7	[511]
$AlBr_3{\cdot}$1.5pyz (s) = $AlBr_3{\cdot}$pyz (s) + (1/2)pyz(g)		408	14	28	[548]
	401–414	408	59[a]	140[a]	
$ZrCl_4{\cdot}2POCl_3$ (s) = $ZrCl_4{\cdot}POCl_3$ (s) + $POCl_3$ (g)	378–452	415	59.5 ± 3.4	118.9 ± 8.0	[545]
$HfCl_4{\cdot}2POCl_3$ (s) = $HfCl_4{\cdot}POCl_3$ (s) + $POCl_3$ (g)	383–462	423	81.2 ± 5.0	164.0 ± 8.4	[545]

Table 28 (*Continued*)

Process	Temperature range, K	Mean temperature, K	ΔH_T°, kJ mol^{-1}	ΔS_T°, J mol^{-1} K^{-1}	Ref.
$MnCl_2 \cdot H_2O$ (s) = $MnCl_2$ (s) + H_2O (g)	353–500	425	62.5 ± 0.2	124.6 ± 0.5	[490]
		298	63.5 ± 0.5	127.5 ± 1.2	[490]
(1/2)$CuCl_2 \cdot 2H_2O$ (s) = (1/2)$CuCl_2$ (s) + H_2O (g)		358	58.04 ± 0.07	143.3 ± 0.2	[491]
		298	58.6 ± 0.2	145.1 ± 0.6	[491]
Vaporization					
$AlBr_3 \cdot NH_3$ (l) = $AlBr_3 \cdot NH_3$ (g)	514–698	606	80.3 ± 2.1	115.9 ± 3.8	[525]
$GaCl_3 \cdot NH_3$ (l) = $GaCl_3 \cdot NH_3$ (g)	531–716	624	68.4 ± 0.4	96.3 ± 0.4	[496]
$GaBr_3 \cdot NH_3$ (l) = $GaBr_3 \cdot NH_3$ (g)			67.4 ± 1.3	94.1 ± 2.5	[496]
$AlI_3 \cdot py$ (l) = $AlI_3 \cdot py$ (g)	506–688	597	66.3 ± 0.7	90.5 ± 2	[492]
$GaI_3 \cdot py$ (l) = $GaI_3 \cdot py$ (g)	465–695	580	82 ± 2.7	111.1	[499]
		630	78.8 ± 3.5	103.9	
$AlBr_3 \cdot pyz$ (l) = $AlBr_3 \cdot pyz$ (g)	552–586	569	48 ± 2	65 ± 3	[548]
$GaCl_3 \cdot pyz$ (l) = $GaCl_3 \cdot pyz$ (g)	477–543	510	54.6 ± 2.4	78.5 ± 4.6	[527]
$GaCl_3 \cdot pip$ (l) = $GaCl_3 \cdot pip$ (g)	463–548	506	66.8 ± 0.2	98.1 ± 0.4	[550]
$AlCl_3 \cdot POCl_3$ (l) = $AlCl_3 \cdot POCl_3$ (g)	461–621	541	69.9 ± 3.8	106.3 ± 6.3	[528]
$GaCl_3 \cdot POCl_3$ (l) = $GaCl_3 \cdot POCl_3$ (g)	473–273	473	(50)	(88)	[537]
$FeCl_3 \cdot POCl_3$ (l) = $FeCl_3 \cdot POCl_3$ (g)	408–588	498	59.9 ± 7.5	94.6 ± 13.4	[549]
$FeCl_3 \cdot PCl_5$ (l) = $FeCl_3 \cdot PCl_5$ (g)[a]			107.1[a]	105[a]	[549]
$[Li(dpm)]_4$ (l) = $[Li(dpm)]_4$ (g)	550–581	566	96.5 ± 1.3	142.1 ± 2.3	[486]
$Hf(tfac)_4$ (l) = $Hf(tfac)_4$ (g)[b]	403–423	413	83.2 ± 2.0	149.5 ± 5.0	[489]
$Hf(ptac)_4$ (l) = $Hf(ptac)_4$ (g)[b]	424–472	448	91.2 ± 0.3	153.7 ± 0.6	[489]
$Zr(hfac)_4$ (l) = $Zr(hfac)_4$ (g)	366–456	411	48.6 ± 0.6	94.5 ± 1.3	[551]
Melting					
$AlCl_3 \cdot NH_4Cl$ (s) = $AlCl_3 \cdot NH_4Cl$ (l)			11.7	37.7	[549]
$AlBr_3 \cdot pyz$ (s) = $AlBr_3 \cdot pyz$ (l)	549	549	27 ± 5	53 ± 9	[548]
$GaCl_3 \cdot pyz$ (s) = $GaCl_3 \cdot pyz$ (l)	475	475	12 ± 5	23 ± 13	[527]
$AlCl_3 \cdot POCl_3$ (s) = $AlCl_3 \cdot POCl_3$ (l)	461	461	37.7 ± 6.3	81.6 ± 13.4	[528]
$TiCl_4 \cdot POCl_3$ (s) = $TiCl_4 \cdot POCl_3$ (l)	379	379	37.7 ± 8	104.6 ± 8	[524]
			40.6 ± 4.6	107.5 ± 10.0	[519]
$AlCl_3 \cdot PCl_5$ (s) = $AlCl_3 \cdot PCl_5$ (l)	627	627	75 ± 17	121 ± 29	[549]
Sublimation					
$AlBr_3 \cdot NH_3$ (s) = $AlBr_3 \cdot NH_3$ (g)	609	609	(92)	(142)	[537]
$GaCl_3 \cdot NH_3$ (s) = $GaCl_3 \cdot NH_3$ (g)	624	624	(88)	(138)	[537]
$InCl_3 \cdot NH_3$ (s) = $InCl_3 \cdot NH_3$ (g)	298	298	(146)		[526,537]
$AlBr_3 \cdot pyz$ (s) = $AlBr_3 \cdot pyz$ (g)	496–546	521	75 ± 5	118 ± 9	[548]
$GaCl_3 \cdot pyz$ (s) = $GaCl_3 \cdot pyz$ (g)	347–472	410	66.2 ± 4.8	101.0 ± 11.6	[527]
$GaCl_3 \cdot pyz \cdot GaCl_3$ (s) = $GaCl_3 \cdot pyz \cdot GaCl_3$ (g)	537	537	92.1 ± 9.4	182.7 ± 17.5	[527]
$AlCl_3 \cdot POCl_3$ (s) = $AlCl_3 \cdot POCl_3$ (g)	461	461	107.5 ± 5.0	187.9 ± 14.6	[528]
$GaCl_3 \cdot POCl_3$ (s) = $GaCl_3 \cdot POCl_3$ (g)	298	298	64	(146)	[537]
$TiBr_4 \cdot POCl_3$ (s) = $TiBr_4 \cdot POCl_3$ (g)	298	298	126	(226)	[536]
$SbCl_5 \cdot POCl_3$ (s) = $SbCl_5 \cdot POCl_3$ (g)	298	298	(109)	(218)	[532]
$NbCl_5 \cdot POCl_3$ (s) = $NbCl_5 \cdot POCl_3$ (g)	298	298	107.5	(218)	[532]
$TaCl_5 \cdot POCl_3$ (s) = $TaCl_5 \cdot POCl_3$ (g)	298	298	(113)	(230)	[532]
$[Li(dpm)]_4$(s) = $[Li(dpm)]_4$(g)	537–545	541	198.0 ± 1.5	329.4 ± 27.8	[486]
$Cu(thd)_2$(s) = $Cu(thd)_2$(g)	434–468	451	111.6 ± 2.1	199.8 ± 4.2	[552]
$Al(acac)_3$(s) = $Al(acac)_3$(g)	423–467	446	121.8 ± 1.5	235.5 ± 4.3	[488]
$Hf(tfac)_4$(s) = $Hf(tfac)_4$ (g)[b]	358–398	378	126.5 ± 1.8	257.5 ± 4.7	[489]
$Hf(ptac)_4$(s) = $Hf(ptac)_4$ (g)[b]	386–423	405	121.5 ± 0.8	225.3 ± 2.0	[489]
$Hf(dpm)_4$(s) = $Hf(dpm)_4$ (g)[b]	453–603	528	99.1 ± 0.8	141.8 ± 1.4	[489]

[a] Entropy of the process is fixed (either computed by quantum chemical methods or estimated), enthalpy is computed using equation $\Delta H_T^\circ = -RT \ln K_T + T\Delta H_T^\circ$.
[b] Joint treatment of data, obtained by static and flow methods.

marize all systems studied in our laboratory using static method with membrane null-manometer and report the approximate content of the complex molecules in vapors. The results show, that the presence of the DA complexes in vapors is significant in many systems.

In the present review reported thermodynamic characteristics of processes are attributed to the mean temperature of the studied temperature interval. In order to correct these data to the standard temperature, the knowledge of the heat capacities of all studied compounds is required. Such data are not known for the majority of the studied complexes. There are several methods for estimation of vaporization and sublimation heat capacities. Application of these methods for organic compounds has been analyzed by Chickos et al. [523]. In some cases the uncertainty in the estimated value is greater than the value itself, and in the present review we report original experimental data obtained at elevated temperatures.

7. Estimation of the sublimation enthalpies for Donor–acceptor complexes

7.1. A critical note about the widely used approach toward estimation of vaporization enthalpies of the donor–acceptor complexes

The strength of the metal–ligand donor–acceptor bond is one of the fundamental characteristics of the complex. The closest value which can be measured directly is the enthalpy of the homogeneous complex dissociation in the gas phase. Since the experimental stud-

Table 29
Summary of the experimentally studied donor–acceptor systems and complex content in vapor.

System (adduct)	Temperature range, K	Adduct content in vapor[a], %	Ref.
$TiCl_4 \cdot POCl_3$	323–418	Not observed	[524]
$TiCl_4 \cdot POCl_3$	373–433	Not observed	[519]
$TiCl_4 \cdot 2POCl_3$	308–378	Not observed	[545]
$TiCl_4$–PCl_3[b]	411–559	Not observed	[547]
$TiCl_4 \cdot PCl_5$	373–673	Not observed	[547]
$TiCl_4 \cdot 2py$	460–615	Not observed	[540]
$TiCl_4 \cdot bipy$	573–663	Not observed	[543]
$TiCl_4 \cdot 2CH_3CN$	413–658	Not observed	[538]
$TiBr_4 \cdot POCl_3$	472–653	6%	[531]
$TiBr_4 \cdot POBr_3$	471–673	Not observed	[531]
$TiBr_4 \cdot 2POBr_3$	473–573	Not observed	[536]
$ZrCl_4 \cdot POCl_3$	597–749	14%	[519]
$ZrCl_4 \cdot 2POCl_3$	<453–463	Not observed	[545]
$ZrCl_4$–$POBr_3$	>573	Not observed[c]	[536]
$ZrBr_4$–$POCl_3$	>573	Not observed[c]	[536]
$ZrBr_4 \cdot POBr_3$	623–673	16%	[536]
$HfCl_4 \cdot POCl_3$	629–756	10%	[519]
$HfCl_4 \cdot 2POCl_3$	453–463	Not observed	[545]
$NbCl_5 \cdot POCl_3$	533–685	5–10%	[533]
$TaCl_5 \cdot POCl_3$	293–673	Present	[534]
$TaCl_5 \cdot POCl_3$	533–661	10% (at 533 K)	[532]
WCl_6–$POCl_3$[b]	527–653	Not observed	[553]
$WOCl_4 \cdot POCl_3$	503–623	Not observed	[553]
$WCl_5 \cdot POCl_3$	543–653	Not observed	[534,554]
$FeCl_3 \cdot PCl_5$	744–813	2.5% (at 747 K)	[549]
$FeCl_3 \cdot POCl_3$	793–868		
	573–808	91% (at 573 K)	[549]
$BCl_3 \cdot POCl_3$	348–373	Not observed	[544]
$BBr_3 \cdot POCl_3$	413–561	Not observed	[537]
$AlCl_3$–PCl_3[b]	452–672	Not observed	[549]
$AlCl_3$–$SbCl_3$	504–672	Not observed	[549]
$AlCl_3 \cdot PCl_5$	529–653	8% (at 653 K)	[549]
$AlCl_3$–$SbCl_5$[b]	467–660	Not observed	[549]
$AlCl_3 \cdot POCl_3$	630–818	90% (at 684 K)	[528]
$AlCl_3 \cdot NH_3$	663–815	94% (at 773 K)	[549]
$AlBr_3 \cdot AsBr_3$	513–693	Not observed	[106]
$AlBr_3 \cdot PBr_3$	483–549	7–18%	[106]
$AlBr_3 \cdot SbBr_3$	525–620	12–20%	[106]
$AlBr_3 \cdot POCl_3$		Not observed[c]	[537]
$AlBr_3 \cdot POBr_3$		Not observed (decomposition to $AlOBr + PBr_3 + Br_2$)[c]	[537]
$AlBr_3 \cdot NH_3$	711–773	96% (at 711 K)	[525]
$AlBr_3 \cdot pyz$	603–660	100% (at 660 K)	[548]
$AlBr_3 \cdot pyz \cdot AlBr_3$	>543	60% (at 543 K)	[548]
AlI_3–$POCl_3$		Not observed[c]	[537]
$AlI_3 \cdot NH_3$	573–723	Present (ammonolysis)[c]	[537]
$AlI_3 \cdot Py$	671–747	100% (until 683 K), 92% (at 743 K)	[492]
$AZ(Py)_3$	369–422	Not observed	[511]
$AZ(Py)_2$	435–468	Not observed	[511]
$GaCl_3 \cdot PCl_3$	473–643	Not observed	[107]
$GaCl_3 \cdot SbCl_3$	483–529	6%	[107]
$GaCl_3 \cdot PCl_5$	653–773	Not observed	[546]
$GaCl_3 \cdot POCl_3$	573–583	55%	[537]
$GaCl_3 \cdot NH_3$	703–783	94% (at 703 K)	[496]
$GaCl_3 \cdot pyz$	559–692	91% (at 673 K)	[527]
$GaCl_3 \cdot pyz \cdot GaCl_3$	627–736	0.2% (at 383 K) 0.05% (at 673 K)	[527]
$GaCl_3 \cdot pip$	463–548	Present[c]	[550]
$GaBr_3 \cdot NH_3$	675–783	90% (at 675 K)	[496]
$GaI_3 \cdot py$	665–695	70% (at 690 K)	[499]
$InCl_3 \cdot POCl_3$	<373–273	Not observed	[537]

Table 29 (*Continued*)

System (adduct)	Temperature range, K	Adduct content in vapor[a], %	Ref.
$InCl_3 \cdot NH_3$	703–803	60%	[526]
$InBr_3 \cdot NH_3$	703–803	60%	[526]
$SiCl_4 \cdot 2py$	328–463	Not observed	[539]
$SiCl_4 \cdot bipy$	523–573	Not observed	[541]
$GeCl_4 \cdot bipy$	523–663	Not observed	[542]
$GeBr_4$–$POCl_3$[b]	410–562	3% (at 410 K)	[530,536]
$GeBr_4$–$POBr_3$[b]	<573	Not observed	[530,536]
$SnCl_4 \cdot 2POCl_3$	<328	Not observed	[545]
$SnCl_4 \cdot C_4H_8O_2$(dioxan)	423–573	Not observed	[505]
$SnCl_4 \cdot C_4H_{10}O_2$	423–573	Not observed	[505]
$SnBr_4$–$POCl_3$[b]	423–573	Not observed	[535,536]
$SnBr_4$–$POBr_3$[b]	443–573	1% (at 443 K)	[535,536]
$SbCl_3 \cdot POCl_3$	473–673	Not observed	[532]
$SbCl_5 \cdot POCl_3$	<623	1%	[532]
$BiCl_3 \cdot 2POCl_3$	653–773	Not observed	[532]

[a] Maximal adduct content.
[b] No complex exists in the solid state.
[c] Side reactions occur.

ies of the dissociation of the gas phase complexes (presented in Sections 5.2 and 5.3) are relatively rare, most thermochemical studies are carried out in solutions and data for the gas phase processes are derived by means of the thermochemical cycles. For example, for the evaluation of the metal–ligand donor–acceptor bond strength the following cycle is widely used (Scheme 1):

In order to complete the thermochemical cycle, the sublimation enthalpy of the complex $\Delta_{sub}H$(AD) is required. Sublimation enthalpies can be measured directly by calorimetry method [555–557]; derived from the vapor pressure measurements by the static tensimetry method (vide supra). Knudsen-effusion technique [485,557–565] and flow (transpiration) method [486,489,566–568] are also used for their determination. However, such experimental studies are very demanding and relatively rare. Recent examples include comprehensive determination of the sublimation enthalpy of copper(II) complex with 3-methylpentane-2,4-dione by the Knudsen-effusion technique as well as direct microcalorimetry [557]. Similar Knudsen-effusion technique was employed to determine standard enthalpy of sublimation of bis(2,2,6,6-tetramethylheptane-3,5-dionato) dioxouranium(VI) {uranyl(VI) dipivaloylmethanate, $UO_2(dpm)_2$} [558]. The sublimation enthalpy of the complex of Li with dipivaloylmethane has been obtained by the Knudsen-effusion method with MS analysis of the gas phase in the temperature range 400–450 K [559]. Enthalpies of vaporization of volatile nickel complexes bis(N-R-salicylaldimine)nickel(II) (R = Me, Et, *n*-Pr, *n*-Bu or *n*-pentyl) have been determined by transpiration method [568]. Static method with capacitance gauge was used for the determination of low vapor pressures (10^{-1} to 10^3 Pa) of four low volatility precursors [569].

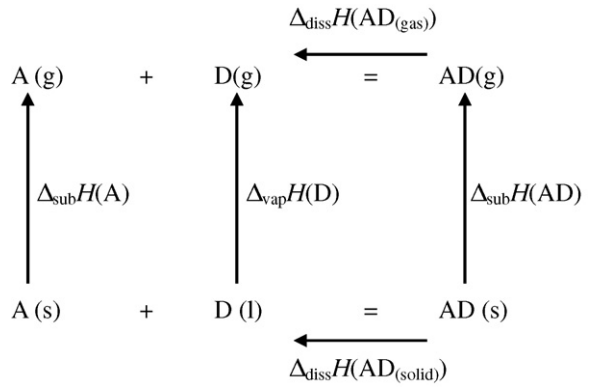

Scheme 1. Thermochemical cycle for the DA complex of 1:1 composition.

It should be noted, that for some complexes the sublimation/vaporization enthalpy cannot be measured directly due to the thermal instability of the complex in the gas phase. Since sublimation enthalpies of many complexes are not readily available, the estimation of the sublimation enthalpy of the complex becomes an important issue. The most widely used approach states that the sublimation enthalpy of the complex is equal to the sublimation enthalpy of one mole of the ligand:

$$\Delta_{sub}H^{\circ}{}_T(EX_m \cdot n\mathrm{L}) = \Delta_{sub}H^{\circ}_T(\mathrm{L}) \quad (11)$$

This approximation was proposed for the sublimable group 12 adducts by Jorge, Airnoldi and Chagas [29]. Approximation (11) was justified in a sense that the intramolecular interactions in crystal structure of the free ligand L and the complexes MX_2nL are similar, since the primary intramolecular contacts are those between atoms of the ligand L. These results are in accord with recent theoretical findings [566,570] that that the metal atom has only moderate (less than 10 kJ mol^{-1}) contribution to the lattice energy. The larger the molecule, the smaller the metal contribution [566]. Approach (11) is supposed to hold for the complexes with large ligands L. Validity of this approach for the sublimable group 12 adducts is illustrated in upper part of Table 30. Approximation (11) works within ±10 kJ mol^{-1} for the complexes of the group 12 element halides. It also works well for Zn porphyrine complexes, as follows from the experimental works of Patiño [571,572]. However, when other transition metal complexes are taken into account (the bottom part of Table 30), the approximation (11) is off by about 40 kJ mol^{-1}.

In 1989, Chagas and Airnoldi [573] tested several models for the estimation of the sublimation enthalpy of the complexes and concluded that the approximation (11) provides the best fit. From this time, many authors cite Chagas and Airoldi paper and use approximation (11) for the estimation of the enthalpies of dissociation of gas phase complexes [574]. In recent years, approximation (11) has become so widespread in the literature, that it is considered a mere routine by some researches [575–599]. Authors simple state that "it was necessary to assume that the molar standard enthalpies of the adducts were equal to the enthalpy of sublimation or vaporization of one mol of the respective ligand".

Table 30
Sublimation enthalpies (kJ mol^{-1}) of the adducts of group 12 metal halides and their ligands and other transition metal complexes.

Complex	$\Delta_{sub}H^{\circ}$ (complex)	$\Delta_{sub}H^{\circ}$ (L)	$\Delta(\Delta_{sub}H^{\circ})$[a]	Ref.
$[Cd(mcyt)_2Cl_2]$	145 ± 20	141.8 ± 8.8	3.2 ± 22	[600]
$[Hg(mcyt)_2Cl_2]$	159 ± 19	141.8 ± 8.8	17.2 ± 21	[600]
$ZnCl_2{\cdot}4tu$	90 ± 20	93.7 ± 10	−3.7 ± 22	[605]
$CdCl_2{\cdot}4tu$	75 ± 20	93.7 ± 10	−18.7 ± 22	[605]
$HgCl_2{\cdot}4tu$	101 ± 20	93.7 ± 10	7.3 ± 22	[605]
Zn(TPP)porphirine	183 ± 3	171 ± 2	12 ± 4	[571,572]
Mean asolute deviation (group 12 halides)			9.3 ± 22	
$[Co(cyt)_2Cl_2]$	162 ± 14	147.2 ± 2.6	14.8 ± 14	[600]
$[Mn(cyt)_2Cl_2]$	153 ± 21	147.2 ± 2.6	5.8 ± 21	[600]
$Ni(pd)_2$	132 ± 10	68 ± 10	64 ± 14	[600]
$Pd(pd)_2$	132 ± 17	68 ± 10	64 ± 20	[600]
$Pt(pd)_2$	133 ± 9	68 ± 10	65 ± 13	[600]
$Cd(pd)_2$	154 ± 22	68 ± 10	86 ± 24	[600]
$Ni(salox)_2$	112 ± 29	105.2 ± 10	6.8 ± 31	[600]
$Ni(Hdmg)_2$	139 ± 6	91.1 ± 1	47.9 ± 6	[600]
$Pt(Hdmg)_2$	153 ± 13	91.1 ± 1	61.9 ± 13	[600]
$[Mn(hoqu)_2]$	226 ± 14	108.8 ± 10	117.2 ± 17	[600]
$[Co(hoqu)_2]$	200 ± 10	108.8 ± 10	91.2 ± 14	[600]
$[Ni(hoqu)_2]$	139 ± 6	108.8 ± 10	30.2 ± 12	[600]
$[Cu(hoqu)_2]$	170 ± 3	108.8 ± 10	61.2 ± 10	[600]
$[Zn(hoqu)_2]$	178 ± 6	108.8 ± 10	69.2 ± 12	[600]
$[Cd(hoqu)_2]$	154 ± 22	108.8 ± 10	45.2 ± 24	[600]
$[Pd(hoqu)_2]$	168 ± 4	108.8 ± 10	59.2 ± 11	[600]
$Fe(Cp)_2$	74.9 ± 1.7	36.4 ± 0.3	38.5 ± 1.7	[606]
Mean asolute deviation (all data)			43 ± 32	

[a] $\Delta(\Delta_{sub}H^{\circ}) = \Delta_{sub}H^{\circ}$ (complex) − $\Delta_{sub}H^{\circ}$ (L).

However, the Chagas and Airnoldi fit was based on the assumption that the metal-oxygen dissociation energy should be linearly dependent on the reaction enthalpy of the complex formation in the solid state. It is obvious, that different adducts have different structures in the solid state, and therefore intramolecular interactions (packing) should affect the reaction enthalpy in the solid state. Different complexes have different coordination environment (for example, octahedral and tetrahedral complexes) and therefore their sublimation enthalpies should be different. This is especially significant in the case when the complexes adopt polymeric (oligomeric) structures in the solid state, as for example Mn and Ni complexes with bridging halide ions. Different complexes, therefore, should have very different sublimation enthalpies.

Widespread use of approach (11) leads to results which clearly contradict the experimental observations. If one assumes that the sublimation enthalpy of the $EX_n{\cdot}mL$ complex is indeed equal to the sublimation enthalpy of the ligand L, then the complex would be sublimable more easily than the ligand L. This follows from the fact that sublimation entropy of the complex is equal or larger than that of the ligand, and therefore the partial pressure of the complex at a given temperature should be equal or even larger than the pressure of the ligand. Therefore, sublimation of any $EX_n{\cdot}mL$ complex should proceed even more easily compared to the free ligand L. This is not the case observed experimentally, since it is clearly stated that complexes do not exist in vapors below their decomposition temperature [575–599]. The fact that complex does not undergo sublimation at the same conditions when ligand L sublimes, directly indicates the failure of the approximation (11).

The melting point of the compound is one of the indicators of the intramolecular interactions in the crystal. It is interesting, that some correlation exists between the melting points of complexes and respective ligands for the adducts of group 13 metal halides ($n - v$ type molecular complexes) [501]. Melting point of the adduct is always higher compared to the melting point of free ligand L, which indicates different intermolecular interactions. This may be due to "head-to-tail" interactions of polar adduct molecules, which are responsible for the dramatic donor–acceptor bond shortening from the gaseous to the silid state in so called "partially bonded" molecules [100].

Already in 1984 Burkinshaw and Mortimer [600] stated: "When values for the enthalpies of sublimation of transition metal complexes have not been available, a number of authors have assumed these values to be the same as those of the uncomplexed ligand. Only where the structure of the crystalline ligand remains virtually unchanged on complexing with the metal, so that intermolecular forces will be similar in both the uncomplexed ligand and metal complex, do we expect the enthalpies of sublimation to be similar. Unfortunately, there are insufficient structural data to take this analysis further". Except for $Ni(salox)_2$, the intrermolecular hydrogen bonding in the ligand differs considerably from that in transition metal complex [601].

Now, when more thermochemical and structural information is available, it is clear, that the approximation (11) does not hold. For example, it completely fails for the complexes of the group 13-14 halides, as can be seen from Table 31. It is not surprising, since usually donors are much more volatile compounds than complexes. Almost all donor molecules do exist in vapors, while examples of gas phase complexes are limited. Most donor molecules have molecular crystal structure, while many complexes are ionic. One should not use the sublimation enthalpy of a molecular donor compound as a valid estimation for the sublimation enthalpy of the ionic (or polymeric) complex.

One can trust neither trends nor values for the gas phase metal–ligand bond dissociation energies, obtained with use of the approximation (11). Nevertheless, using estimated $\Delta_{sub}H(AD)$ values in the thermochemical cycle (Scheme 1), in many works [575–599] authors repeatedly state that "standard enthalpies of the Lewis acid/base reactions in the gaseous phase" have been obtained. Especially troubling is the fact that authors report the standard deviation of the gas phase dissociation energy of the Metal–ligand bond with accuracy of about 6 kJ mol^{-1} or less, while the sublimation enthalpy used to calculate those values may be as wrong as 90 kJ mol^{-1} (Table 31). Sevast'yanova and Suvorov [27] reviewed sublimation enthalpies of 8 donor–acceptor complexes of group 13 halides with pyridine, obtained by differ-

Table 31
Sublimation enthalpies (kJ mol^{-1}) of the adducts of group 13–14 metal halides and their ligands.

Complex	$\Delta_{sub}H^{\circ}$ (complex)	$\Delta_{sub}H^{\circ}$ (L)	$\Delta(\Delta_{sub}H^{\circ})$[a]	Ref.
BBr_3·Py	110.0 ± 2.5	40.0 ± 0.2	70.0 ± 2.5	[607]
$AlCl_3$·Py	128.4 ± 2.3	40.0 ± 0.2	88.4 ± 2.3	[607]
$AlBr_3$·Py	109.4 ± 2.1	40.0 ± 0.2	69.4 ± 2.1	[607]
$GaCl_3$·Py	106.6 ± 6.0	40.0 ± 0.2	66.6 ± 6.0	[607]
$GaBr_3$·Py	99.0 ± 3.0	40.0 ± 0.2	59.0 ± 3.0	[607]
$AlCl_3$·Et_3N	96.3 ± 1.9	34.94 ± 0.06	61.4 ± 1.9	[607]
$AlBr_3$·Et_3N	107.1 ± 2.5	34.94 ± 0.06	72.2 ± 2.5	[607]
$AlCl_3$·Pip	110.7 ± 2.8	39.3 ± 0.2	71.4 ± 2.5	[607]
$AlBr_3$·Pip	116.8 ± 3.2	39.3 ± 0.2	77.5 ± 3.2	[607]
		Mean	70.6 ± 3.0	
$GaCl_3$·pyz·$GaCl_3$	92.1 ± 9.4	40.5 ± 1.7	51.6 ± 9.6	[527]
$GaCl_3$·pyz	66.2 ± 4.8	40.5 ± 1.7	25.7 ± 5.1	[527]
$AlBr_3$·pyz	75.0 ± 5	40.5 ± 1.7	34.5 ± 5.3	[548]
$AlBr_3$·NH_3	(92)[b]	31 (195 K)	61	[537]
$GaCl_3$·NH_3	(88)[b]	31	57	[537]
$InCl_3$·NH_3	(146)[b]	31	115	[526,537]
$AlCl_3$·$POCl_3$	107.5 ± 5.0	53.0 (274 K)	54.5	[528]
$GaCl_3$·$POCl_3$	64	53.0	11	[537]
$TiBr_4$·$POCl_3$	126	53.0	73	[536]
$SbCl_5$·$POCl_3$	(109)	53.0	56	[532]
$NbCl_5$·$POCl_3$	107.5	53.0	54.5	[532]
$TaCl_5$·$POCl_3$	(113)	53.0	60	[532]

[a] $\Delta(\Delta_{sub}H^{\circ}) = \Delta_{sub}H^{\circ}$ (complex) − $\Delta_{sub}H^{\circ}$ (L).
[b] Estimated value.

ent methods. Most reliable sublimation enthalpies of complexes (directly measured by the sublimation calorimetry) are in the range of 100–125 kJ mol^{-1}, while sublimation enthalpy of Py is only 43 kJ mol^{-1}. In this particular case approximation (11) leads to the mean error of the metal–ligand dissociation energy of about 70 kJ mol^{-1}. This value is clearly higher than the overoptimistic error bars of 1–6 kJ mol^{-1} repeatedly reported in the literature [575–599].

Nowadays much more thermochemical information is available for the gas phase complexes (Table 28), see also references [485,560–565] for recent data obtained by Knudsen method. Now it is a time to re-evaluate the widespread usage of the approach (11). We must stress the point, that many metal–ligand bond energies, reported in the literature [575–599] as "experimental" values, in fact result from the approximation (11) and cannot be trusted. The mere fact of publication [575–599] of more than 20 papers containing such values does not make them correct. All these "experimental gas phase metal–ligand dissociation energies" are in fact very crude approximation.

7.2. Estimation of the sublimation enthalpies based on structural data

From the previous discussion, it is clear that more reliable models for the estimation of the sublimation enthalpies of donor–acceptor complexes should be developed. Such approaches must include the structural information, since the structure of the solid compound determines its volatility. Nowadays the solid-state structures are available for many complex compounds. Notable efforts in the direction of the development of the structure-thermochemical approach include programmed use of the Cambridge structural database. The TOPOS program package was employed to analyze the intermolecular contacts and calculate vaporization enthalpies of 570 molecular organotitanium coordination compounds [601].

There are lattice energy computations on the basis of structural data in the solid state using atom–atom potential (AAP) method [565,570,602]. However, validity of current semiempirical approaches is not very high and depends on the studied system. For example, calculated lattice energies for Pd(II) chelates satisfactory agree (largest deviation 22.7 kJ mol^{-1}) with the experimental sublimation enthalpies [566]. However, for some compounds data obtained using different potentials are different by 60 kJ mol^{-1}, while for other compounds the difference is not so dramatic. Authors conclude, that the "classical AAP technique is problematic for the most interesting complexes with weak intermolecular contacts" [570]. Computed and experimental sublimation enthalpies of molecular strontium and barium β-diketonates with crown ligands differ by 38 and 61 kJ mol^{-1} for [Sr(15C5)($C_5O_2F_6H)_2$] and [Ba(18C6)($C_5O_2F_6H)_2$], respectively [603]. Results of the X-ray photoelectron study of electron density distribution in palladium(II) β-diketonate complexes [604] indicate that vaporization enthalpy depends not only on van der Waals interactions but also on the electrostatic interactions between molecules in the crystal. A new method, which will take into account "interaction between the electron density in the crystal, but not between atoms" is proposed [570].

Further developments in the structure-thermochemistry approach, in particularly experimental studies on the vaporization/sublimation enthalpies and crystal structures of the complexes are needed in order to build a more reliable model for the estimation of the sublimation enthalpy of the complex to make prognosis of volatility of novel promising single-source precursors based on structural data.

8. Conclusions

In the present review basics of the static tensimetric method with membrane null-manometer and its application for studying donor–acceptor complexes have been summarized. Several case cases of the application of the tensimetry method for studying thermal behavior of different DA complexes were discussed. Thermodynamic characteristics for more than 90 processes for about 50 adducts have been summarized for the first time. On the basis of our findings, the widely used approximation of the sublimation enthalpy of the complex as the sublimation enthalpy of one mole of donor molecule should not be used. Published literature data on the gas phase bond dissociation energies, based on such approx-

imation, can be as wrong as 70 kJ mol^{-1} and shall not be trusted. Further experiments are needed to recommend a new scheme for the estimation of sublimation enthalpies of complexes. This new scheme is expected to be based on the structural information which is nowadays available for many molecular complex compounds.

Acknowledgements

Authors are grateful to all our former and present colleagues from the Laboratory of High Temperature Chemistry, Department of Inorganic Chemistry at Leningrad (now St. Petersburg) State University.

References

[1] G.B. Stringfellow, Organometallic Vapor Phase Epitaxy: Theory and Practice, Academic Press, New York, 1989.
[2] A.C. Jones, P. O'Brien, CVD of Compound Semiconductors. Precursor Synthesis, Development and Applications, VCH, Weinheim, 1997.
[3] G.B. Stringfellow, Organometallic Vapor Phase Epitaxy, 2nd ed., Academic Press, New York, 1998.
[4] H.O. Pierson (Ed.), Handbook of Chemical Vapor Deposition: Principles, Technology and Applications, 2nd ed., William Andrew Publishing, LLC, New York, USA, 2000.
[5] E.N. Gur'yanova, I.P. Gol'dshtein, I.P. Romm, Donor–Acceptor Bond, Halsted, New York, 1975.
[6] S. Mishra, E. Jeanneau, S. Daniele, Polyhedron 29 (2010) 500.
[7] C.J. Carmalt, J.D. Mileham, A.J.P. White, D.J. Williams, Dalton Trans. (2003) 4255.
[8] M.F. Mahon, N.L. Moldovan, K.C. Molloy, A. Muresan, I. Silaghi-Dumitrescu, L. Silaghi-Dumitrescu, Dalton Trans. (2004) 4017.
[9] C.S. Blackman, C.J. Carmalt, I.P. Parkin, L. Apostolico, K.C. Molloy, A.J.P. White, D.J. Williams, J. Chem. Soc., Dalton Trans. (2002) 2702.
[10] R.L. Wells, S.R. Aubuchon, S.S. Kher, M.I.S. Lube, P.S. White, Chem. Mater. 7 (1995) 793.
[11] K. Sardar, M. Dan, B. Schwenzer, C.N.R. Rao, J. Mater. Chem. 15 (2005) 2175.
[12] O.-S. Joo, K.-D. Jung, S.-H. Cho, J.-H. Kyoung, C.-K. Ahn, S.-C. Choi, Y. Dong, H. Yun, S.-H. Han, Chem. Vap. Dep. 8 (2002) 273.
[13] P. Hasan, S.E. Potts, C.J. Carmalt, R.G. Palgrave, H.O. Davies, Polyhedron 27 (2008) 1041.
[14] Q.M. Cheng, O. Stark, F. Stowasser, A. Wohlfart, R.A. Fischer, J. Mater. Chem. 12 (2002) 2470.
[15] A. Villinger, P. Mayer, A. Schulz, Chem. Commun. (2006) 1236.
[16] C. Hubrich, A. Schulz, A. Villinger, Z. Anorg. Allg. Chem. 633 (2007) 2362.
[17] P. Mayer, A. Schulz, A. Villinger, J. Organomet. Chem. 692 (2007) 2839.
[18] J.S. Chickos, W.E. Acree Jr., J. Phys. Chem. Ref. Data 31 (2002) 537.
[19] J.S. Chickos, W.E. Acree Jr., J. Phys. Chem. Ref. Data 32 (2003) 519.
[20] H.C. Brown, J. Chem. Soc. (1956) 1248.
[21] H.L. Morris, N.I. Kulevsky, M. Tamres, S. Searles Jr., Inorg. Chem. 5 (1966) 124.
[22] D.E. McLaughlin, M. Tamres, J. Am. Chem. Soc. 82 (1960) 5618.
[23] D.E. McLaughlin, M. Tamres, J. Am. Chem. Soc. 82 (1960) 5621.
[24] P.M. Burkinshaw, C.T. Mortimer, Coord. Chem. Rev. 48 (1983) 101.
[25] C. Airoldi, A.P. Chagas, Coord. Chem. Rev. 119 (1992) 29.
[26] T.N. Sevast'yanova, A.V. Suvorov, Russ. J. Coord. Chem. 23 (1997) 812.
[27] T.N. Sevast'yanova, A.V. Suvorov, Russ. J. Coord. Chem. 25 (1999) 679.
[28] I.P. Romm, Yu.G. Noskov, A.A. Malkov, Russ. Chem. Bull., Int. Ed. 56 (2007) 1935.
[29] R.A. Jorge, C. Airoldi, A.P. Chagas, J. Chem. Soc., Dalton Trans. (1978) 1102.
[30] J.-L. Gay-Lussac, Mémoires de Physique et de Chimie, de la Société d'Arcueil 2 (1809) 207.
[31] R.S. Ghadwal, S.S. Sen, H.W. Roesky, G. Tavcar, S. Merkel, D. Stalke, Organometallics 28 (2009) 6374.
[32] C.H. Winter, T.S. Lewkebandara, J.W. Proscia, A.L. Rheingold, Inorg. Chem. 33 (1994) 1227.
[33] M.F. Davis, W. Levason, G. Reid, M. Webster, Polyhedron 25 (2006) 930.
[34] N. Bricklebank, S.M. Godfrey, C.A. McAuliffe, R.G. Pritchard, J. Chem. Soc., Chem. Commun. (1994) 695.
[35] L. Kozlov, I. Goldberg, Acta Crystallogr. C 64 (2008) m123.
[36] J.A.J. Pardoe, A.R. Cowley, A.J. Downs, T.M. Greene, Acta Crystallogr. C 61 (2005) m200.
[37] M. Hargittai, I. Hargittai, V.P. Spiridonov, A.A. Ivanov, J. Mol. Struct. 39 (1977) 225.
[38] M. Hargittai, I. Hargittai, V.P. Spiridonov, J. Mol. Struct. 30 (1976) 31.
[39] M. Hargittai, I. Hargittai, J. Mol. Struct. 39 (1977) 79.
[40] M. Hargittai, I. Hargittai, V.P. Spiridonov, M. Pelissier, J.F. Labarre, J. Mol. Struct. 24 (1975) 27.
[41] A. Almenningen, A. Haaland, T. Haugen, D.P. Novak, Acta Chem. Scand. 27 (1973) 1821.
[42] E. Rytter, M.-A. Einarsrud, C.E. Sjøgren, Spectrochim. Acta 42A (1986) 1317.
[43] C.E. Sjøgren, E. Rytter, M.-A. Einarsrud, C.E. Sjøgren, Spectrochim. Acta 42A (1986) 1317.
[44] T. Østvold, E. Rytter, G.N. Papatheodorou, Polyhedron 5 (1986) 821.
[45] G.N. Papatheodorou, I.A. Curtiss, V.A. Maroni, J. Chem. Phys. 78 (1983) 3303.
[46] H. Jacobs, F.O. Schröder, Z. Anorg. Allg. Chem. 628 (2002) 327.
[47] C. Trinh, M. Bodensteiner, A.V. Virovets, E.V. Peresypkina, M. Scheer, S.M. Matveev, A.Y. Timoshkin, Polyhedron 29 (2010) 414.
[48] H. Jacobs, F.O. Schröder, Z. Anorg. Allg. Chem. 628 (2002) 951.
[49] P. Woodward, T. Vogt, W. Weber, E. Schweda, J. Solid State Chem. 138 (1998) 350.
[50] J. Pauls, S. Chitsaz, B. Neumüller, Z. Anorg. Allg. Chem. 627 (2001) 1723.
[51] M. Roos, G. Meyer, Z. Anorg. Allg. Chem. 625 (1999) 1129.
[52] C. Plitzko, M. Strecker, G. Meyer, Z. Anorg. Allg. Chem. 623 (1997) 79.
[53] S. Boghosian, D.A. Karydis, G.A. Voyiatzis, Polyhedron 12 (1993) 771.
[54] E. Gerding, J.A. Koningstein, E.R. van der Worm, Spectrochim. Acta 16 (1960) 881.
[55] S. Boghosian, G.N. Papatheodorou, R.W. Berg, N.J. Bjerrum, Polyhedron 5 (1986) 1393.
[56] N. Burford, A.D. Phillips, R.W. Schurko, R.E. Wasylishen, J.F. Richardson, Chem. Commun. (1997) 2363.
[57] D.H. Brown, D.T. Stewart, D.E.H. Jones, Spectrochim. Acta 29A (1973) 213.
[58] J.W. Wilson, I.J. Worrall, J. Inorg. Nucl. Chem. 31 (1969) 1205.
[59] J.W. Wilson, I.J. Worrall, J. Inorg. Nucl. Chem. 30 (1968) 715.
[60] J.W. Wilson, I.J. Worrall, J. Inorg. Nucl. Chem. 30 (1968) 1457.
[61] G. Beran, K. Dymock, H.A. Patel, A.J. Carty, P.M. Boorman, Inorg. Chem. 11 (1972) 896.
[62] I.R. Beatti, M. Milne, W. Webster, H.E. Blayden, P.J. Jones, R.C.G. Killean, J.L. Lawrence, J. Chem. Soc. A (1969) 482.
[63] A.Y. Timoshkin, H.F. Schaefer, J. Phys. Chem. C 112 (2008) 13816.
[64] A.Y. Timoshkin, A.V. Suvorov, H.F. Bettinger, H.F. Schaefer, J. Am. Chem. Soc. 121 (1999) 5687.
[65] A.Y. Timoshkin, H.F. Schaefer, J. Am. Chem. Soc. 125 (2003) 9998.
[66] V. Jonas, G. Frenking, M.T. Reetz, J. Am. Chem. Soc. 116 (1994) 8741.
[67] C. Loschen, K. Voigt, J. Frunzke, A. Diefenbach, M. Diedenhofen, G. Frenking, Z. Anorg. Allg. Chem. 628 (2002) 1294.
[68] I.S. Ignatyev, T. Sundius, J. Mol. Struct. 480–481 (1999) 667.
[69] E.I. Davydova, T.N. Sevastianova, A.Y. Timoshkin, A.V. Suvorov, G. Frenking, Int. J. Quant. Chem. 100 (2004) 419.
[70] A.Y. Timoshkin, E.I. Davydova, T.N. Sevastianova, A.V. Suvorov, H.F. Schaefer, Int. J. Quant. Chem. 88 (2002) 436.
[71] E.I. Davydova, A.Y. Timoshkin, T.N. Sevastianova, A.V. Suvorov, G. Frenking, J. Mol. Struct. Theochem. 767 (2006) 103.
[72] H. Fleischer, Eur. J. Inorg. Chem. (2001) 393.
[73] I.S. Ignatyev, H.F. Schaefer, J. Phys. Chem. A 105 (2001) 7665.
[74] M. Siodmiak, G. Frenking, A. Korkin, J. Mol. Model. 6 (2000) 413.
[75] O. Holloczki, L. Nyulaszi, Organometallics 28 (2009) 4159.
[76] B.D. Rowsell, R.J. Gillespie, G.L. Heard, Inorg. Chem. 38 (1999) 4659.
[77] H. Hirao, K. Omoto, H. Fujimoto, J. Phys. Chem. A 103 (1999) 5807.
[78] F. Bessac, G. Frenking, Inorg. Chem. 42 (2003) 7990.
[79] V. Horvath, A. Kovacs, I. Hargittai, J. Phys. Chem. A 107 (2003) 1197.
[80] V. Horvath, I. Hargittai, Struct. Chem. 15 (2004) 233.
[81] G. Frenking, K. Wichmann, N. Fröhlich, C. Loschen, M. Lein, J. Frunzke, V.M. Rayón, Coord. Chem. Rev. 238–239 (2003) 55.
[82] F. Bessac, G. Frenking, Inorg. Chem. 45 (2006) 6956.
[83] R. Hart, W. Levason, B. Patel, G. Reid, J. Chem. Soc., Dalton Trans. (2002) 3153.
[84] R. Hart, W. Levason, B. Patel, G. Reid, Eur. J. Inorg. Chem. (2001) 2927.
[85] S. Abram, C. Maichle-Mössmer, U. Abram, Polyhedron 16 (1997) 2183.
[86] A.C. Legon, H.E. Warner, J. Chem. Soc. Chem. Commun. (1991) 1397.
[87] K. Iijima, S. Shibata, Bull. Chem. Soc. Jpn. 52 (1979) 711.
[88] P.S. Bryan, R.L. Kuczkowski, Inorg. Chem. 10 (1971) 200.
[89] P. Cassoux, R.L. Kuczkowski, A. Serafini, Inorg. Chem. 16 (1977) 3005.
[90] K. Iijima, T. Noda, M. Maki, T. Sasase, S. Shibata, J. Mol. Struct. 144 (1986) 169.
[91] W. Caminati, D. Damiani, J. Mol. Struct. 147 (1986) 389.
[92] S.W. Reeve, W.A. Burns, F.J. Lovas, R.D. Suenram, K.R. Leopold, J. Phys. Chem. 97 (1993) 10630.
[93] M.A. Dvorak, R.S. Ford, R.D. Suenram, F.J. Lovas, K.R. Leopold, J. Am. Chem. Soc. 114 (1992) 108.
[94] K. Iijima, T. Yamada, S. Shibata, J. Mol. Struct. 77 (1981) 271.
[95] K. Iijima, S. Shibata, Bull. Chem. Soc. Jpn. 53 (1980) 1908.
[96] K. Iijima, S. Shibata, Bull. Chem. Soc. Jpn. 52 (1979) 3204.
[97] K. Iijima, E. Koshimizu, S. Shibata, Bull. Chem. Soc. Jpn. 54 (1981) 2255.
[98] V.P. Spiridonov, A.S. Malkova, Zh. Strukt. Khim. (Russ.) 10 (1969) 332.
[99] R.S. Ruoff, T.C. Emilsson, A.I. Jaman, T.C. Germann, H.S. Gutowsky, J. Chem. Phys. 96 (1992) 3441.
[100] K.R. Leopold, M. Canagaratna, J.A. Phillips, Acc. Chem. Res. 30 (1997) 57, and references therein.
[101] G.H. Penner, B. Ruscitti, J. Reynolds, I. Swainson, Inorg. Chem. 41 (2002) 7064.
[102] J.A. Phillips, C.J. Cramer, J. Chem. Theory Comput. 1 (2005) 827.
[103] J.A. Phillips, J.A. Halfen, J.P. Wrass, C.C. Knutson, C.J. Cramer, Inorg. Chem. 45 (2006) 722.
[104] J.A. Phillips, C.J. Cramer, J. Phys. Chem. B 111 (2007) 1408.
[105] E.M. Cabaleiro-Lago, M.A. Rios, Chem. Phys. Lett. 294 (1998) 272.
[106] A.V. Suvorov, A.S. Malkova, V.I. Avrorina, Zh. Neorg. Khim. 14 (1969) 1374.
[107] M.V. Volkova, T.N. Sevast'yanova, S.G. Semenov, A.V. Suvorov, A.Sh. Tarasova, Koord. Khim. (Russ.) 12 (1986) 1490.
[108] C. Peylhard, P. Teulon, A. Potier, Z. Anorg. Allg. Chem. 483 (1981) 236.
[109] D. Mootz, M. Steffen, Z. Anorg. Allg. Chem. 483 (1981) 171.
[110] J.L. Hoard, S. Geller, W.M. Cashin, Acta Crystallogr. 4 (1951) 396.

[111] J.L. Hoard, S. Geller, T.B. Owen, Acta Crystallogr. 4 (1951) 405.
[112] D. Göbbels, G. Meyer, Z. Anorg, Allg. Chem. 628 (2002) 1799.
[113] S. Geller, J.L. Hoard, Acta Crystallogr. 3 (1950) 121.
[114] S. Geller, J.L. Hoard, Acta Crystallogr. 4 (1951) 399.
[115] Z.V. Zvonkova, Kristallografiya 1 (1956) 73.
[116] K. Töpel, K. Hensen, J.W. Bats, Acta Crystallogr. C 40 (1984) 828.
[117] M.J.G. Lesley, A. Woodward, N.J. Taylor, T.B. Marder, I. Cazenobe, I. Ledoux, J. Zyss, A. Thornton, D.W. Bruce, A.K. Kakkar, Chem. Mater. 10 (1998) 1355.
[118] W.A. Burns, K.R. Leopold, J. Am. Chem. Soc. 115 (1993) 11622.
[119] J.L. Hoard, T.B. Owen, A. Buzzell, O.N. Salmon, Acta Crystallogr. 3 (1950) 130.
[120] B. Swanson, D.F. Shriver, J.A. Ibers, Inorg. Chem. 8 (1969) 2182.
[121] J.A. Phillips, D.J. Giesen, N.P. Wells, J.A. Halfen, C.C. Knutson, J.P. Wrass, J. Phys. Chem. A 109 (2005) 8199.
[122] M. Haddad, J.P. Legros, L. Lopez, M.T. Boisdon, J. Barrans, Phosph. Sulf. Silicon Relat. Elem. 69 (1992) 189.
[123] M. Haddad, F. Dahan, J.-P. Legros, L. Lopez, M.-T. Boisdon, J. Barrans, J. Chem. Soc., Perkin Trans. 2 (1992) 671.
[124] S.E. Denmark, J.I. Montgomery, L.A. Kramps, J. Am. Chem. Soc. 128 (2006) 11620.
[125] M. Güizado-Rodríguez, A. Ariza-Castolo, G. Merino, A. Vela, H. Nöth, V.I. Bakhmutov, R. Contreras, J. Am. Chem. Soc. 123 (2001) 9144.
[126] R.E. Banks, M.K. Besheesh, R.G. Pritchard, I. Sharif, Acta Crystallogr. C 49 (1993) 1804.
[127] I.I. Padilla-Martinez, M.J. Rosalez-Hoz, H. Tlahuext, C. Camacho-Camacho, A. Ariza-Castolo, R. Contreras, Chem. Ber. 129 (1996) 441.
[128] D. Görz, H. Pritzkow, W. Siebert, Eur. J. Inorg. Chem. (2003) 2783.
[129] W. Pieper, D. Schmitz, P. Paetzold, Chem. Ber. 114 (1981) 3801.
[130] M. Schröter, E. Lork, R. Mews, Z. Anorg. Allg. Chem. 631 (2005) 1609.
[131] M. Möhlen, K. Harms, K. Dehnicke, J. Magull, H. Goesmann, D. Fenske, Z. Anorg. Allg. Chem. 622 (1996) 1692.
[132] F. Heshmatpour, D. Nußhär, R. Garbe, S. Wocadlo, W. Massa, K. Dehnicke, H. Goesmann, D. Fenske, Z. Anorg. Allg. Chem. 621 (1995) 443.
[133] Y. Ma, E. Lobkovsky, D.B. Collum, J. Org. Chem. 70 (2005) 2335.
[134] R. Mahrwald, B. Ziemer, S. Troyanov, Tetrahedron Lett. 42 (2001) 6843.
[135] A. Galland, J.M. Paris, T. Schlama, R. Guillot, J.-C. Fiaud, M. Toffano, Eur. J. Org. Chem. (2007) 863.
[136] J. Nikolai, G. Taubmann, G. Maas, Z. Naturforsch. B 58 (2003) 217.
[137] E.J. Corey, T.-P. Loh, S. Sarshar, M. Azimioara, Tetrahedron Lett. 33 (1992) 6945.
[138] M. Well, A. Fischer, P.G. Jones, R. Schmutzler, Phosph. Sulf. Silicon Relat. Elem. 80 (1993) 189.
[139] D.H. Ryu, T.W. Lee, E.J. Corey, J. Am. Chem. Soc. 124 (2002) 9992.
[140] M.T. Reetz, M. Huellmann, W. Massa, S. Berger, P. Rademacher, P. Heymanns, J. Am. Chem. Soc. 108 (1986) 2405.
[141] N. Burford, R.E.v.H. Spence, A. Linden, T.S. Cameron, Acta Crystallogr. C 46 (1990) 92.
[142] A.J. Arduengo III, F. Davidson, R. Krafczyk, W.J. Marshall, R. Schmutzler, Monatsh. Chem. 131 (2000) 251.
[143] J.M. Stoddard, K.J. Shea, Organometallics 22 (2003) 1124.
[144] D.J. Nielsen, K.J. Cavell, B.W. Skelton, A.H. White, Inorg. Chim. Acta 352 (2003) 143.
[145] X. Cattoën, H. Gornitzka, D. Bourissou, G. Bertrand, J. Am. Chem. Soc. 126 (2004) 1342.
[146] N. Kuhn, R. Fawzi, H. Kotowski, M. Steimann, Z. Kristallogr.-New Cryst. Struct. 212 (1997) 259.
[147] U. Monkowius, S. Nogai, H. Schmidbaur, Dalton Trans. (2003) 987.
[148] A.G. Avent, P.B. Hitchcock, M.F. Lappert, D.-S. Liu, G. Mignani, C. Richard, E. Roche, J. Chem. Soc. Chem. Commun. (1995) 855.
[149] P.H. Clippard, J.C. Hanson, R.C. Taylor, J. Cryst. Mol. Struct. 1 (1971) 363.
[150] H. Hess, Acta Crystallogr. B 25 (1969) 2338.
[151] R. Minkwitz, R. Nass, M. Rieland, H. Preut, Z. Anorg. Allg. Chem. 550 (1987) 133.
[152] R. Minkwitz, R. Nass, H. Preut, Z. Anorg. Allg. Chem. 546 (1987) 99.
[153] K. Töpel, K. Hensen, M. Trömel, Acta Crystallogr. B 37 (1981) 969.
[154] K. Anton, H. Nöth, H. Pommerening, Chem. Ber. 117 (1984) 2479.
[155] R.A. Baber, A.E.A. Bull, J.P.H. Charmant, N.C. Norman, A.G. Orpen, Acta Crystallogr. E 61 (2005) o553.
[156] M. Weinmann, J. Nuss, M. Jansen, Acta Crystallogr. E 62 (2006) o5590.
[157] M.L. Levin, J.W. Fieldhouse, H.R. Allcock, Acta Crystallogr. B 38 (1982) 2284.
[158] D.L. Boucher, M.A. Brown, B.R. McGarvey, D.G. Tuck, J. Chem. Soc. Dalton Trans. (1999) 3445.
[159] D.L. Black, R.C. Taylor, Acta Crystallogr. B 31 (1975) 1116.
[160] M.S. Lube, R.L. Wells, P.S. White, Inorg. Chem. 35 (1996) 5007.
[161] J.P.H. Charmant, C. Fan, N.C. Norman, P.G. Pringle, Dalton Trans. (2007) 114.
[162] M.S. Lube, R.J. Jouet, R.L. Wells, P.S. Whtte, V.G. Young Jr., Main Group Chem. 2 (1997) 89.
[163] P. Biagini, F. Calderazzo, F. Marchetti, G. Pampaloni, S. Ramello, M. Salvalaggio, R. Santi, S. Spera, Dalton Trans. (2004) 2364.
[164] R.K. Chadha, J.M. Chehayber, J.E. Drake, J. Crystallogr. Spectrosc. Res. 15 (1985) 53.
[165] B. Krebs, G. Schwetlik, M. Wienkenhöver, Acta Crystallogr. B 45 (1989) 257.
[166] I. Vargas-Baca, M. Findlater, A. Powell, K.V. Vasudevan, A.H. Cowley, Dalton Trans. (2008) 6421.
[167] D.F. Grant, R.C.G. Killean, J.L. Lawrence, Acta Crystallogr. B25 (1969) 377.
[168] F. Weller, M. Möhlen, K. Dehnicke, Z. Kristallogr.-New Cryst. Struct. 212 (1997) 159.
[169] K. Iijima, I. Oonishi, S. Shibata, Chem. Lett. (1983) 251.
[170] C. Aubauer, G. Engelhardt, T.M. Klapötke, H. Nöth, A. Schulz, M. Warchhold, Eur. J. Inorg. Chem. (2000) 2245.
[171] F. Dornhaus, M. Bolte, H.-W. Lerner, M. Wagner, Eur. J. Inorg. Chem. (2006) 1777.
[172] C. Aubauer, K. Davidge, T.M. Klapötke, P. Mayer, H. Piotrowski, A. Schulz, Z. Anorg. Allg. Chem. 626 (2000) 2373.
[173] Y. Wang, B. Quillian, P. Wei, C.S. Wannere, Y. Xie, R.B. King, H.F. Schaefer III, P.v.R. Schleyer, G.H. Robinson, J. Am. Chem. Soc. 129 (2007) 12412.
[174] T. Gelbrich, J. Sieler, U. Dümichen, Z. Kristallogr. 215 (2000) 127.
[175] M. Jansen, T. Jäschke, Z. Naturforsch. B 55 (2000) 763.
[176] M. Heckel, W. Hiller, Z. Kristallogr. 211 (1996) 661.
[177] M.-R. Mazieres, T.-C. Kim, R. Wolf, M. Sanchez, J. Jaud, Z. Kristallogr. 184 (1988) 147.
[178] N. Burford, R.G. Hicks, B.W. Royan, B. Borecka, T.S. Cameron, Acta Crystallogr. C 47 (1991) 1066.
[179] W. Clegg, U. Klingebiel, J. Neemann, G.M. Sheldrick, J. Organomet. Chem. 249 (1983) 47.
[180] L.M. Engelhardt, P.C. Junk, C.L. Raston, B.W. Skelton, A.H. White, J. Chem. Soc., Dalton Trans. (1996) 3297.
[181] A. Dimitrov, D. Heidemann, E. Kemnitz, Inorg. Chem. 45 (2006) 10807.
[182] F. Thomas, T. Bauer, S. Schulz, M. Nieger, Z. Anorg. Allg. Chem. 629 (2003) 2018.
[183] I. Krossing, H. Nöth, H. Schwenk-Kircher, T. Seifert, C. Tacke, Eur. J. Inorg. Chem. (1998) 1925.
[184] Q.M. Cheng, O. Stark, K. Merz, M. Winter, R.A. Fischer, J. Chem. Soc., Dalton Trans. (2002) 2933.
[185] H. Ott, C. Matthes, S. Schmatz, U. Klingebiel, D. Stalke, Z. Naturforsch. B 63 (2008) 1023.
[186] C.M. Ong, P. McKarns, D.W. Stephan, Organometallics 18 (1999) 4197.
[187] B. Jäschke, M. Jansen, Z. Kristallogr. - New Cryst. Struct. 218 (2003) 381.
[188] U. Klingebiel, M. Noltemyer, H.-G. Schmidt, D. Schmidt-Bäse, Chem. Ber. 130 (1997) 753.
[189] A.H. Cowley, M.C. Cushner, P.E. Riley, J. Am. Chem. Soc. 102 (1980) 624.
[190] S. Tragl, K. Gibson, H.-J. Meyer, Z. Anorg. Allg. Chem. 633 (2007) 470.
[191] A.J. Heston, M.J. Panzner, W.J. Youngs, C.A. Tessier, Inorg. Chem. 44 (2005) 6518.
[192] J.C. Gálvez-Ruiz, C. Guadarrama-Pérez, H. Nöth, A. Flores-Parra, Eur. J. Inorg. Chem. (2004) 601.
[193] R.L. Wells, A.T. McPhail, J.A. Laske, P.S. White, Polyhedron 13 (1994) 2737.
[194] A. Bittner, D. Männig, H. Nöth, Z. Naturforsch. B 41 (1986) 587.
[195] S.E. Rasmussen, N.C. Broch, Chem. Commun. 13 (1965) 289b.
[196] S.E. Rasmussen, N.C. Broch, Acta Chem. Scand. 20 (1966) 1351.
[197] J.-M. Le Carpentier, R. Weiss, Acta Crystallogr. B 28 (1972) 1437.
[198] P. Sobota, M.O. Mustafa, J. Utko, T. Lis, J. Organomet. Chem. 368 (1989) 257.
[199] N. Burford, B.W. Royan, R.E.v.H. Spence, T.S. Cameron, A. Linden, R.D. Rogers, J. Chem. Soc., Dalton Trans. (1990) 1521.
[200] A.M. Arif, A.H. Cowley, R.M. Kren, D.L. Westmoreland, Heteroat. Chem. 1 (1990) 117.
[201] F. Bigi, G. Sartori, R. Maggi, C. Valerio-Papa, E. Marzi, M. Lanfranchi, M.A. Pellinghelli, J. Chem. Soc., Perkin Trans. 1 (1996) 1815.
[202] B. Chevrier, J.-M. Le Carpentier, R. Weiss, Acta Crystallogr. B 28 (1972) 2659.
[203] N. Burford, B.W. Royan, R.E.v.H. Spence, R.D. Rogers, J. Chem. Soc., Dalton Trans. (1990) 2111.
[204] N. Burford, R.E.v.H. Spence, R.D. Rogers, J. Chem. Soc., Dalton Trans. (1990) 3611.
[205] A. Stasch, S. Singh, H.W. Roesky, M. Noltemeyer, H.-G. Schmidt, Eur. J. Inorg. Chem. (2004) 4052.
[206] A. Hinchliffe, F.S. Mair, E.J.L. McInnes, R.G. Pritchard, J.E. Warren, Dalton Trans. (2008) 222.
[207] C. Hubrich, D. Michalik, A. Schulz, A. Villinger, Z. Anorg. Allg. Chem. 634 (2008) 1403.
[208] S.A. Sangokoya, B. Lee, M.F. Self, W.T. Pennington, G.H. Robinson, Polyhedron 8 (1989) 1497.
[209] J. Utko, M. Wróblewska, T. Lis, P. Sobota, J. Organomet. Chem. 447 (1993) 159.
[210] P. Sobota, S. Szafert, T. Glowiak, J. Organomet. Chem. 526 (1996) 329.
[211] M. Lanfranchi, M.A. Pellinghelli, G. Predieri, F. Bigi, R. Maggi, G. Sartori, J. Chem. Soc., Dalton Trans. (1993) 1463.
[212] L. Hubener, H.-W. Lerner, M. Bolte, Acta Crystallogr. E 59 (2003) m929.
[213] K. Anton, H. Fußstetter, H. Nöth, Chem. Ber. 114 (1981) 2723.
[214] J. Vollet, R. Burgert, H. Schnöckel, Angew. Chem. Int. Ed. 44 (2005) 6956.
[215] P.F. Kelly, A.M.Z. Slawin, J. Chem. Soc., Dalton Trans. (1996) 4029.
[216] M. Rastätter, P.W. Roesky, Eur. J. Inorg. Chem. (2008) 5287.
[217] C.S. Branch, S.G. Bott, A.R. Barron, J. Organomet. Chem. 666 (2003) 23.
[218] S. Scholz, H.-W. Lerner, M. Bolte, Acta Crystallogr. E 59 (2003) m289.
[219] C. Klemp, C. Üffing, E. Baum, H. Schnöckel, Z. Anorg. Allg. Chem. 626 (2000) 1787.
[220] L. Jakobsmeier, I. Krossing, H. Nöth, M.J.H. Schmidt, Z. Naturforsch. B 51 (1996) 1117.
[221] A. Weiss, R. Plass, A. Weiss, Z. Anorg. Allg. Chem. 283 (1956) 390.
[222] I. Krossing, H. Nöth, H. Schwenk-Kircher, Eur. J. Inorg. Chem. (1998) 927.
[223] C. Jones, P.C. Junk, M. Kloth, K.M. Proctor, A. Stasch, Polyhedron 25 (2006) 1592.
[224] K. Anton, H. Nöth, Chem. Ber. 115 (1982) 2668.
[225] T. Pell, D.P. Mills, A.J. Blake, W. Lewis, S.T. Liddle, Polyhedron 29 (2010) 120.
[226] K. Anton, C. Euringer, H. Nöth, Chem. Ber. 117 (1984) 1222.
[227] M. Schaffrath, A. Schulz, A. Villinger, Acta Crystallogr. E 63 (2007) m2764.

[228] S. Nogai, A. Schriewer, H. Schmidbaur, Dalton Trans. (2003) 3165.
[229] D.A. Atwood, V.O. Atwood, D.F. Carriker, A.H. Cowley, F.P. Gabbai, R.A. Jones, M.R. Bond, C.J. Carrano, J. Organomet. Chem. 463 (1993) 29.
[230] H. Schmidbaur, S.D. Nogai, Z. Anorg. Allg. Chem. 630 (2004) 2218.
[231] Z. Yu, A.V. Korolev, M.J. Heeg, C.H. Winter, Polyhedron 21 (2002) 1117.
[232] S. Zanias, C.P. Raptopoulou, A. Terzis, T.F. Zafiropoulos, Inorg. Chem. Commun. 2 (1999) 48.
[233] F. Cheng, H.L. Codgbrook, A.L. Hector, W. Levason, G. Reid, M. Webster, W. Zhang, Polyhedron 26 (2007) 4147.
[234] S. Nogai, H. Schmidbaur, Inorg. Chem. 41 (2002) 4770.
[235] N. Burford, T.S. Cameron, D.J. LeBlanc, P. Losier, S. Sereda, G. Wu, Organometallics 16 (1997) 4712.
[236] J.F. Janik, R.A. Baldwin, R.L. Wells, W.T. Pennington, G.L. Schimek, A.L. Rheingold, L.M. Liable-Sands, Organometallics 15 (1996) 5385.
[237] J.C. Carter, G. Jugie, R. Enjalbert, J. Galy, Inorg. Chem. 17 (1978) 1248.
[238] J.J. Weigand, N. Burford, A. Decken, Eur. J. Inorg. Chem. (2008) 4343.
[239] F. Cheng, A.L. Hector, W. Levason, G. Reid, M. Webster, W. Zhang, Acta Crystallogr. E 63 (2007) m1761.
[240] S. Herler, P. Mayer, J. Schmedt auf der Günne, A. Schulz, A. Villinger, J.J. Weigand, Angew. Chem. Int. Ed. 44 (2005) 7790.
[241] A. Schulz, A. Villinger, Angew. Chem. Int. Ed. 47 (2008) 603.
[242] F. Cheng, A.L. Hector, W. Levason, G. Reid, M. Webster, W. Zhang, Inorg. Chem. 46 (2007) 7215.
[243] S. Scholz, H.-W. Lerner, M. Bolte, Acta Crystallogr. E 58 (2002) m586.
[244] M.G. Davlieva, S.V. Lindeman, I.S. Neretin, J.K. Kochi, J. Org. Chem. 70 (2005) 4013.
[245] C. Gurnani, W. Levason, R. Ratnani, G. Reid, M. Webster, Dalton Trans. (2008) 6274.
[246] N. Marion, E.C. Escudero-Adán, J. Benet-Buchholz, E.D. Stevens, L. Fensterbank, M. Malacria, S.P. Nolan, Organometallics 26 (2007) 3256.
[247] J.D. Masuda, D. Martin, C. Lyon-Saunier, A. Baceiredo, H. Gornitzka, B. Donnadieu, G. Bertrand, Chem. Asian J. 2 (2007) 178.
[248] M. Sigl, A. Schier, H. Schmidbaur, Z. Naturforsch. B 53 (1998) 1301.
[249] S.P. Green, C. Jones, A. Stasch, R.P. Rose, New J. Chem. 31 (2007) 127.
[250] J.D. Johansen, A.T. McPhail, R.L. Wells, Adv. Mater. Opt. Electron. 1 (1992) 29.
[251] L.-J. Baker, L.A. Kloo, C.E.F. Rickard, M.J. Taylor, J. Organomet. Chem. 545–546 (1997) 249.
[252] M.A. Brown, J.A. Castro, D.G. Tuck, Can. J. Chem. 75 (1997) 333.
[253] B. Beagley, S.M. Godfrey, K.J. Kelly, S. Kungwankunakorn, C.A. McAuliffe, R.G. Pritchard, Chem. Commun. (1996) 2179.
[254] F. Chen, G. Ma, R.G. Cavell, V.V. Terskikh, R.E. Wasylishen, Chem. Commun. (2008) 5933.
[255] C.D. Abernethy, M.L. Cole, C. Jones, Organometallics 19 (2000) 4852.
[256] R.J. Baker, A.J. Davies, C. Jones, M. Kloth, J. Organomet. Chem. 656 (2002) 203.
[257] S.J. Black, D.E. Hibbs, M.B. Hursthouse, C. Jones, K.M.A. Malik, N.A. Smithies, J. Chem. Soc., Dalton Trans. (1997) 4313.
[258] S. Kühner, H.-D. Hausen, J. Weidlein, Z. Anorg. Allg. Chem. 624 (1998) 13.
[259] N.W. Alcock, I.A. Degnan, O.W. Howarth, M.G.H. Wallbridge, J. Chem. Soc., Dalton Trans. (1992) 2775.
[260] M.A. Brown, D.G. Tuck, E.J. Wells, Can. J. Chem. 74 (1996) 1535.
[261] S.M. Godfrey, K.J. Kelly, P. Kramkowski, C.A. McAuliffe, R.G. Pritchard, Chem. Commun. (1997) 1001.
[262] M.A. Brown, D.G. Tuck, Can. J. Chem. 78 (2000) 536.
[263] M. Sigl, A. Schier, H. Schmidbaur, Z. Naturforsch. B 54 (1999) 21.
[264] T. Gelbrich, U. Dümichen, J. Sieler, Acta Crystallogr. C 55 (1999) 1797.
[265] A. Ahmed, W. Schwarz, J. Weidlein, H. Hess, Z. Anorg. Allg. Chem. 434 (1977) 207.
[266] E.B. Lobkovskii, I.I. Korobov, K.N. Semenenko, Zh. Strukt. Khim. (Russ.) 19 (1978) 1063.
[267] G. Müller, C. Krüger, Acta Crystallogr. C 40 (1984) 628.
[268] A.H. Cowley, M.C. Cushner, R.E. Davis, P.E. Riley, Inorg. Chem. 20 (1981) 1179.
[269] A. Ecker, H. Schnöckel, Z. Anorg. Allg. Chem. 624 (1998) 813.
[270] S.D. Nogai, H. Schmidbaur, Dalton Trans. (2003) 2488.
[271] R. Karia, G.R. Willey, M.G.B. Drew, Acta Crystallogr. C 42 (1986) 558.
[272] R.L. Beddoes, D. Collison, F.E. Mabbs, J. Temperley, Acta Crystallogr. C 47 (1991) 58.
[273] W.T. Robinson, C.J. Wilkins, Z. Zeying, J. Chem. Soc., Dalton Trans. (1988) 2187.
[274] D.J. Williams, V.L.H. Bevilacqua, P.A. Morson, K.J. Dennison, W.T. Pennington, G.L. Schimek, D. VanDerveer, J.S. Kruger, N.T. Kawai, Inorg. Chim. Acta 285 (1999) 217.
[275] S.P. Sinha, T.T. Pakkanen, T.A. Pakkanen, L. Niinistö, Polyhedron 1 (1982) 355.
[276] M.F. Self, A.T. McPhail, R.L. Wells, Polyhedron 12 (1993) 455.
[277] B.R. Whittlesey, I.P. Ittycheriah, Acta Crystallogr. C 50 (1994) 693.
[278] H.V.R. Dias, W. Jin, Inorg. Chem. 35 (1996) 267.
[279] S. Jin, V. McKee, M. Nieuwenhuyzen, W.T. Robinson, C.J. Wilkins, J. Chem. Soc., Dalton Trans. (1993) 3111.
[280] I.A. Degnan, N.W. Alcock, S.M. Roe, M.G.H. Wallbridge, Acta Crystallogr. C 48 (1992) 995.
[281] M.V. Veidis, G.J. Palenik, J. Chem. Soc. D (1969) 586b.
[282] S. Chitsaz, T. Breyhan, J. Pauls, B. Neumüller, Z. Anorg. Allg. Chem. 628 (2002) 956.
[283] G.R. Willey, D.R. Aris, J.V. Haslop, W. Errington, Polyhedron 20 (2001) 423.
[284] W. Clegg, N.C. Norman, N.L. Pickett, Acta Crystallogr. C 50 (1994) 36.
[285] G. Beran, A.J. Carty, H.A. Patel, G.J. Palenik, J. Chem. Soc. D (1970) 222.
[286] M. Itazaki, R. Ujihara, H. Nakazawa, Acta Crystallogr. E 62 (2006) m1649.
[287] S.E. Jeffs, R.W.H. Small, I.J. Worrall, Acta Crystallogr. C 40 (1984) 1329.
[288] R.J. Butcher, C. George, N. Muratore, A.P. Purdy, Acta Crystallogr. E 59 (2003) m1107.
[289] M. Green, S. Norager, P. Moriarty, M. Motevalli, P. O'Brien, J. Mater. Chem. 10 (2000) 1939.
[290] S. Das, C.-H. Hung, S. Goswami, Inorg. Chem. 42 (2003) 5153.
[291] R.L. Wells, S.S. Kher, R.A. Baldwin, P.S. White, Polyhedron 13 (1994) 2731.
[292] A. Dashti, K. Niediek, B. Werner, B. Neumüller, Z. Anorg. Allg. Chem. 623 (1997) 394.
[293] W.T. Robinson, C.J. Wilkins, Z. Zeying, J. Chem. Soc., Dalton Trans. (1990) 219.
[294] R.W.H. Small, I.J. Worrall, Acta Crystallogr. B 38 (1982) 932.
[295] M.A. Brown, D.G. Tuck, Inorg. Chim. Acta 247 (1996) 135.
[296] P. Müller, I. Usón, J. Prust, H.W. Roesky, Acta Crystallogr. C 56 (2000) 1300.
[297] K. Hensen, A. Lemke, M. Bolte, Z. Naturforsch. B 55 (2000) 877.
[298] N. Kuhn, T. Kratz, D. Bläser, R. Boese, Chem. Ber. 128 (1995) 245.
[299] Y. Wang, Y. Xie, P. Wei, R.B. King, H.F. Schaefer III, P.v.R. Schleyer, G.H. Robinson, Science 321 (2008) 1069.
[300] I.M. Lazarev, Y.E. Ovchinnikov, G.V. Dolgushin, Y.T. Struchkov, Mendeleev Commun. 7 (1997) 16.
[301] M.S. Bilton, M. Webster, J. Chem. Soc. Dalton Trans. (1972) 722.
[302] K. Hensen, A. Lemke, M. Bolte, Acta Crystallogr. C 56 (2000) 1196.
[303] K. Hensen, A. Lemke, M. Bolte, Acta Crystallogr. C 56 (2000) e565.
[304] C.-I. Bränden, I. Lindqvist, Acta Chem. Scand. 14 (1960) 726.
[305] M. Boyer, Y. Jeannin, C. Rocchiccioli-Deltcheff, R. Thouvenot, J. Coord. Chem. 7 (1978) 219.
[306] L. Brun, Acta Crystallogr. 20 (1966) 739.
[307] I.W. Bassi, M. Calcaterra, R. Intrito, J. Organomet. Chem. 127 (1977) 305.
[308] T. Carofiglio, P.G. Cozzi, C. Floriani, A. Chiesi-Villa, C. Rizzoli, Organometallics 12 (1993) 2726.
[309] N.R. Strel'tsova, L.V. Ivakina, V.K. Bel'skii, P.A. Storozhenko, B.M. Bulichev, Koord. Khim. (Russ.) 14 (1988) 421.
[310] T.S. Lewkebandara, P.J. McKarns, B.S. Haggerty, G.P.A. Yap, A.L. Rheingold, C.H. Winter, Polyhedron 17 (1998) 1.
[311] E. Gauch, H. Hoppe, J. Strähle, J. Organomet. Chem. 593–594 (2000) 175.
[312] K. Hensen, A. Lemke, C. Näthe, Z. Anorg. Allg. Chem. 623 (1997) 1973.
[313] U. Thewalt, K. Holl, Z. Naturforsch. B 43 (1988) 467.
[314] P.G. Cozzi, E. Solari, C. Floriani, A. Chiesi-Villa, C. Rizzoli, Chem. Ber. 129 (1996) 1361.
[315] H.W. Roesky, J. Schimkowiak, H.-G. Schmidt, M. Noltemeyer, G.M. Sheldrick, Chem. Ber. 123 (1990) 1345.
[316] V. Di Noto, S. Bresadola, R. Zannetti, M. Viviani, G. Valle, Z. Kristallogr. 194 (1991) 267.
[317] G. Quinkert, M. del Grosso, A. Bucher, M. Bauch, W. Döring, J.W. Bats, G. Dürner, Tetrahedron Lett. 33 (1992) 3617.
[318] H. Wei, Y.-H. Li, Y. Zhang, Acta Crystallogr. E 63 (2007) m798.
[319] B. Schweder, H. Görls, D. Walther, Inorg. Chim. Acta 286 (1999) 14.
[320] L.M. Liable-Sands, A.L. Rheingold, Private Commun. (1999).
[321] D.A. Young, J. Mol. Catal. 53 (1989) 433.
[322] P. Sobota, M.O. Mustafa, T. Lis, J. Organomet. Chem. 377 (1989) 69.
[323] S.I. Troyanov, M.A. Simonov, Koord. Khim. (Russ.) 12 (1986) 1276.
[324] C. Plitzko, G. Meyer, Z. Anorg. Allg. Chem. 622 (1996) 1646.
[325] O.J. Rutt, A.R. Cowley, S.J. Clarke, Acta Crystallogr. E 63 (2007) o3406.
[326] V.A. Bain, R.C.G. Killean, M. Killean, Acta Crystallogr. (B) 25 (1969) 156.
[327] A.D. Adley, P.H. Bird, A.R. Fraser, M. Onyszchuk, Inorg. Chem. 11 (1972) 1402.
[328] A.N. Chekhlov, V.V. Tkachev, S.A. Lermontov, Zh. Strukt. Khim. (Russ.) 44 (2003) 1165.
[329] O. Bechstein, B. Ziemer, D. Hass, S.I. Trojanov, V.B. Rybakov, G.N. Maso, Z. Anorg. Allg. Chem. 582 (1990) 211.
[330] K. Hensen, R. Mayr-Stein, B. Spangenberg, M. Bolte, Acta Crystallogr. C 56 (2000) 610.
[331] S.E. Denmark, B.M. Eklov, Chem.-Eur. J 14 (2008) 234.
[332] K. Hensen, R. Mayr-Stein, B. Spangenberg, M. Bolte, S. Rühl, Z. Naturforsch. B 55 (2000) 248.
[333] M. Bolte, K. Hensen, B. Spangenberg, J. Chem. Crystallogr. 30 (2000) 245.
[334] D.T. Tran, P.Y. Zavalij, S.R.J. Oliver, Acta Crystallogr. E 58 (2002) m742.
[335] F. Cheng, M.F. Davis, A.L. Hector, W. Levason, G. Reid, M. Webster, W. Zhang, Eur. J. Inorg. Chem. (2007) 4897.
[336] M.F. Davis, W. Levason, G. Reid, M. Webster, Dalton Trans. (2008) 2261.
[337] M.F. Davis, W. Levason, G. Reid, M. Webster, W. Zhang, Dalton Trans. (2008) 533.
[338] F. Cheng, M.F. Davis, A.L. Hector, W. Levason, G. Reid, M. Webster, W. Zhang, Eur. J. Inorg. Chem. (2007) 2488.
[339] N.W. Mitzel, U. Losehand, K. Vojinovic, Inorg. Chem. 40 (2001) 5302.
[340] R. Hulme, G.J. Leigh, I.R. Beattie, J. Chem. Soc. (1960) 366.
[341] G.R. Willey, U. Somasunderam, D.R. Aris, W. Errington, Inorg. Chim. Acta 315 (2001) 191.
[342] J. Ejfler, S. Szafert, H. Jiao, P. Sobota, New J. Chem. 26 (2002) 803.
[343] M. Bolte, K. Hensen, A. Faber, Acta Crystallogr. C 56 (2000) e497.
[344] S.M. Godfrey, I. Mushtaq, R.G. Pritchard, J. Chem. Soc., Dalton Trans. (1999) 1319.
[345] K. Hensen, A. Faber, M. Bolte, Acta Crystallogr. C 55 (1999) 1774.
[346] M. Bolte, K. Hensen, A. Faber, Acta Crystallogr. C 56 (2000) e499.
[347] M.F. Davis, M. Clarke, W. Levason, G. Reid, M. Webster, Eur. J. Inorg. Chem. (2006) 2773.
[348] V.N. Zaharov, A.V. Yatsenko, A.L. Kamushnui, L.A. Aslanov, Koord. Khim. (Russ.) 71 (1991) 789.
[349] Z.-H. Su, B.-B. Zhou, Z.-F. Zhao, S.W. Ng, Acta Crystallogr. E 63 (2007) m394.

[350] M. Webster, H.E. Blayden, J. Chem. Soc. A (1969) 2443.
[351] C.-I. Bränden, Acta Chem. Scand. 17 (1963) 759.
[352] M.M. Ebrahim, H. Stoeckli-Evans, K. Panchanatheswaran, J. Organomet. Chem. 692 (2007) 2168.
[353] A.V. Yatsenko, L.A. Aslanov, Yu.M. Burtsev, E.A. Kravchenko, Zh. Neorg. Khim. (Russ.) 36 (1991) 2031.
[354] L.A. Aslanov, V.M. Ionov, V.M. Attiya, A.B. Permin, V.S. Petrosyan, Zh. Strukt. Khim. (Russ.) 18 (1977) 1103.
[355] A.V. Yatsenko, L.A. Aslanov, Yu.M. Burtsev, E.A. Kravchenko, Zh. Neorg. Khim. (Russ.) 36 (1991) 2035.
[356] M.A. Porai-Koshits, T.S. Khodashova, R.A. Slavinskaya, A.E. Shalamov, T.N. Sumarokova, Koord. Khim. (Russ.) 6 (1980) 1751.
[357] G.G. Mather, G.M. McLaughlin, A. Pidcock, J. Chem. Soc., Dalton Trans. (1973) 1823.
[358] K. Ruth, H.-W. Lerner, M. Bolte, Acta Crystallogr. E 61 (2005) m1852.
[359] M.M. Olmstead, K.A. Williams, W.K. Musker, J. Am. Chem. Soc. 104 (1982) 5567.
[360] A.R.J. Genge, W. Levason, G. Reid, J. Chem. Soc., Dalton Trans. (1997) 4479.
[361] S.E. Dann, A.R.J. Genge, W. Levason, G. Reid, J. Chem. Soc., Dalton Trans. (1996) 4471.
[362] S. Calogero, U. Russo, G. Valle, P.W.C. Barnard, J.D. Donaldson, Inorg. Chim. Acta 59 (1982) 111.
[363] D. Tudela, M.A. Khan, J.J. Zuckerman, J. Chem. Soc., Dalton Trans. (1991) 999.
[364] Y. Zhang, H.-B. Tong, D.-S. Liu, S.-P. Huang, M.-S. Zhou, Acta Crystallogr. E 61 (2005) m1697.
[365] G.A. Koutsantonis, T.S. Morien, B.W. Skelton, A.H. White, Acta Crystallogr. C 59 (2003) m361.
[366] S. Parsons, I. Maley, C. Pulham, P. Wood, Private Commun. (2004).
[367] T. Chivers, S.W. Liblong, J.F. Richardson, T. Ziegler, Inorg. Chem. 27 (1988) 860.
[368] W.A. Grigsby, T.S. Morien, C.L. Raston, B.W. Skelton, A.H. White, Aust. J. Chem. 57 (2004) 507.
[369] K.G. Rasmussen, K. Juhl, R.G. Hazell, K.A. Jørgensen, J. Chem. Soc. Perkin Trans. 2 (1998) 1347.
[370] V.J. Hall, E.R.T. Tiekink, Z. Kristallogr. 211 (1996) 247.
[371] B.Z. Momeni, F. Rominger, S.S. Hosseini, Acta Crystallogr. E 65 (2009) m690.
[372] J.M. Kisenyi, G.R. Willey, M.G.B. Drew, Acta Crystallogr. C 41 (1985) 700.
[373] T. Szymanska-Buzar, T. Glowiak, I. Czelusniak, Main Group Met. Chem. 24 (2001) 821.
[374] G.R. Willey, T.J. Woodman, R.J. Deeth, W. Errington, Main Group Met. Chem. 21 (1998) 583.
[375] F.D. Lewis, J.D. Oxman, J.C. Huffman, J. Am. Chem. Soc. 106 (1984) 466.
[376] S.E. Denmark, B.R. Henke, E. Weber, J. Am. Chem. Soc. 109 (1987) 2512.
[377] D. Dakternieks, H. Zhu, E.R.T. Tiekink, Main Group Met. Chem. 17 (1994) 519.
[378] G. Quinkert, H. Becker, M. Del Grosso, G. Dambacher, J.W. Bats, G. Dürner, Tetrahedron Lett. 34 (1993) 6885.
[379] F. Kunkel, K. Dehnicke, H. Goesmann, D. Fenske, Z. Naturforsch. B 50 (1995) 848.
[380] D. Tudela, J.D. Tornero, A. Monge, A.J. Sanchez-Herencia, Inorg. Chem. 32 (1993) 3928.
[381] M. Gregorkiewitz, D. Tudela, Acta Crystallogr. C 46 (1990) 210.
[382] A.I. Tursina, A.V. Yatsenko, S.V. Medvedev, V.V. Chernyshev, L.A. Aslanov, Zh. Strukt. Khim. (Russ.) 27 (1986) 157.
[383] A.V. Yatsenko, S.V. Medvedev, A.I. Tursina, L.A. Aslanov, Zh. Obshch. Khim. (Russ.) 56 (1986) 2330.
[384] T.S. Khodashova, M.A. Porai-Koshits, R.A. Slavinskaya, T.N. Sumarokova, Koord. Khim. (Russ.) 7 (1981) 301.
[385] G.R. Willey, R.J. Baker, J.V. Haslop, M.P. Spry, M.G.B. Drew, Polyhedron 17 (1998) 3291.
[386] K.A. Paseshnichenko, L.A. Aslanov, A.V. Yatsenko, S.V. Medvedev, Koord. Khim. (Russ.) 10 (1984) 1279.
[387] A.I. Tursina, L.A. Aslanov, V.V. Chernyshev, S.V. Medvedev, A.V. Yatsenko, Koord. Khim. (Russ.) 12 (1986) 420.
[388] M. Hitosugi-Levesque, J.M. Tanski, Acta Crystallogr. E 64 (2008) m1107.
[389] A.V. Jatsenko, S.V. Medvedev, K.A. Paseshnitchenko, L.A. Aslanov, J. Organomet. Chem. 284 (1985) 181.
[390] A.R.J. Genge, W. Levason, G. Reid, Inorg. Chim. Acta 288 (1999) 142.
[391] E.G. Il'in, G.B. Nikiforov, G.G. Aleksandrov, Dokl. Akad. Nauk SSSR (Russ.) 396 (2004) 500.
[392] V.K. Rotaru, M.Yu. Cheban, A.Yu. Simonov, T.I. Malinovskii, Dokl. Akad. Nauk SSSR (Russ.) 280 (1985) 631.
[393] G.B. Nikiforov, H.W. Roesky, P.G. Jones, J. Magull, A. Ringe, R.B. Oswald, Inorg. Chem. 47 (2008) 2171.
[394] S.I. Troyanov, G.N. Mazo, Vestn. MGU, Chem. 25 (1984) 606.
[395] S.I. Troyanov, G.N. Mazo, M.A. Simonov, Koord. Chem. 11 (1985) 1147.
[396] T. Carofiglio, C. Floriani, A. Chiesi-Villa, C. Guastini, Inorg. Chem. 28 (1989) 4417.
[397] G.N. Mazo, A.P. Bobylev, S.I. Troyanov, Vestn. MGU, Chem. 28 (1987) 459.
[398] C.-I. Bränden, Acta Chem. Scand. 16 (1962) 1806.
[399] S.I. Troyanov, G.N. Mazo, V.B. Rybakov, K.V. Budkina, Koord. Chem. 16 (1990) 466.
[400] A.S. Batsanov, J.A.K. Howard, A.K. Hughes, A.J. Kingsley, Acta Crystallogr. C 55 (1999) IUC9900137.
[401] C.H. Winter, T.S. Lewkebandara, J.W. Proscia, A.L. Rheingold, Inorg. Chem. 32 (1993) 3807.
[402] J. Utko, P. Sobota, T. Lis, J. Organomet. Chem. 334 (1987) 341.
[403] W. Levason, B. Patel, G. Reid, V.-A. Tolhurst, M. Webster, J. Chem. Soc., Dalton Trans. (2000) 3001.
[404] F.A. Cotton, C.A. Murillo, M.A. Petrukhina, J. Organomet. Chem. 573 (1999) 78.
[405] F.A. Cotton, C.A. Murillo, M.A. Petrukhina, J. Organomet. Chem. 593 (2000) 1.
[406] S.I. Troyanov, G.N. Mazo, M.A. Simonov, A.L. Il'inskii, Zh. Neorg. Khim. (Russ.) 31 (1986) 3022.
[407] S.I. Troyanov, G.N. Mazo, M.A. Simonov, Koord. Khim. (Russ.) 12 (1986) 1000.
[408] L. Chen, F.A. Cotton, Polyhedron 17 (1998) 3727.
[409] S. Rabe, U. Müller, Z. Anorg. Allg. Chem. 627 (2001) 201.
[410] M.S. Hill, P.B. Hitchcock, N. Smith, Polyhedron 23 (2004) 801.
[411] K. Hensen, A. Lemke, M. Bolte, Acta Crystallogr. C 55 (1999) 863.
[412] H.W. Roesky, B. Meller-Rehbein, M. Noltemeyer, Z. Naturforsch. B 46 (1991) 1059.
[413] I.A. Guzei, C.H. Winter, Inorg. Chem. 36 (1997) 4415.
[414] P. Sobota, J. Utko, S. Szafert, K. Szczegot, J. Chem. Soc., Dalton Trans. (1997) 679.
[415] G. Guolin, P. Zuohua, Z. Zeying, Wuli Huaxue Xuebao(Chin.) 2 (1986) 278.
[416] T. Lis, J. Ejfler, J. Utko, P. Sobota, Pol. J. Chem. 66 (1992) 93.
[417] M.-F. Li, Y.-K. Shan, Z. Kristallogr.-New Cryst. Struct. 221 (2006) 41.
[418] W. Clegg, P.A. O'Neil, K.W. Henderson, R.E. Mulvey, Acta Crystallogr. C 49 (1993) 2108.
[419] F. Weller, S. Wocadlo, H.-J. Mai, K. Dehnicke, Z. Kristallogr. 209 (1994) 634.
[420] D. Jones, A. Roberts, K. Cavell, W. Keim, U. Englert, B.W. Skelton, A.H. White, J. Chem. Soc. Dalton Trans. (1998) 255.
[421] J. Strauch, T.H. Warren, G. Erker, R. Frohlich, P. Saarenketo, Inorg. Chim. Acta 300 (2000) 810.
[422] B. Viard, M. Poulain, D. Grandjean, J. Amaudrut, J. Chem. Res. 84 (1983) 853.
[423] T. Poll, J.O. Metter, G. Helmchen, Angew. Chem. Int. Ed. Engl. 24 (1985) 112.
[424] G. Maier, U. Seipp, R. Boese, Tetrahedron Lett. 28 (1987) 4515.
[425] P. Sobota, J. Utko, T. Lis, J. Organomet. Chem. 393 (1990) 349.
[426] H.J. Kakkonen, J. Pursiainen, T.A. Pakkanen, M. Ahlgren, E. Iiskola, J. Organomet. Chem. 453 (1993) 175.
[427] P. Sobota, S. Szafert, T. Lis, J. Organomet. Chem. 443 (1993) 85.
[428] K. Ishimaru, K. Monda, Y. Yamamoto, K. Akiba, Tetrahedron 54 (1998) 727.
[429] S.I. Troyanov, G.N. Mazo, V.B. Rybakov, Zh. Neorg. Khim. 33 (1988) 2798.
[430] G.N. Mazo, V.B. Rybakov, A.L. Il'inskii, S.I. Troyanov, Koord. Khim. (Russ.) 16 (1990) 185.
[431] S.I. Troyanov, G.N. Mazo, B.V. Merinov, B.A. Maksimov, Kristallografiya (Russ.) 34 (1989) 235.
[432] M. Niehues, G. Kehr, G. Erker, B. Wibbeling, R. Fröhlich, O. Blacque, H. Berke, J. Organomet. Chem. 663 (2002) 192.
[433] E.V. Avtomonov, K.A. Rufanov, Z. Naturforsch. (B) 54 (1999) 1563.
[434] S.I. Troyanov, Koord. Khim. (Russ.) 13 (1987) 1123.
[435] J. Guery, M. Leblanc, C. Jacoboni, Eur. J. Solid State Inorg. Chem. 26 (1989) 289.
[436] C.E.F. Rickard, M.W. Glenny, A.J. Nielson, Acta Crystallogr. E 59 (2003) m183.
[437] B. Richter, J. Scholz, B. Neumüller, R. Weimann, H. Schumann, Z. Anorg. Allg. Chem. 621 (1995) 365.
[438] M. Eberle, C. Röhr, Acta Crystallogr. C 52 (1996) 566.
[439] B. Galeffi, M. Simard, J.D. Wuest, Inorg. Chem. 29 (1990) 951.
[440] R.A. Johnson, R.B. Von Dreele, T.M. Brown, Inorg. Chem. 23 (1984) 4302.
[441] S.I. Troyanov, Yu.M. Subbotin, Zh. Neorg. Khim. (Russ.) 32 (1987) 58.
[442] F.A. Cotton, W.A. Wojtczak, Acta Crystallogr. C 50 (1994) 1662.
[443] I.H.T. Sham, B.O. Patrick, B. von Ahsen, S. von Ahsen, H. Willner, R.C. Thompson, F. Aubke, Solid State Sci. 4 (2002) 1457.
[444] I.C. Tornieporth-Oetting, T.M. Klapötke, T.S. Cameron, J. Valkonen, P. Rademacher, K. Kowski, J. Chem. Soc., Dalton Trans. (1992) 537.
[445] H. Binas, Z. Anorg. Allg. Chem. 352 (1967) 271.
[446] T.M. Klapötke, H. Nöth, T. Schütt, M. Suter, M. Warchhold, Z. Anorg. Allg. Chem. 627 (2001) 1582.
[447] J.C. Jochims, R. Abu-El-Halawa, L. Zsolnai, G. Huttner, Chem. Ber. 117 (1984) 1161.
[448] C.-I. Bränden, I. Lindqvist, Acta Chem. Scand. 17 (1963) 353.
[449] H. Kietaibl, H. Völlenkle, A. Wittmann, Monatsh. Chem. 103 (1972) 1360.
[450] B. Chevrier, J.-M. Le Carpentier, R. Weiss, Acta Crystallogr. B 28 (1972) 2667.
[451] B. Chevrier, J.-M. Le Carpentier, R. Weiss, J. Am. Chem. Soc. 94 (1972) 5718.
[452] T. Laube, A. Weidenhaupt, R. Hunziker, J. Am. Chem. Soc. 113 (1991) 2561.
[453] R. Minkwitz, U. Lohmann, H. Preut, Z. Naturforsch. B 51 (1996) 133.
[454] E.G. Zaitseva, S.V. Medvedev, L.A. Aslanov, Metalloorg. Khim. (Russ.) 1 (1988) 1360.
[455] B. Neumuller, R. Meyer zu Kocker, K. Dehnicke, Z. Kristallogr. 209 (1994) 90.
[456] E. Anders, F. Markus, H. Meske, J. Tropsch, G. Maas, Chem. Ber. 120 (1987) 735.
[457] L. Brun, C.-I. Brändén, Acta Crystallogr. 20 (1966) 749.
[458] J. Yamamoto, S. Ito, T. Tsuboi, T. Tsuboi, K. Tsukihara, Bull. Chem. Soc. Jpn. 58 (1985) 470.
[459] A. Schmidpeter, H. Nöth, Inorg. Chim. Acta 269 (1998) 7.
[460] J.-M. Le Carpentier, R. Weiss, Acta Crystallogr. B 28 (1972) 1442.
[461] Y. Hermodsson, Acta Chem. Scand. 21 (1967) 1313.
[462] G.R. Willey, T.J. Woodman, M.G.B. Drew, Polyhedron 16 (1997) 351.
[463] I.-A. Ahmed, R. Blachnik, H. Reuter, K. Stumpf, Z. Kristallogr.-New Cryst. Struct. 214 (1999) 117.
[464] K. Stumpf, R. Blachnik, H. Reuter, Z. Kristallogr.-New Cryst. Struct. 214 (1999) 279.
[465] K. Stumpf, R. Blachnik, G. Roth, Z. Kristallogr.-New Cryst. Struct. 213 (1998) 151.
[466] K. Stumpf, R. Blachnik, H. Reuter, Z. Kristallogr.-New Cryst. Struct. 214 (1999) 281.

[467] K. Stumpf, R. Blachnik, G. Roth, Z. Kristallogr.-New Cryst. Struct. 214 (1999) 397.
[468] I.-A. Ahmed, R. Blachnik, H. Reuter, K. Stumpf, Z. Kristallogr.-New Cryst. Struct. 214 (1999) 119.
[469] C. Chavant, G. Constant, Y. Jeannin, R. Morancho, Acta Crystallogr. B 31 (1975) 1823.
[470] F. Marchetti, G. Pampaloni, S. Zacchini, Inorg. Chem. 47 (2008) 365.
[471] F. Marchetti, G. Pampaloni, S. Zacchini, Eur. J. Inorg. Chem. (2008) 453.
[472] F.A. Cotton, M.P. Diebold, W.J. Roth, Acta Crystallogr. C 46 (1990) 1624.
[473] K. Stumpf, R. Blachnik, G. Roth, G. Kastner, Z. Kristallogr.-New Cryst. Struct. 215 (2000) 589.
[474] R.E. Desimone, M.D. Glick, J. Coord. Chem. 5 (1976) 181.
[475] F. Marchetti, G. Pampaloni, S. Zacchini, Dalton Trans. (2007) 4343.
[476] C.-T. Chen, L.H. Doerrer, V.C. Williams, M.L.H. Green, J. Chem. Soc., Dalton Trans. (2000) 967.
[477] C. Ritter III, T.L. Groy, J. Kouvetakis, Acta Crystallogr. E 58 (2002) m684.
[478] A.V. Suvorov, Thermodynamic Chemistry of the Vapor State. Tensimetric Studies of Heterogeneous Equilibria, Khimia, Leningrad, 1970 (in Russian).
[479] H. Ipser, Ber. Bunsenges. Phys. Chem. 102 (1998) 1217.
[480] A.B. Nikol'skii (Ed.), Physical Methods for Studying Inorganic Substances, Academia, Moskow, 2006 (in Russian).
[481] T.P. Melia, R. Merrifield, J. Inorg. Nucl. Chem. 32 (1970) 1489.
[482] S. Boghosian, G.A. Voyiatzis, G.N. Papatheodorou, J. Chem. Soc. Dalton Trans. (1996) 3405.
[483] T.P. Chusova, L.N. Zelenina, Yu.G. Stenin, Z.I. Semenova, V.A. Titov, Russ. Chem. Bull. Int. Ed. 56 (2007) 1313.
[484] A.D. Rusin, L.A. Nisel'son, Russ. J. Phys. Chem. A 82 (2008) 1801.
[485] P.P. Semyannikov, I.K. Igumenov, S.V. Trubin, T.P. Chusova, Z.I. Semenova, Thermochim. Acta 432 (2005) 91.
[486] E.S. Filatov, S.V. Sysoev, L.N. Zelenina, T.P. Chusova, V.A. Logvinenko, P.P. Semyannikov, I.K. Igumenov, J. Therm. Anal. Calorim. 86 (2006) 537.
[487] L.N. Zelenina, V.A. Titov, T.P. Chusova, Yu.G. Stenin, A.A. Titov, J. Chem. Thermodyn. 35 (2003) 1601.
[488] P.P. Semyannikov, I.K. Igumenov, S.V. Trubin, T.P. Chusova, Z.I. Semenova, Thermochim. Acta 451 (2006) 80.
[489] K.V. Zherikova, N.B. Morozova, L.N. Zelenina, S.V. Sysoev, T.P. Chusova, I.K. Igumenov, J. Therm. Anal. Calorim. 92 (2008) 729.
[490] O.G. Polyachenok, E.N. Dudkina, L.D. Polyachenok, J. Chem. Thermodyn. 41 (2009) 414.
[491] O.G. Polyachenok, E.N. Dudkina, L.D. Polyachenok, J. Chem. Thermodyn. 41 (2009) 74.
[492] A.Y. Timoshkin, A.V. Suvorov, A.D. Misharev, Russ. J. Gen. Chem. 72 (2002) 1874.
[493] H.C. Brown, R.R. Holmes, J. Am. Chem. Soc. 78 (1956) 2173.
[494] J.W. Wilson, I.J. Worral, J. Chem. Soc. (A) (1968) 316.
[495] J.H. Kiefer, Q. Zhang, R.D. Kern, J. Yao, B. Jursic, J. Phys. Chem. A 101 (1997) 7061.
[496] V.I. Trusov, A.V. Suvorov, R.N. Abakumova, Zh. Neorg. Khim. 20 (1975) 501.
[497] H.L. Friedman, H. Taube, J. Am. Chem. Soc. 72 (1950) 2236.
[498] W. Klemm, W. Tilk, H. Jacobi, Z. Anorg. Allg. Chem. 207 (1932) 187.
[499] A.Y. Timoshkin, A.A. Grigoriev, A.V. Suvorov, Zh. Obsh. Khim. 65 (1995) 1634.
[500] V.N. Kuliukin, E.S. Petrov, Izv. SO AN USSR, Ser. Khim. khim. nauk. (1970) 69.
[501] A.A. Grigoriev, G.G. Tchernik, A.Y. Timoshkin, A.V. Suvorov, Zh. Obsh. Khim. 64 (1994) 564.
[502] R.C. Reid, J.M. Prausnitz, T.K. Sherwood, The Properties of Gases and Liquids, McGraw-Hill Inc., New York, 1977.
[503] H. Rheinboldt, R. Boy, J. Prakt. Chem. 29 (1931) 268.
[504] V.I. Vasil'eva, M.A. Yazkovskaya, S.S. Medvedev, Doklady Acad. Sci. USSR 188 (1969) 351.
[505] E.A. Kolesnikova, T.N. Sevast'yanova, A.V. Suvorov, Zh. Neorg. Khim. 32 (1987) 1571.
[506] K.M. Waggoner, H. Hope, P.P. Power, Angew. Chem. Int. Ed. 27 (1988) 1699.
[507] K.M. Waggoner, P.P. Power, J. Am. Chem. Soc. 113 (1991) 3385.
[508] P.P. Power, J. Organomet. Chem. 400 (1990) 49.
[509] J. Pinkas, J. Lőbl, H.W. Roesky, Phosph. Sulf. Silic. 179 (2004) 759.
[510] J. Lőbl, M. Necas, J. Pinkas, Main Group Chem. 5 (2006) 79.
[511] J.L. Lőbl, A.Y. Timoshkin, C. Trinh, M. Necas, H.W. Roesky, J. Pinkas, Inorg. Chem. 46 (2007) 5678.
[512] E.M. Larsen, J. Howatson, A.M. Camill, L.J. Wittenberg, J. Am. Chem. Soc. 74 (1952) 3489.
[513] I.A. Sheka, B.A. Voitovich, Zh. Neorg. Khim. 1 (1956) 964.
[514] B.A. Voitovich, A.S. Barabanova, V.P. Klochkov, E.V. Sharkina, Ukr. Khim. Zh. 32 (1966) 167.
[515] D.M. Gruen, J.J. Katz, J. Am. Chem. Soc. 71 (1949) 3843.
[516] L.A. Nisel'son, B.N. Ivanov-Emin, Zh. Neorg. Khim. 1 (1956) 1766.
[517] E.K. Krzhizhanovskaya, Cand. Sci. thesis, Leningrad, 1970.
[518] A.V. Suvorov, E.K. Krzhizhanovskaya, Zh. Neorg. Khim. 14 (1969) 835.
[519] A.V. Suvorov, E.K. Krzhizhanovskaya, Y.V. Kondrat'ev, Problems of Modern Chemistry of Coordination Compounds, vol. 3, 1970, p. 57 (in Russian).
[520] V.P. Glushko (Ed.), Thermal constants of Substances, Academy of Science, vols. I–VII. USSR, Moskow, 1965–1982.
[521] O. Kubaschewski, E.L. Evans, Thermochemistry in Metallurgy, In. Lit, Moskow, 1954.
[522] R.R. Wenner, Thermochemical calculations, McGraw-Hill, New York, 1941.
[523] J.S. Chickos, S. Hosseini, P.G. Hesse, J.F. Liebman, Struct. Chem. 4 (1993) 271.
[524] A.V. Suvorov, E.K. Krzhizhanovskaya, Zh. Neorg. Khim. 14 (1969) 898.
[525] V.I. Trusov, A.V. Suvorov, Zh. Neorg. Khim. 19 (1974) 3253.
[526] V.I. Trusov, A.V. Suvorov, A.S. Tarasova, Zh. Neorg. Khim. 21 (1976) 3102.
[527] A.Y. Timoshkin, E.A. Berezovskaya, A.V. Suvorov, A.D. Misharev, Russ. J. Gen. Chem. 75 (2005) 1173.
[528] A.V. Suvorov, V.L. Shubaev, Zh. Neorg. Khim. 16 (1971) 318.
[529] A.V. Suvorov, V.I. Trusov, Zh. Neorg. Khim. 18 (1973) 1953.
[530] A.V. Suvorov, D. Sharipov, Zh. Neorg. Khim. 20 (1975) 1064.
[531] A.V. Suvorov, D. Sharipov, Zh. Neorg. Khim. 19 (1974) 512.
[532] A.M. German, Cand. Sci. thesis, Leningrad, 1974.
[533] A.V. Suvorov, A.M. German, N.P. Bondareva, Zh. Neorg. Khim. 16 (1971) 2413.
[534] A.M. German, A.V. Suvorov, V.A. Titov, V.I. Trusov, Zh. Neorg. Khim. 17 (1972) 3101.
[535] A.V. Suvorov, D. Sharipov, Zh. Neorg. Khim. 20 (1975) 1393.
[536] D. Sharipov, Cand. Sci. thesis, Leningrad, 1974.
[537] V.I. Trusov, Cand. Sci. thesis, Leningrad, 1974.
[538] T.N. Sevast'yanova, A.V. Suvorov, N.L. Yaremchuk, Zh. Obsh. Khim. 66 (1996) 894.
[539] I.I. Konysheva, T.N. Sevast'yanova, A.V. Suvorov, Zh. Neorg. Khim. 36 (1991) 1260.
[540] T.N. Sevast'yanova, A.M. German, A.V. Suvorov, A.N. Cherviakov, Zh. Obsh. Khim. 65 (1995) 1084.
[541] E.I. Davydova, T.N. Sevast'yanova, A.V. Suvorov, D.A. Kirichenko Vestnik, St. Petersburg University, ser. 4 Khim. (2004) 33.
[542] T.N. Sevast'yanova, E.V. Korobkina, A.V. Suvorov, Zh. Neorg. Khim. 33 (1988) 2900.
[543] T.N. Sevast'yanova, A.V. Suvorov, A.D. Misharev, Zh. Obsh. Khim. 66 (1996) 195.
[544] A.V. Suvorov, T.N. Sevast'yanova, A.I. Burliand, Zh. Fiz. Khim. 56 (1982) 1112.
[545] E.K. Krzhizhanovskaya, A.V. Suvorov, Zh. Neorg. Khim. 16 (1971) 2542.
[546] T.N. Sevast'yanova, A.Sh. Tarasova, A.V. Suvorov, Zh. Neorg. Khim. 24 (1979) 2322.
[547] O.V. Plutova, T.N. Sevast'yanova, A.V. Suvorov, Zh. Neorg. Khim. 21 (1976) 1305.
[548] T.V. Susliakova, Diploma thesis, St. Petersburg State University, St. Petersburg, 2008.
[549] V.L. Shubaev, Cand. Sci. thesis, Leningrad State University, Leningrad, 1971.
[550] A.S. Litvinenko, A.Y. Timoshkin, H.F. Schaefer, Polyhedron 25 (2006) 2465.
[551] N.B. Morozova, Doct. Sci. Diss. Novosibirsk, 2009.
[552] I.K. Igumenov, Y.I. Chumachenko, S.V. Zemskov, Problems of Chemistry and Applications of Metal beta-diketonates, Nauka, Moskow, 1982, p. 100 (in Russian).
[553] V.I. Trusov, A.V. Suvorov, Zh. Neorg. Khim 19 (1974) 549.
[554] V.I. Trusov, Diploma thesis, Leningrad, 1971.
[555] S. Murata, M. Sakiyama, S. Seki, Thermochim. Acta 88 (1985) 121.
[556] C.M. Lousada, S.S. Pinto, J.N.C. Lopes, M.F.M. da Piedade, H.P. Diogo, M.E.M. da Piedade, J. Phys. Chem. A 112 (2008) 2977.
[557] M.A.V. Ribeiro da Silva, M.L.C.C.H. Ferrao, M.J.S. Monte, R.M.G.E. da Silva, J.C. Ribeiro, J. Chem. Thermodyn. 24 (1992) 585.
[558] M.A.V. Ribeiro da Silva, M.J.S. Monte, E. Giera, W. Kakolowicz, J. Chem. Thermodyn. 25 (1993) 1263.
[559] E.S. Filatov, P.A. Stabnikov, P.P. Semyannikov, S.V. Trubin, I.K. Igumenov, Russ. J. Coord. Chem. 32 (2006) 126.
[560] N.B. Morozova, P.P. Semyannikov, S.V. Trubin, P.P. Stabnikov, A.A. Bessonov, K.V. Zherikova, I.K. Igumenov, J. Therm. Anal. Calorim. 96 (2009) 261.
[561] A.A. Bessonov, N.B. Morozova, N.V. Gelfond, P.P. Semyannikov, I.A. Baidina, S.V. Trubin, Y.V. Shevtsov, I.K. Igumenov, J. Organomet. Chem. 693 (2008) 2572.
[562] A.A. Bessonov, N.B. Morozova, P.P. Semyannikov, S.V. Trubin, N.V. Gelfond, I.K. Igumenov, Russ. J. Coord. Chem. 34 (2008) 186.
[563] N.B. Morozova, K.V. Zherikova, I.A. Baidina, S.V. Sysoev, P.P. Semyannikov, L.V. Yakovkina, T.P. Smirnova, N.V. Gelfond, I.K. Igumenov, G. Carta, G. Rossetto, J. Phys. Chem. Solids 69 (2008) 673.
[564] N.B. Morozova, P.A. Stabnikov, I.A. Baidina, P.P. Semyannikov, S.V. Trubin, I.K. Igumenov, J. Struct. Chem. 48 (2007) 889.
[565] A.A. Bessonov, N.B. Morozova, N.V. Gelfond, P.P. Semyannikov, S.V. Trubin, Y.V. Shevtsov, Y.V. Shubin, I.K. Igumenov, Surf. Coat. Technol. 201 (2007) 9099.
[566] G.I. Zharkova, P.A. Stabnikov, S.A. Sysoev, I.K. Igumenov, J. Struct. Chem. 46 (2005) 320.
[567] K.V. Zherikova, N.B. Morozova, I.A. Baidina, S.V. Sysoev, I.K. Igumenov, J. Struct. Chem. 49 (2008) 58.
[568] S. Arockiasamy, O.M. Sreedharan, C. Mallika, V.S. Raghunathan, K.S. Nagaraja, Chem. Eng. Sci. 62 (2007) 1703.
[569] T. Ohta, F. Cicoira, P. Doppelt, L. Beitone, P. Hoffmann, Chem. Vap. Dep. 7 (2001) 33.
[570] O.V. Prokuda, V.R. Belosludov, I.K. Igumenov, P.A. Stabnikov, J. Struct. Chem. 47 (2006) 1032.
[571] L.A. Torres, M. Campos, E. Enriquez, R. Patiño, J. Chem. Thermodyn. 34 (2002) 293.
[572] R. Patiño, M. Campos, L.A. Torres, J. Chem. Thermodyn. 34 (2002) 193.
[573] A.P. Chagas, C. Airoldi, Polyhedron 8 (1989) 1093.
[574] L.C.R. dos Santos, J. de Queiroz Caluete, A.G. de Souza, Thermochim. Acta 292 (1997) 71.
[575] P.O. Dunstan, L.C.R. dos Santos, Thermochim. Acta 156 (1989) 163.
[576] P.O. Dunstan, Thermochim. Acta 279 (1996) 167.
[577] P.O. Dunstan, Thermochim. Acta 317 (1998) 165.
[578] P.O. Dunstan, Thermochim. Acta 333 (1999) 5.

[579] A.G. Souza, M.M. Oliveira, A.D. Gondim, P.O. Dunstan, D.M. de, A. Melo, Thermochim. Acta 344 (2000) 29.
[580] P.O. Dunstan, Thermochim. Acta 345 (2000) 117.
[581] J.A. de, A.I. Sales, A.G. Souza, G.F. Goncalves de Freitas, S. Prasad, M.F.S. Trindade, L.H. Carvalho, P.O. Dunstan, Thermochim. Acta 356 (2000) 9.
[582] P.O. Dunstan, Thermochim. Acta 356 (2000) 19.
[583] P.O. Dunstan, Thermochim. Acta 369 (2001) 9.
[584] P.O. Dunstan, Thermochim. Acta 376 (2001) 17.
[585] J.R. Botelho, A.G. Souza, L.M. Nunes, A.P. Chagas, I.M. Garcia dos Santos, M.M. da Conceicao, P.O. Dunstan, J. Therm. Anal. Calorim. 67 (2002) 413.
[586] P.O. Dunstan, Thermochim. Acta 389 (2002) 25.
[587] P.O. Dunstan, Thermochim. Acta 398 (2003) 1.
[588] P.O. Dunstan, Thermochim. Acta 404 (2003) 117.
[589] P.O. Dunstan, Thermochim. Acta 409 (2004) 19.
[590] P.O. Dunstan, Thermochim. Acta 419 (2004) 89.
[591] J.R. Botelho, A.D. Gondim, I.M.G. Santos, P.O. Dunstan, A.G. Souza, V.J. Fernandes Jr., A.S. Araujo, J. Therm. Anal. Calorim. 75 (2004) 607.
[592] J.R. Botelho, A.G. Souza, A.D. Gondim, P.F. Athayde-Fihlo, P.O. Dunstan, C.D. Pinheiro, E. Longo, L.H. Carvalho, J. Therm. Anal. Calorim. 79 (2005) 309.
[593] P.O. Dunstan, J. Therm. Anal. Calorim. 79 (2005) 355.
[594] P.O. Dunstan, Thermochim. Acta 437 (2005) 100.
[595] P.O. Dunstan, Thermochim. Acta 441 (2006) 1.
[596] P.O. Dunstan, Thermochim. Acta 450 (2006) 5.
[597] P.O. Dunstan, Thermochim. Acta 456 (2007) 32.
[598] P.O. Dunstan, Thermochim. Acta 468 (2008) 21.
[599] P.O. Dunstan, J. Chem. Eng. Data 54 (2009) 842.
[600] P.M. Burkinshaw, C.T. Mortimer, J. Chem. Soc. Dalton Trans. (1984) 75.
[601] V.G. Sevast'yanov, D.V. Sevast'yanov, E.V. Peresypkina, V.A. Blatov, N.T. Kuznetsov, Russ. J. Coord. Chem. 30 (2004) 679.
[602] G.I. Zharkova, S.V. Sysoev, I.A. Baidina, P.A. Stabnikov, I.K. Igumenov, J. Struct. Chem. 46 (2005) 494.
[603] V.G. Sevast'yanov, E.P. Simonenko, D.V. Sevast'yanov, N.T. Kuznetsov, Russ. J. Coord. Chem. 30 (2004) 755.
[604] L.N. Mazalov, S.V. Trubina, N.A. Kryuchkova, O.A. Tarasenko, S.V. Trubin, G.I. Zharkova, J. Struct. Chem. 48 (2007) 253.
[605] S.J. Ashcroft, J. Chem. Soc. (A) (1970) 1020.
[606] L.M.N.B.F. Santos, B. Schröder, O.O.P. Fernandes, M.A.V. Ribeiro da Silva, Thermochim. Acta 415 (2004) 15.
[607] A.A. Grigoriev, Cand. Sci. Diss. Leningrad, 1987.
[608] D.R. Aris, W. Errington, G.R. Willey, Acta Crystallogr. C 55 (1999) 1746.